Acta Universitatis Tamperensis 2081

MARISA OJALA

Cardiac Differentiation of Pluripotent Stem Cells and Modeling Hypertrophic Cardiomyopathy

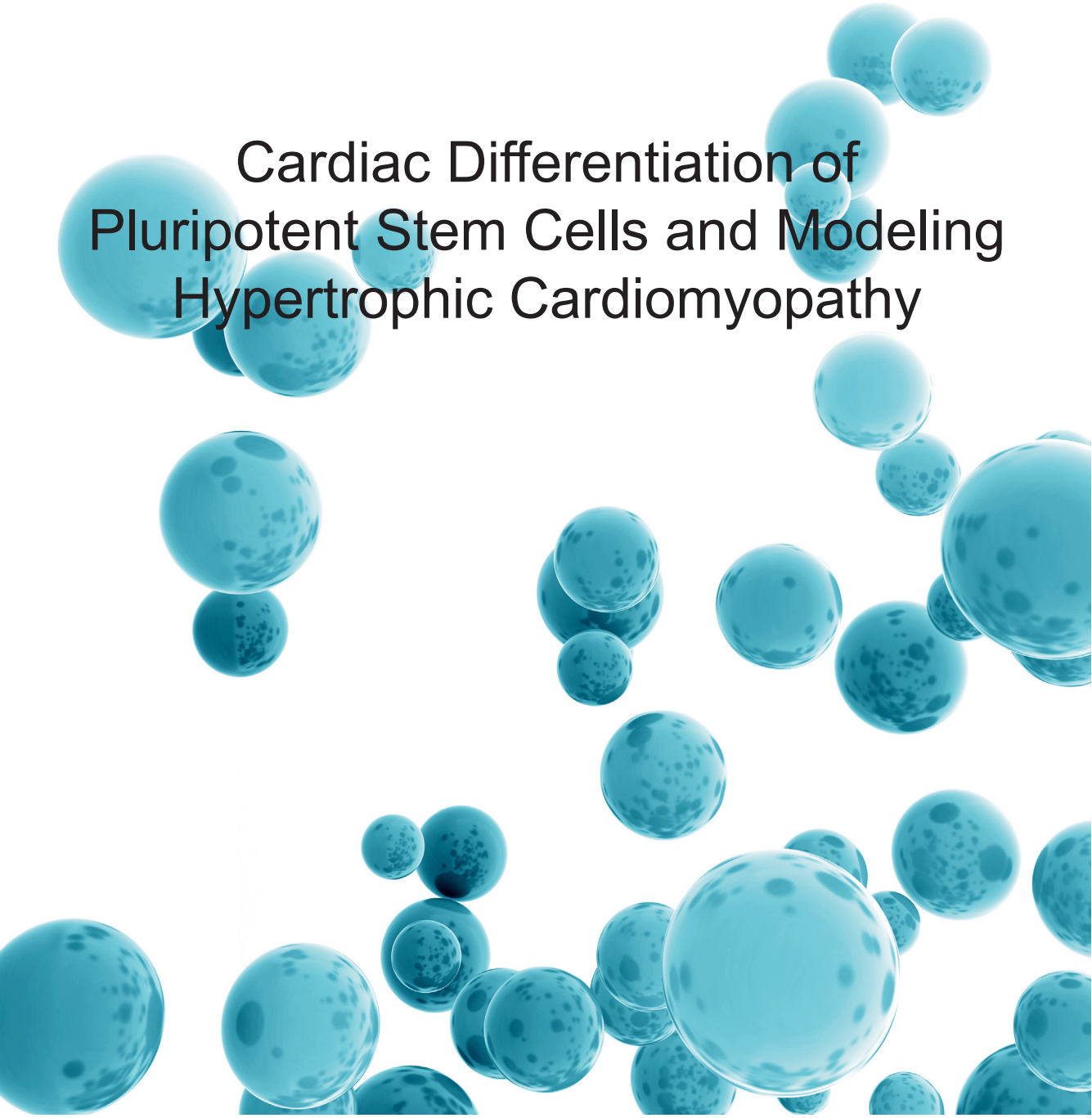

MARISA OJALA

Cardiac Differentiation of Pluripotent Stem Cells and Modeling Hypertrophic Cardiomyopathy

ACADEMIC DISSERTATION
To be presented, with the permission of
the Board of the BioMediTech of the University of Tampere,
for public discussion in the auditorium of Finn-Medi 5,
Biokatu 12, Tampere, on 28 August 2015, at 12 o'clock.

UNIVERSITY OF TAMPERE

MARISA OJALA

Cardiac Differentiation of Pluripotent Stem Cells and Modeling Hypertrophic Cardiomyopathy

Acta Universitatis Tamperensis 2081
Tampere University Press
Tampere 2015

UNIVERSITY OF TAMPERE

ACADEMIC DISSERTATION
University of Tampere, BioMediTech
Tampere University Hospital, Heart Hospital
Finland

Supervised by
Professor Katriina Aalto-Setälä
University of Tampere
Finland
PhD Kristiina Rajala
University of Tampere
Finland

Reviewed by
Docent Riikka Lund
University of Turku
Finland
Professor Heikki Ruskoaho
University of Helsinki
Finland

The originality of this thesis has been checked using the Turnitin OriginalityCheck service in accordance with the quality management system of the University of Tampere.

Cover design by
Mikko Reinikka

Distributor:
verkkokauppa@juvenesprint.fi
https://verkkokauppa.juvenes.fi

Acta Universitatis Tamperensis 2081
ISBN 978-951-44-9875-6 (print)
ISSN-L 1455-1616
ISSN 1455-1616

Acta Electronica Universitatis Tamperensis 1575
ISBN 978-951-44-9876-3 (pdf)
ISSN 1456-954X
http://tampub.uta.fi

Suomen Yliopistopaino Oy – Juvenes Print
Tampere 2015

To my Family

Abstract

The derivation of human embryonic stem cells (hESCs) from developing embryos, as well as the more recent discovery of human induced pluripotent stem cells (hiPSCs), has revolutionized the research of genetic diseases, also in the cardiovascular field. These cells are collectively called human pluripotent stem cells (hPSCs), and they possess the ability to self-renew and differentiate into all cell types of the human body. Thus, hPSCs represent a potential source of cells for future regenerative medicine applications and *in vitro* modeling of genetic diseases as well as a platform for drug screening.

hPSCs can be cultured under laboratory conditions and differentiated into desired cell types. *In vitro* culture methods for hPSCs have improved markedly in recent years, from the use of animal-derived feeder cell layers and serum-containing medium to more defined feeder cell-free culture methods, including protein or synthetic attachment matrices and defined cell culture medium compositions. Current cardiac differentiation methods are based on EB (embryoid body) formation, co-culturing hPSCs with mouse endodermal-like cells (END-2), or to more guided monolayer cardiac differentiation applying various growth factors in feeder cell-free cultures.

Hypertrophic cardiomyopathy (HCM) is one the most common genetic cardiovascular diseases, with a prevalence of 1:500 in the general population. In HCM, typically the interventricular septum (IVS) is thickened, which may lead to progressive heart failure and sudden cardiac death (SCD). The mutations that lead to HCM are typically located in the genes encoding sarcomeric proteins. In Finland, two founder mutations account for approximately 18% of Finnish HCM cases. These mutations are located either in the myosin-binding protein C (*MYBPC3-Gln1061X*) or in α-tropomyosin (*TPM1-Asp175Asn*) genes.

Conventionally, cardiomyopathies have been studied using animal models, primarily rodents, or human tissue samples collected from end-stage HCM patients from surgical myectomies. The properties of rodent cardiomyocytes differ greatly from human cardiomyocytes, and cardiomyocytes derived from adults rapidly lose their typical properties, e.g., beating, when cultured *in vitro*. Using hiPSC technology, we are now able

to reprogram patient somatic cells into hiPSCs that contain the same genetic information, including mutations, as the patient. These patient-specific hiPSCs can be differentiated into cardiomyocytes, and their morphological and electrophysiological properties can be studied *in vitro*.

The first two aims of this thesis were to compare the cardiac differentiation efficiencies of various hESC and hiPSC lines and to evaluate the effects of hPSC culture methods on the cardiac differentiation efficiencies of hPSCs. We observed marked variations in the cardiac differentiation potential of individual hPSC lines. Furthermore, hESCs were more efficient in producing cardiomyocytes than hiPSCs. This phenomenon could partially be explained by the use of integrating retroviruses in hiPSC production. Furthermore, culture conditions had a significant effect on the cardiac differentiation potential of hPSCs, revealing the superiority of mouse feeder cell layer-based methods over the tested feeder cell-free culture method. The third aim was to develop cell models for studying HCM *in vitro* using patient-specific hiPSCs. hiPSC-derived HCM cardiomyocytes exhibited the HCM phenotype but simultaneously revealed significant differences between cardiomyocytes carrying the *MYBPC3-Gln1061X* or *TPM1-Asp175Asn* mutations. The hiPSC-derived *in vitro* models established in this thesis represent a valuable tool to study the pathophysiological mechanisms of HCM, drug screening and potentially optimize the drug treatments in a mutation-specific manner.

Tiivistelmä

Ihmisen alkion kantasolut (hESC-solut) ja indusoidut kantasolut (hiPSC-solut) ovat erittäin monikykyisiä eli pluripotentteja kantasoluja. Pluripotentit kantasolut (hPSC-solut) pystyvät jakautumaan rajattomasti, minkä lisäksi niitä voidaan erilaistaa halutuksi solutyypiksi laboratorio-olosuhteissa. Tällä hetkellä pluripotentteja kantasoluja voidaan jo hyödyntää erilaisten tautien tutkimisessa sekä lääkekehityksessä. Ainutlaatuisten ominaisuuksiensa ansiosta erittäin monikykyisiä kantasoluja voidaan tulevaisuudessa käyttää erilaisista solupuutoksista tai solujen toimintojen häiriöistä johtuvien sairauksien hoitoon.

Hypertrofinen kardiomyopatia (HCM) on periytyvä sydänlihassairaus, jossa sydämen kammioiden välinen seinämä paksuuntuu. Kudoksen liikakasvun vuoksi paksuuntunut kammiolihas rentoutuu huonosti, mikä voi aiheuttaa potilaille sydämen vajaatoiminta-oireita sekä pitkälle edettyään rytmihäiriöitä ja jopa äkkikuolemia. Tautiin ei ole olemassa parannusta, ja nykyiset hoitomenetelmät keskittyvät potilaiden oireiden hoitoon. Tyypillisesti taudin aiheuttavat geenimutaatiot sijaitsevat sarkomeeriproteiineja koodaavissa geeneissä. Suomessa kaksi valtamutaatiota kattaa noin 18% HCM-potilaista. Mutaatiot sijaitsevat myosiinia sitovassa proteiinissa (*MYBPC3-Gln1061X*) tai α-tropomyosiinissa (*TPM1-Asp175Asn*).

Aikaisemmin perinnöllisiä sydänsairauksia on tutkittu joko eläinmallien tai aikuisen yksilön sydämestä eristettyjen solujen avulla. Eläinten sydänlihassolut poikkeavat paljon ihmisen sydänlihassoluista, ja aikuisesta yksilöstä eristettyjen sydänlihassolujen kasvattaminen laboratorio-olosuhteissa on vaativaa. hiPSC-soluteknologian avulla aikuisen yksilön jo täysin erilaistuneet solut voidaan muuttaa takaisin alkion kantasoluja muistuttaviksi pluripotenteiksi soluiksi. hiPSC-soluja voidaan tuottaa esimerkiksi perinnöllisiä sydänsairauksia sairastavien potilaiden ihosoluista. Nämä potilasspesifiset solut sisältävät saman geneettisen informaation kuin potilaan perimä, mukaan lukien sairauden aiheuttavan geenivirheen. Potilasspesifisiä hiPSC-soluja on mahdollista erilaistaa laboratoriossa sydänlihassoluiksi, joiden morfologisia ja toiminnallisia ominaisuuksia voidaan sen jälkeen tutkia tarkemmin.

Tämä väitöskirja käsittelee hESC- ja hiPSC-solujen erilaistamista sydänlihassoluiksi sekä solumallin kehittämistä HCM-taudin mallintamista varten. Ensimmäisessä osatyössä hPSC-solulinjojen välillä havaittiin merkitseviä eroja niiden kyvyssä erilaistua sydänlihassoluiksi, minkä lisäksi hiPSC-solujen valmistustavan huomattiin vaikuttavan solujen erilaistumistehokkuuteen. Toisessa osatyössä hPSC-soluja kasvatettiin kolmessa eri kasvatusolosuhteessa, joiden havaittiin vaikuttavan solujen erilaistumispotentiaaliin merkitsevästi. Näin ollen sekä hiPSC-solujen valmistustapa että hPSC-solujen kasvatusmenetelmät tulisi optimoida tulevissa tutkimuksissa. Väitöskirjan kolmannessa osatyössä kehitettiin solumalleja HCM-taudin tutkimusta varten. Suomalaisia valtamutaatioita (*TPM1-Asp175Asn* tai *MYBPC3-Gln1061X*) kantavilta potilailta eristettiin fibroblasteja, jotka uudelleenohjelmoitiin hiPSC-soluiksi. Potilaiden hiPSC-soluista erilaistettujen sydänlihassolujen ominaisuuksia verrattiin keskenään sekä kontrollihenkilöiden hiPSC-soluista erilaistettujen sydänlihassolujen ominaisuuksiin. Tutkimuksessa havaittiin merkitseviä eroja sekä HCM-potilaiden ja kontrollihenkilöiden sydänlihassolujen välillä että kahden eri HCM-mutaation sisältävien sydänlihassolujen välillä. Tässä väitöskirjassa kehitettyjä HCM-solumalleja voidaan tulevaisuudessa käyttää tarkempien tautimekanismien tutkimisessa ja lääkekehityksessä.

Table of Contents

List of original communications

This thesis is based on the three original publications listed below. These publications are referred to in the thesis by using their Roman numbers (I-III).

I Toivonen S*, **Ojala M***, Hyysalo A*, Ilmarinen T, Rajala K, Pekkanen-Mattila M, Äänismaa R, Lundin K, Palgi J, Weltner J, Trokovic R, Silvennoinen O, Skottman H, Narkilahti S, Aalto-Setälä K, Otonkoski T. Comparative analysis of targeted differentiation of human induced pluripotent stem cells (hiPSCs) and human embryonic stem cells reveals variability associated with incomplete transgene silencing in retrovirally derived hiPSC lines. Stem Cells Transl Med, 2013, 2(2):83-93.

II **Ojala M**, Rajala K, Pekkanen-Mattila M, Miettinen M, Huhtala H, Aalto-Setälä K. Culture conditions affect cardiac differentiation potential of human pluripotent stem cells. PLoS ONE, 2012, 7(10):e48659.

III **Ojala M**, Prajapati C, Pölönen RP, Rajala K, Pekkanen-Mattila M, Rasku J, Larsson K, Aalto-Setälä K. Mutation-specific phenotypes in hiPSC-derived cardiomyocytes carrying either myosin-binding protein C or α-tropomyosin mutation for hypertrophic cardiomyopathy. Submitted.

* Authors contributed equally

List of abbreviations

ACTC1	α-cardiac actin
AFP	α-fetoprotein
APD	action potential duration
ARVC	arrhythmogenic cardiomyopathy
ATP	adenosine triphosphate
BMP	bone morphogenetic protein
BPM	beats per minute
bFGF	basic fibroblast growth factor
Brachyury T	T-box factor Brachyury
BSA	bovine serum albumin
CICR	Ca^{2+}-induced Ca^{2+} release
C-MYC	myelocytomatosis viral oncogene homolog
CNV	copy number variation
CRISPR	clustered regularly interspaced short palindromic repeat
DAD	delayed after depolarization
DCM	dilated cardiomyopathy
Dkk-1	Dickkopf homolog 1
DMEM	Dulbecco's modified Eagle's medium
EAD	early after depolarization
EB	embryoid body
ECG	electrocardiogram
ECM	extracellular matrix
EHS	Engelbreth-Holm-Swarm
EHT	engineered heart tissue
EM	electron microscopy
EMT	epithelial to mesenchymal transformation
END-2	mouse endodermal-like cell
ET-1	endothelin 1
FACS	fluorescence activated cell sorting
FBS	fetal bovine serum

FGF	fibroblast growth factor
GATA4	GATA-binding protein 4
hAFSC	human amniotic fluid stem cell
HCM	hypertrophic cardiomyopathy
HCMM	HCM with *MYBPC3-Gln1061X* mutation
HCMT	HCM with *Asp175Asn* mutation
hESC	human embryonic stem cell
hFF	human foreskin fibroblast
hiPSC	human induced pluripotent stem cell
hPSC	human pluripotent stem cell
HSA	human serum albumin
ICD	implantable cardioverter defibrillator
ICM	inner cell mass
IVF	*in vitro* fertilization
IVS	interventricular septum
KDR	kinase insert domain receptor
KLF4	Kruppel-like factor 4
ko-SR	knockout serum replacement
LEFTY-1	left-right determination factor 1
LIF	leukemia inhibitory factor
lncRNA	long non-coding RNA
LTR	long terminal repeat
MAP-2	microtubule associated protein 2
MEA	microelectrode array
MEF	mouse embryonic fibroblast
MEF-CM	medium conditioned on mouse embryonic fibroblasts
mESC	mouse embryonic stem cell
MESP-1	mesoderm posterior 1
miRNA	micro RNA
mRNA	messenger RNA
MHC	myosin heavy chain
MLC	myosin light chain
MSC	mesenchymal stem cell
MYBPC	myosin-binding protein C
NCX	Na^+/Ca^{2+} exchanger
NEAA	non-essential amino acids

NF-68	neurofilament 68
NKX2.5	NK2 transcription factor-related gene, locus 5
OCT3/4	octamer-binding transcription factor 3/4
PAX6	paired box protein 6
PSA-NCAM	polysialylated-neural cell adhesion molecule
qRT-PCR	quantitative real-time polymerase chain reaction
REX1	RNA exonuclease 1
ROCK	Rho-associated protein kinase
RPE	retinal pigmented epithelium
RPMI	Roswell Park Memorial Institute
RT-PCR	reverse transcriptase polymerase chain reaction
RYR2	ryanodine receptor
SCD	sudden cardiac death
SCID	severe combined immunodeficient
SCNT	somatic cell nuclear transfer
SEM	standard error of the mean
SERCA	sarcoplasmic reticulum Ca^{2+}-ATPase
SIRPA	signal regulatory protein alpha
SNL	feeder cells expressing neomycin-resistance and LIF genes
SOX	sex-determining region Y-box
SR	sarcoplasmic reticulum
SSEA	stage-specific embryonic antigen
TALEN	transcription activator-like effector nuclease
TGFβ	transforming growth factor β
Tn	troponin
TPM1	α-tropomyosin
TRA	tumor-related antigen
T tubule	transverse tubule
UPS	ubiquitin proteasome system
UTF-1	undifferentiated embryonic cell transcription factor 1
VCAM1	vascular cell adhesion molecule 1
VEGF	vascular endothelial growth factor
WNT	wingless/INT protein
WT	wildtype

1 Introduction

The derivation of human embryonic stem cells (hESCs) (Thomson et al., 1998) and, more recently, the invention of human induced pluripotent stem cells (hiPSCs) (Takahashi et al., 2007) have opened new opportunities for research and cellular therapies in regenerative medicine. These cells, collectively called human pluripotent stem cells (hPSCs), have the ability to self-renew indefinitely and to differentiate into derivatives of all three germ layers (Takahashi et al., 2007; Thomson et al., 1998). Thus, hPSCs provide a potential source of cells for regenerative medicine applications as well as *in vitro* modeling of genetic diseases and drug screening.

Traditionally, hiPSCs have been reprogrammed from skin fibroblasts by virally transferring four pluripotency factors, specifically octamer-binding transcription factor 3/4 (*OCT3/4*), sex-determining region Y-box 2 (*SOX2*), Kruppel-like factor 4 (*KLF4*), and myelocytomatosis viral oncogene homolog (*C-MYC*), which integrate into the genome of the target cell (Takahashi et al., 2007). More recent methods have aimed to produce hiPSCs using non-integrative viral transfection (Fusaki et al., 2009), integrative vectors that can be excised after reprogramming (Soldner et al., 2009), or non-viral delivery methods, such as the introduction of episomal vectors into target cells using electroporation (Yu et al., 2009).

hPSCs have turned out to be one of the most demanding cell types to grow stably under *in vitro* conditions. Since mouse embryonic fibroblast (MEF) feeder cell layers and fetal bovine serum (FBS)-containing culture medium (Thomson et al., 1998), culture methods have developed toward more defined, serum- and xeno-free conditions. A substantial variety of culture conditions are based on the use of either mouse (Amit et al., 2000; Thomson et al., 1998) or human (Hovatta et al., 2003; Richards et al., 2002) feeder cell layers or extracellular matrix (ECM) proteins (Amit et al., 2004; Ludwig et al., 2006a,b; Rodin et al., 2010; Xu et al., 2001), which provide an adequate attachment matrix for the undifferentiated growth of hPSCs. hPSC culture media are composed of either serum or serum-replacement (Amit et al., 2000; Thomson et al., 1998), and various growth factors (Chen et al., 2011; Ludwig et al., 2006a,b). In more recent methods, expensive ECM proteins have been replaced by synthetic polymer surfaces (Nandivada et al., 2011).

hPSCs can be differentiated into cardiomyocytes under laboratory conditions. Differentiation methods are based on embryoid body (EB) formation (Itskovitz-Eldor et al., 2000), co-culturing hPSCs with mouse endodermal-like cells (END-2) (Mummery et al., 2003) or more direct differentiation on a monolayer using different growth factors and small molecules (Laflamme et al., 2007). However, the efficiency of cardiac differentiation appears to vary when using different cell lines and differentiation methods (Osafune et al., 2008).

Hypertrophic cardiomyopathy (HCM) is one of the most common genetic cardiovascular diseases, with a worldwide prevalence of 1:500. In HCM, the cardiac muscle tissue in the interventricular septum (IVS), which separates the ventricles from each other or in the free wall of the left ventricle is thickened. The most severe symptoms of HCM are progressive heart failure and sudden cardiac death (SCD). (Maron et al., 2014.) HCM is caused by more than 1400 mutations, which reside primarily in genes coding for sarcomeric proteins (Roma-Rodrigues & Fernandes, 2014). The clinical phenotype of the disease is variable, and most of the patients carrying the mutations live their lives without any symptoms (Maron et al., 2014). In Finland, two founder mutations in genes coding for myosin-binding protein C (MYBPC) and α-tropomyosin (TPM1) proteins account for approximately 18% of Finnish HCM cases (Jääskeläinen et al., 2013).

Research of genetic cardiovascular diseases has lacked of good disease models because rodents, which are primarily used, differ greatly from humans. The ability to derive hiPSCs from patients carrying inherited cardiac diseases has revolutionized research in the cardiovascular field. Thus far, hiPSCs have been used to model a variety of cardiac diseases, including channelopathies (Fatima et al., 2011; Kujala et al., 2012a; Lahti et al., 2012; Moretti et al., 2010), which are electrical defects caused by the malfunctioning of certain ion channels or receptors, as well as cardiomyopathies, in which the structure of the heart muscle is affected (Lan et al., 2013; Sun et al., 2012).

The first aim of this thesis was to compare the cardiac differentiation capacities of both hESCs and hiPSCs. These hPSCs were derived in two different laboratories from different cell sources with distinct methods. The second aim was to determine which hPSC culture method would be optimal when considering cardiac differentiation potential after long-term culture. The effects of two feeder cell layer-based methods and one feeder cell-free method on the cardiac differentiation potential of hPSCs were studied. The final aim of this thesis was to develop cell models for HCM with patient-specific hiPSCs by exploiting the knowledge learned from the previous studies.

2 Review of the literature

2.1 Stem cells

Stem cells are defined as cells that have the ability to self-renew as well as to differentiate into other cell types. Stem cells can be categorized into subgroups based on their differentiation potential (Figure 1).

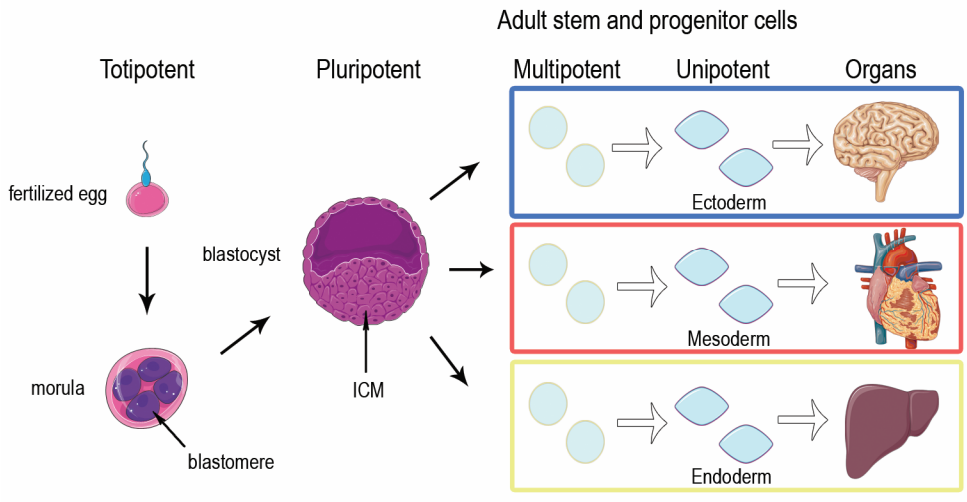

Figure 1. Differentiation potential of stem cells. After fertilization of the egg through the eight-cell stage of the morula, cells are *totipotent* and are able to form an individual. In the blastocyst structure, cells are divided into pluripotent cells in the inner cell mass (ICM) and into trophoblast cells in the outer layer of the blastocyst. The cells in the ICM are *pluripotent* and are able to form all tissues in the human body, while the trophoblast cells form extraembryonic tissues such as the placenta. Later in development, the cells are divided into three germ layers, ectoderm, mesoderm and endoderm, from which different tissues are formed. In adult tissues, cells derived from adult stem and progenitor cells, which have *multipotent* or *unipotent* differentiation potential, continuously replace aging cells. However, it is believed that adult stem cells also have the ability to transdifferentiate into cells of other tissue lineages. (Wobus & Boheler, 2005.) The figure is composed of images from the Servier Medical Art image bank (www.servier.com/Powerpoint-image-bank).

In the beginning of human development, the fertilized egg and the cells from the first divisions are called *totipotent* cells, which have the ability to form a whole individual. This totipotency is retained until the eight-cell stage of the morula. Later in development, the cells are divided into two distinct groups in the structure called a blastocyst. The cells in the inner cell mass (ICM) of the blastocyst are *pluripotent*, and they form the embryo, while the outer trophoblast cells form extraembryonic tissues such as the placenta. Although pluripotent stem cells have the ability to form all tissues in the human body, they have lost the ability to form extraembryonic tissues and are therefore not able to form an individual. In adults, stem cells are needed for tissue regeneration and normal cellular turnover, as most cell types in the human body have a relatively short lifespan. Adult stem and precursor cells, which have either *multipotent* or *unipotent* differentiation potential, are found in almost every tissue in the human body. (Wobus & Boheler, 2005; Wolpert et al., 2007; Yamanaka et al., 2008a.)

2.1.1 Human pluripotent stem cells

Both hESCs and hiPSCs have the unique ability to form cell types of all three germ layers: endoderm, mesoderm and ectoderm (Figure 2). The first hESC line was derived by Thomson and co-workers in 1998 (Thomson et al., 1998). Traditionally, hESCs are derived from the ICM of the blastocyst but early blastomeres or morula stage embryos have also been used (Klimanskaya et al., 2006; Strelchenko et al., 2004). In Finland, hESCs are derived from surplus embryos donated for research by couples undergoing *in vitro* fertilization (IVF) treatments (Skottman, 2010).

For a long time, the scientific community believed that cell differentiation was a one-way route and that there was no turning back when a cell reached a fully differentiated state. In 2006, Yamanaka and co-workers were able to reprogram already fully differentiated mouse cells back into the pluripotent stage via retroviral induction with specific pluripotency factors: *OCT3/4*, *SOX2*, *KLF4* and *C-MYC*. These four transcription factors, so called "Yamanaka factors," were able to force endogenous pluripotency genes to be turned on in the transfected cell, changing the cell back to a pluripotent state (Takahashi & Yamanaka, 2006). In 2007, the team repeated the reprogramming using human fibroblasts, creating hiPSCs (Takahashi et al., 2007). Similar to hESCs, hiPSCs also have the ability to self-renew and give rise to all somatic cell types. Although the discovery of hiPSCs has been a revolutionary invention in the stem cell field, it would not have been possible without earlier

research, including somatic cell nuclear transfer (SCNT) (Briggs & King, 1952; Gurdon, 1962; Wilmut et al., 1997), which suggested that the nuclear status of a differentiated cell could be reverted back to totipotency by factors in the cytoplasm of an oocyte (Yamanaka, 2008b).

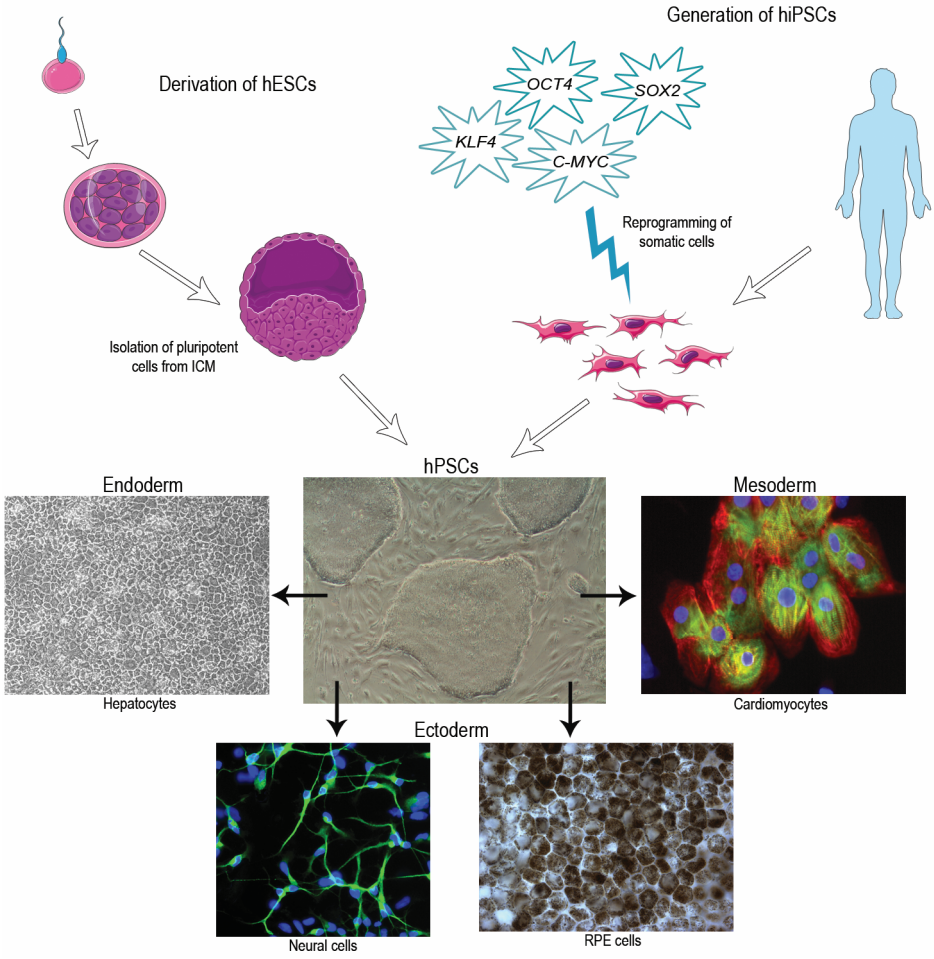

Figure 2. Human pluripotent stem cells (hPSCs). Human embryonic stem cells (hESCs) are derived from the inner cell mass (ICM) of a blastocyst. Somatic cells from a patient or from control individual are reprogrammed into human induced pluripotent stem cells (hiPSCs) by transferring exogenous pluripotency factors into the cells. hESCs and hiPSCs, collectively called hPSCs, have the ability to form all three germ layers. In the laboratory, hPSCs can be cultured for extended periods of time and differentiated into derivatives of different germ layers, such as hepatocytes, neural cells, retinal pigmented epithelial (RPE) cells and cardiomyocytes. The figure is composed of images from the Servier Medical Art image bank (www.servier.com/Powerpoint-image-bank) and cell pictures from BioMediTech.

Because of their unique properties, hPSCs can be maintained in the laboratory for extended periods of time in their undifferentiated state and differentiated into various cell types, including cardiomyocytes (Itskovitz-Eldor et al., 2000), retinal pigmented epithelial (RPE) cells (Vaajasaari et al., 2011), neural cells (Nat et al., 2007) and hepatocytes (Hay et al., 2008) (Figure 2). hPSCs represent a limitless cell source for regenerative medicine applications as well as for studying developmental processes and genetic diseases.

The groundbreaking discovery of hiPSCs has opened completely new opportunities for disease modeling and drug screening also in the cardiac field. Conventionally, cardiac diseases have been modeled using animal models or genetically engineered cell lines. These models often correlate poorly with the results from human studies. In addition, obtaining cardiac tissue directly from patients for research purposes is difficult, and adult human cardiomyocytes also dedifferentiate rapidly under cell culture conditions and lose their characteristic properties. With the hiPSC technique, we are able to derive cells directly from a patient and transfer the same genetic information and mutations into hiPSC-derived cardiomyocytes. Thus, hiPSCs have great potential to revolutionize the research of cardiovascular diseases. (Savla et al., 2014.) Yamanaka received a Nobel Prize and the Millennium Prize in 2012 for his pioneering work in the field of stem cells.

2.1.2 Generation of human induced pluripotent stem cells

In the first conversion of mouse and human fibroblasts into iPSCs, Yamanaka's group used the viral transduction of four transcription factors (*OCT3/4*, *SOX2*, *KLF4* and *C-MYC*) (Takahashi et al., 2007; Takahashi & Yamanaka, 2006). This method involved the integration of viral genes into the host cell genome, which involves a risk of tumorigenicity due to the insertional mutagenesis and uncontrolled gene expression as well as potential reactivation of the virus (Bayart & Cohen-Haguenauer, 2013; Park et al., 2014). To circumvent these problems, a variety of new methods using different non-viral and non-integrative methods have been developed. Technological options for hiPSC transduction are presented in Figure 3.

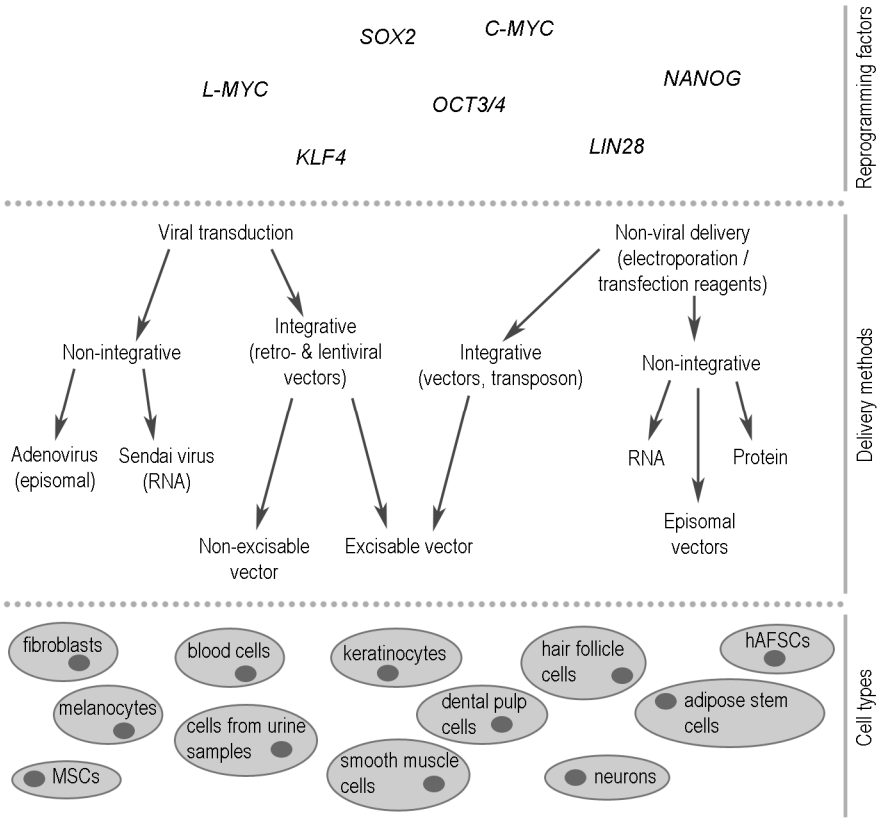

Figure 3. Reprogramming factors, different delivery methods and donor cell types used in hiPSC generation. The data presented in the figure were collected from review articles (Bayart & Cohen-Haguenauer, 2013; Hu, 2014). MSCs, mesenchymal stem cells; hAFSCs, human amniotic fluid stem cells.

Viral transduction can be achieved using either integrating or non-integrating viral vectors. In 2007, two distinct research groups published the first generation of hiPSCs. In the first paper, the delivery was accomplished using retroviral pMXs vectors (Takahashi et al., 2007), while in the second paper the transduction was performed using lentiviruses (Yu et al., 2007). The proteins, which are needed for virus replication and packaging, are deleted from the pMXs vectors. Retroviral vectors are able to target cells according to their envelope pseudotype. These vectors are only able to transduce actively dividing cells. Lentiviruses, in contrast, are also able to transduce non-dividing cells. (Bayart & Cohen-Haguenauer, 2013.) Both retro- and lentivirally transferred genes are expected to be silenced during the reprogramming process through methylation and epigenetic modification (Matsui et al., 2010). Sometimes, however, the process is incomplete, which results in partially

reprogrammed hiPSC lines (Mikkelsen et al., 2008; Sridharan et al., 2009; Takahashi & Yamanaka, 2006).

To overcome the problems related to transgene integration into the genome, excisable vectors have been engineered based on, for example, Cre-recombinase-mediated excision (Soldner et al., 2009). In this method, the sequence of the gene to be integrated into the genome is inserted between two *loxP* sites in the LTR (long terminal repeat) region of the vector. After transfecting the cells, the integrated transgene can be excised from the genome by transfecting the hiPSCs with Cre-recombinase. (Soldner et al., 2009.) When using this method, polycistronic vectors, which express all reprogramming factors in one vector separated by 2A sequences, are favored (Chang et al., 2009; Kaji et al., 2009). Reprogramming factors in distinct vectors are integrated at independent sites, which can lead to genomic instability and genome reorganization when Cre-recombinase is introduced into the cells.

Non-integrative viral methods include the use of Sendai viral and adenoviral vectors. With these two non-integrative viral methods, the Sendai virus has turned out to be more efficient for the generation of hiPSCs. Sendai virus vectors replicate their single-stranded RNA in the cytoplasm without entering the nucleus of the infected cell (Fusaki et al., 2009). In addition, they are able to infect a wide variety of cell species and tissues by attaching to sialic acid receptors, which are present on the surface of various cell types (Fusaki et al., 2009). Adenoviral vectors, in contrast, contain DNA, which is transported to the nucleus of the target cell. However, this adenoviral DNA is not integrated into the genome, and the expression of the adenoviral genes is thus transient. (Stadtfeld et al., 2008; Zhou & Freed, 2009.)

Non-viral methods are based on delivering genes (DNA), RNA copies of the genes or proteins to target cells. Different delivery carriers, such as transposons, and methods, including electroporation and transfection reagents, have been reported (reviewed in Park et al., 2014). The previously mentioned polycistronic vectors can also be transferred into target cells without viral delivery through electroporation (Kaji et al., 2009; Soldner et al., 2009). The *PiggyBac* transposon and transposase system is another integrative non-viral method used in hiPSC generation (Woltjen et al., 2009). In this method, the transposase enzyme cleaves the delivered genes from specific cleavage sites in the *PiggyBac* vector and transfers them into the target genome. The same enzyme can be used to excise exogenous genes from the genome after reprogramming (Woltjen et al., 2009).

For non-integrative non-viral hiPSC production, episomal vectors, messenger RNA (mRNA) molecules or purified protein can be used. Episomal vectors derived from Epstein-Barr virus (oriP/EBNA1) are used in hiPSC production (Okita et al.,

2011; Yu et al., 2009). These vectors can be used to introduce reprogramming factors into cells without a need for viral packaging. The expression of the exogenes is transient and they disappear from the transfected cells during culture (Yu et al., 2009). Lastly, nanoparticles have been used to improve the efficiency of reprogramming, particularly with mRNA molecules and proteins (Khan et al., 2013; Lee et al., 2011).

In most of these methods, the four Yamanaka factors (*OCT3/4*, *SOX2*, *KLF4* and *C-MYC*) are used. Other commonly used factors in reprogramming cocktails, as well as the donor cell types, are presented in Figure 3. Despite the great development of hiPSC induction methods, many research laboratories aiming for basic research are still performing gene delivery via vector systems, as these methods have been demonstrated to be the most effective.

2.1.3 *In vitro* culture of human pluripotent stem cells

The first hESC lines were derived on top of mitotically inactivated MEF feeder cell layers in culture medium containing FBS (Thomson et al., 1998). The first culture methods followed those that had originally been developed for mouse embryonic stem cells (mESCs). However, hESCs soon turned out to be quite different from mESCs; for example, leukemia inhibitory factor (LIF) alone was not able to maintain hESCs undifferentiated, in contrast to mESCs. In the past 10-15 years, much knowledge regarding the key molecular pathways and transcription factors involved in self-renewal and differentiation has been obtained, and this knowledge has been translated for the optimization of hPSC culture conditions. From the use of feeder cells and ECM proteins, hPSC culture is moving toward the use of synthetic components combined with biological motifs and toward fully synthetic culture materials combined with fully defined culture medium. (Villa-Diaz et al., 2013.) The most important culture methods and cornerstones that have changed the direction of hPSC culture development are shown in Table 1.

Initial hPSC culture employed a MEF feeder cell layer and Dulbecco's modified Eagle's medium (DMEM) supplemented with 20% FBS, 1 mM glutamine, 0.1 mM β-mercaptoethanol and 1% non-essential amino acids (NEAA) (Thomson et al., 1998). One important milestone in hPSC culture was the replacement of FBS with knockout serum replacement (ko-SR) and the addition of basic fibroblast growth factor (bFGF) to the medium (Amit et al., 2000). These modifications have enabled the long-term and undifferentiated culture of hPSCs. However, ko-SR still contains

bovine serum albumin (BSA) and is thus not optimal for hPSC culture considering the potential future clinical use of hPSCs (Price et al., 1998). The production of MEF feeder cells is quite laborious, and as is the case for many primary cells, the lifespan is quite short: only 5-6 passages. STO feeder cells, which is an immortalized cell line derived from MEFs, have been used to overcome this problem (Park et al., 2004). The first hiPSCs were derived over SNL feeder cells, which are derived from the STO cell line transfected with neomycin-resistance and murine *Lif* genes (Takahashi et al., 2007).

Table 1. The development of hPSC culture methods.

Feeder cell/substrate	Key media components	Innovation/Achievement	Reference	Company
MEF	FBS	First derivation of hESCs	Thomson et al., 1998	–
MEF	ko-SR, bFGF	Replacement of FBS with ko-SR and the addition of bFGF	Amit et al., 2000	Life Technologies (ko-SR)
Fetal muscle, fetal skin, adult fallopian tube	FBS, HS	First human feeder cell layer	Richards et al., 2002	–
Matrigel™	MEF-CM (ko-SR), bFGF	First publication of feeder cell -free culture	Xu et al., 2001	–
Fibronectin	ko-SR, TGFβ, LIF, bFGF	First feeder- and serum-free culture	Amit et al., 2004	–
Collagen IV, fibronectin, laminin, vitronectin	TeSR1 (TeSR™2)	First defined hPSC culture in feeder and xeno-free conditions	Ludwig et al., 2006a	STEMCELL Technologies
Matrigel™	mTeSR™1	First commercial feeder cell-free method	Ludwig et al., 2006b	STEMCELL Technologies
Laminin-511	TeSR™2	Long-term culture of hPSCs on recombinant laminin surface	Rodin et al., 2010	BioLamina
Vitronectin	E8	Medium that contains only 8 essential components	Chen et al., 2011	Life Technologies
PMEDSAH	StemPro® hESC SFM	Promising fully synthetic polymer surface	Nandivada et al., 2011	Life Technologies

MEF mouse embryonic fibroblast; **FBS** fetal bovine serum; **hESC** human embryonic stem cell; **ko-SR** knockout-serum replacement; **bFGF** basic fibroblast growth factor; **HS** human serum; **MEF-CM** medium conditioned on mouse embryonic fibroblasts; **TGFβ** transforming growth factor β, **LIF** leukemia inhibitory factor; **PMEDSAH** poly[2-(methacryloyloxy)ethyl dimethyl-(3-sulfopropyl)ammonium hydroxide]

Animal-derived feeder cells and culture supplements contain nonhuman animal proteins and represent a potential source of pathogens, which can incorporate into hPSCs during culture (Hisamatsu-Sakamoto et al., 2008; Martin et al., 2005). Thus, many human cells have been tried as feeder cells for hPSCs to overcome the xenogeneic problems related to MEFs. Both adult and fetal fibroblasts have been tested, such as postnatal human foreskin fibroblasts (hFFs) (Hovatta et al., 2003). Lastly, so-called autologous feeders differentiated from hPSCs themselves have also been used (Stojkovic et al., 2005; Xu et al., 2004).

Feeder cell layers provide the appropriate attachment substrate and secrete proteins and growth factors, which are needed for the undifferentiated growth of

hPSCs. However, the secretion profiles of feeder cells derived from different sources vary a great deal. For example MEFs, secrete higher levels of Activin A than human feeder cells while lacking the expression of bFGF, which is produced by human feeder cells (Eiselleova et al., 2008). In addition, the preparation of feeder cells is time-consuming and laborious and the scale-up of hPSC production is difficult when using feeder cell layer-based culture methods. Thus, the research on culture methods has focused on finding well-defined, xeno-free materials and supplements that would allow the large-scale production of hPSCs for drug-screening applications as well as to clinical use. (Celiz et al., 2014.)

The first method for feeder cell-free culture of hPSCs was published in 2001. In this method, Xu and co-workers used Matrigel™ as an attachment matrix and medium conditioned on a MEF feeder cell layer (MEF-CM) (Xu et al., 2001). Matrigel™ is a mixture of various ECM proteins, such as laminin, collagen and fibronectin, as well as growth factors and proteoglycans (Kleinman et al., 1982). It is derived from Engelbreth-Holm-Swarm (EHS) mouse sarcoma cells and is thus prone to batch-to-batch variability. Geltrex® is another basement membrane preparation similar to Matrigel™ but obtained from a different company. From the use of medium conditioned on different feeder cell layers, researchers have moved on to using media with known and defined compositions. The first feeder- and xeno-free medium was published in 2006 (Ludwig et al., 2006a). This medium, called TeSR1 (TeSR™2), is a complex mixture of ingredients including human serum albumin (HSA), vitamins, antioxidants, trace minerals, lipids and growth factors such as high concentrations of bFGF (Ludwig et al., 2006a). In the same year, modified TeSR1 (mTeSR™1) medium was published in which the expensive compounds had been replaced with more affordable animal-sourced components, such as replacing HSA with BSA (Ludwig et al., 2006b). Both media are commercially available from STEMCELL Technologies. In 2011, the same research group published a more simplified medium that contains only the eight most essential components (DMEM/F-12, L-ascorbic acid, selenium, transferrin, $NaHCO_3$, insulin, bFGF and transforming growth factor β (TGFβ)) needed for the undifferentiated growth of hPSCs (Chen et al., 2011).

Undefined animal-derived growth substrates, such as Matrigel™ and Geltrex®, have been replaced by individual ECM proteins, such as fibronectin, laminin or vitronectin, and more recently, fully synthetic substrates. Human recombinant laminins, for example, laminin-511, which is expressed in the ICM of blastocysts, have been discovered to be potential substrates for hPSCs (Rodin et al., 2014, 2010). However, hPSC culture under feeder cell-free and defined conditions is more

demanding for the cells, and hPSCs are more prone to develop karyotypical changes when cultured under these conditions (Celiz et al., 2014). Supplements such as Rho-associated protein kinase (ROCK) inhibitors have been used to reduce the apoptosis observed during the passaging of hPSCs in defined media and substrate compositions (Watanabe et al., 2007).

Despite the broad development of hPSC culture methods in recent years, research laboratories are still widely using either feeder cell layer-based methods or Matrigel™ for the long-term culture of hPSCs. One reason for this is that the usage of ECM proteins and fully defined media is extremely expensive. Thus, it is important to identify not only a defined and xeno-free but also an affordable method that would be easy to scale-up and automatize for the production of the high numbers of hPSCs necessary for regenerative medicine applications.

2.1.4 Characterization of human pluripotent stem cells

According to their definition, hPSCs are undifferentiated cells with the capacity to divide without limit and to differentiate into all somatic cell types. Furthermore, more recently, germ cells have also been derived from hPSCs (reviewed in Hendriks et al., 2015). hPSCs are characterized based on their morphology, the expression of specific pluripotency factors both on the gene and protein levels and their ability to form derivatives from all three germ layers. When considering hiPSCs, artificially transferred exogenous genes must be silenced. It is also important to show that the hPSC karyotype is normal at the beginning of the derivation and that it remains stable during long-term culture.

hPSCs tend to form tightly packed colonies with defined and even borders (Figure 2). Individual cells have a high nucleus-to-cytoplasm ratio and prominent nucleoli (Thomson et al., 1998). hPSCs exhibit high telomerase and alkaline phosphatase activities, and they express surface markers such as the stage-specific embryonic antigens SSEA-3 and SSEA-4 as well as the tumor-related antigens TRA-1-60 and TRA-1-81 (Hoffman & Carpenter, 2005; Thomson et al., 1998). Numerous transcription factors are expressed in hPSCs, including *OCT3/4* (also known as *POU5F1*), *SOX2* and the homeodomain protein Nanog, which form the core network for the maintenance of pluripotency (Boyer et al., 2005). Other characteristic transcription factors include RNA exonuclease 1 (*REX1*), left-right determination factor 1 (*LEFTY-1*) and undifferentiated embryonic cell transcription factor 1 (*UTF-1*) (Hoffman & Carpenter, 2005; Richards et al., 2004; Sato et al., 2003;

Zhao et al., 2012). The expression of surface markers and transcription factors can be studied at the gene expression level using methods based on reverse transcriptase polymerase chain reaction (RT-PCR) or at the protein expression level using immunocytochemical staining or western blotting.

The pluripotency of hPSCs can be studied *in vitro* by EB formation or *in vivo* by teratoma assay. When hPSCs are detached from the feeder cell layer or the culture matrix, they form EB structures in which they spontaneously differentiate into all three germ layers within approximately 4 to 6 weeks (Itskovitz-Eldor et al., 2000). The expression of all three germ layers can be then examined by studying the expression of genes specific for each layer by RT-PCR or by immunocytochemical staining (Itskovitz-Eldor et al., 2000; Pekkanen-Mattila et al., 2010). Another method for proving the pluripotency of hPSCs is to perform an *in vivo* teratoma assay in which the hPSCs are injected into various anatomical sites, including muscles and the testis capsule, of severe combined immunodeficient (SCID) mice. At the injection site, hPSCs form teratoma consisting of all three germ layers. After a certain amount of time, the formed teratoma is removed and can be studied by hematoxylin-eosin staining, immunocytochemistry or RT-PCR (Thomson et al., 1998). Recently, there has been a debate as to whether teratoma assays are still needed to prove pluripotency. From and ethical point of view, the assay may induce pain and suffering in the animals used in the study. In addition, due to the expanding number of hiPSC lines that are being derived, a large number of expensive animals are used. From the experimental point of view, in a teratoma assay, the cells are exposed to a non-physiological environment. In addition, the stem cell community lacks standardized methods for injection, which greatly affects the results of the teratoma assay (Buta et al., 2013). Unfortunately, the reviewers for peer-reviewed journals often demand the teratoma assay as proof of pluripotency.

hPSC lines should have normal diploid karyotypes (46 XX/XY) at the beginning of the cell line derivation, and this should be retained during extended periods of hPSC culture (Hoffman & Carpenter, 2005). Conventionally, the karyotype has been studied using G-banding chromosome analysis (Thomson et al., 1998), but now, easier high-throughput methods, such as the KaryoLite karyotyping assay, are also available (Lund et al., 2012a).

2.2 Heart and cardiomyocytes

2.2.1 Structure of the heart and cardiac cells

The human heart is a four-chambered organ composed of two atria and two ventricles. The chambers are separated from each other by septa, which prevent the mixing of oxygen-rich and oxygen-poor blood. The atria receive blood from the veins, while the ventricles eject the blood into the arteries. The right atrium receives the oxygen-poor blood from the body and ejects it into the right ventricle. The right ventricle pumps the blood to the lungs, and the oxygen-rich blood from the lungs is returned to the left atrium of the heart. From the left atrium, blood moves to the left ventricle, which pumps the blood throughout the body through the aorta. The left ventricle is the thickest chamber of the heart (wall thickness: 6-11 mm), as it pumps the blood to all other parts of the body under high pressure. IVS separates the right and left ventricles from each other. (Tortora & Derrickson, 2011.)

The cardiac muscle tissue, myocardium, is composed of cardiomyocytes, fibroblasts, endothelial cells and smooth muscle cells. Cardiomyocytes can be divided into three subtypes, nodal, atrial and ventricular cardiomyocytes, based on their electrical and mechanical properties. Typically, a ventricular cardiomyocyte is a 100-μm-long cell with a diameter of 10-15 μm. Its structure is branched, and it connects to neighboring cells through intercalated discs. Healthy, mature cardiomyocytes contain one to two nuclei. (Sarantitis et al., 2012; Yang et al., 2014.) The structure of the contractile unit of the cardiomyocyte, the sarcomere, is presented below.

2.2.2 Cardiac action potential

The main function of the heart is to pump the blood through the circulatory system and to deliver oxygenized blood with all necessary nutrients to the tissues and organs as well as to remove the waste products of metabolism. To accomplish this, the heart must contract and relax rhythmically and continuously. This is achieved by the generation of changes in the membrane potential, the so-called cardiac action potential, which includes tightly regulated changes in ion currents. This electrical activity can be measured from the whole human heart by recording an electrocardiogram (ECG, Figure 4A). (George, 2013.)

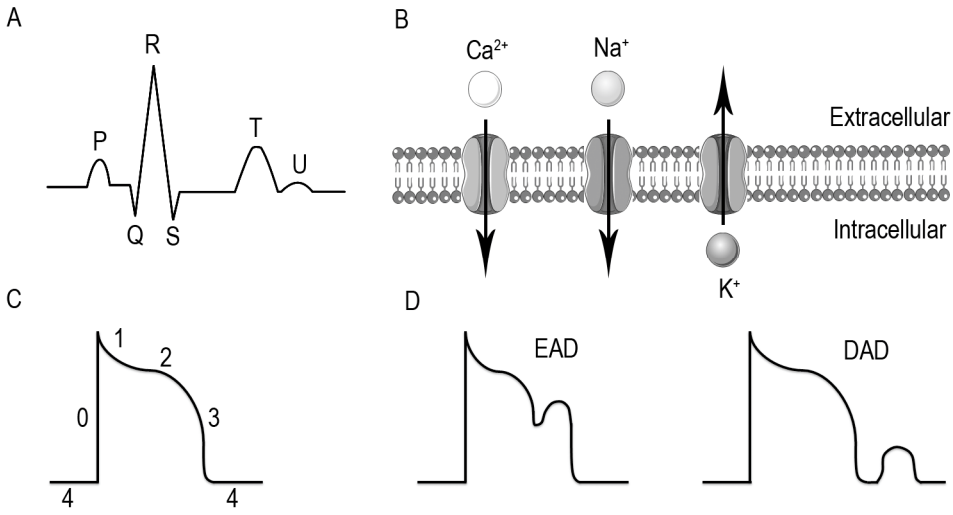

Figure 4. Cardiac action potential. A) Schematic illustration of an electrocardiogram (ECG). The P wave represents the atrial depolarization, while the QRS represents the ventricular depolarization and T wave ventricular repolarization. B) The ionic currents participating in the cardiac action potential. C) The action potential starts when the resting phase (phase 4) is disrupted by rapid depolarization (phase 0), indicating that the voltage across the cell membrane, the so-called membrane potential, shifts from a negative to a more positive charge. Depolarization is attributable to activation of the voltage-gated Na^+ channels, allowing the inward current of Na^+ ions. This is followed by transient repolarization induced by a small outward K^+ current (phase 1) through fast-gating K^+ channels. The long phase 2, or the so-called plateau phase, occurs with the inactivation of Na^+ channels and activation of voltage-gated L-type Ca^{2+} channels, which contribute to membrane depolarization. The final repolarization, when the membrane potential returns back to its resting potential (around -85 mV), occurs with an inward current of K^+ ions (phase 3). D) Early afterdepolarizations (EADs) and delayed afterdepolarizations (DADs), caused by abnormal ionic currents, are the two main mechanisms that trigger arrhythmias. (George, 2013.) The figure is composed of images from the Servier Medical Art image bank (www.servier.com/Powerpoint-image-bank).

The electrical activation of the heart starts from the pacemaker region (sinus node) and propagates from cell to cell via gap junctions through the atria and the ventricles. The waveform of the action potential varies between different cell types in the heart. The main ion channels participating in the generation of the action potential are gateways for Ca^{2+}, Na^+ and K^+ ions (Figure 4B). However, many other ion channels also contribute to the generation and function of cardiac action potentials and are regulated by several factors through complex pathways, such as the β-adrenergic signaling pathway. (George, 2013; Nerbonne & Kass, 2005.) *In vitro*, the electrical activity of a single cardiomyocyte can be measured with the patch-clamp technique (Hamill et al., 1981; Sakmann & Neher, 1984; Zilberter et al., 1982), which gives the

action potential of the cell (Figure 4C), or by microelectrode array (MEA) from a cluster of cardiomyocytes (Kehat et al., 2002; Reppel et al., 2004).

Normally, the heart rate is 60-100 beats per minute (BPM). Arrhythmias occur when the rhythm becomes irregular or the rate is too slow (bradycardias) or too rapid (tachycardias) (Katz, 2001). Arrhythmias can occur due to anatomical conditions or barriers, e.g., scarred myocardium, or ectopic impulses can trigger arrhythmias. At the cellular level, two main mechanisms can trigger arrhythmias and are caused by abnormal depolarizing ionic currents (Figure 4D). Early after depolarization (EAD) appears during the plateau phase (phase 2), and delayed after depolarization (DAD) appears after the completion of the action potential during phase 4. Prolonged action potential duration enhances the risk of EADs, while an increased Ca^{2+} concentration in the sarcoplasmic reticulum increases the risk of DADs. (George, 2013.)

2.2.3 Excitation-contraction coupling

The process by which an electrical signal is transformed into a mechanical contraction is called excitation-contraction coupling. Calcium plays a major role in this process. Transverse tubules (T tubules) are specialized invaginations in the plasma membrane, which contain L-type Ca^{2+} channels. Ca^{2+} influx through these channels during the plateau phase of the action potential (Figure 4C, phase 2) triggers intracellular Ca^{2+} release from the sarcoplasmic reticulum (SR) through the ryanodine receptors (RYR2). This process is called Ca^{2+}-induced Ca^{2+} release (CICR). When intracellular Ca^{2+} levels rise, contraction occurs due to the binding of Ca^{2+} to the Troponin C (TnC) protein that resides in a Tn complex (discussed in more detail below). The relaxation of the cardiomyocyte occurs when the concentration on the intracellular Ca^{2+} is decreased, mainly via the reuptake of Ca^{2+} to the SR by Ca^{2+}-ATPase (SERCA) or by the extrusion of Ca^{2+} to the extracellular space via the Na^{+}/Ca^{2+} exchanger (NCX). (Bers, 2008; George, 2013.) The intracellular Ca^{2+} signaling in cardiomyocytes on a single-cell level can be studied *in vitro* using specific fluorescent probes for Ca^{2+} ions, such as fura-2 (Grynkiewicz et al., 1985).

2.2.4 Sarcomere: the contractile unit of the cardiomyocyte

An adult cardiomyocyte is composed of evenly distributed and organized myofibrils, which are divided into approximately 2.2-μm-long contractile units called sarcomeres. Sarcomeres are composed of thin actin and thick myosin filaments and Z-discs. The thin filaments are attached to Z-discs, which separate the sarcomeres from each other. The thin filament is composed of repeating actin molecules, Tn complexes and TPM1 molecules. Tn complexes consist of TnT, TnI and TnC. The Tn complex works together with TPM1 during cardiac contraction. The thick filament consists of myosin molecules, which are built upon two units of α- and β-myosin heavy chain (α-MHC, β-MHC) and four myosin light chain (MLC) molecules. Among the other proteins of the thick filament, MYBPC plays the most important role in the contraction. It contributes to actin-myosin interactions and cross-bridge formation. (Lopes & Elliott, 2014; Sarantitis et al., 2012.)

When the Ca^{2+} concentration in the cytosol increases, the Ca^{2+} binds to TnC leading to a conformational change in the Tn complex. This leads to TPM1 moving from its inhibitory position, allowing the head region of the MHC to bind to actin, forming a cross-bridge. Then, myosin hydrolyzes adenosine triphosphate (ATP), causing the sliding of actin and myosin filaments and muscle contraction. In addition to the structural proteins mentioned above, the sarcomere consists of many other important proteins, which together form a stabilized and organized structure. (Bers, 2008; Sarantitis et al., 2012; Sequeira et al., 2014).

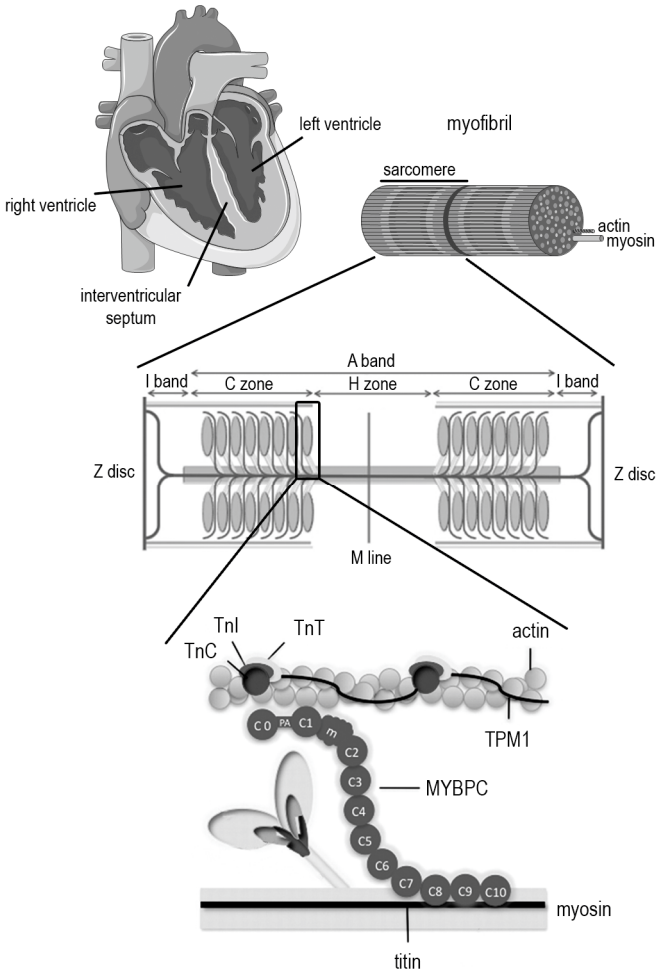

Figure 5. Schematic presentation of the heart and the cardiac sarcomere. Z discs separate the individual sarcomeres from each other. The 2.2-μm long sarcomeres are lined up one after another to form a myofibril. In the A band, thin and thick filaments are overlapping, while the I band consists only of thin filaments, and the H zone consists only of thick filaments. Adjacent thick filaments are connected in the M line. The MYBPC protein is located into the C zone in the cardiac sarcomere. TPM1 is a coiled-coil protein located along the grooves of actin filaments. (Sarantitis et al., 2012.) The figure is composed of images from the Servier Medical Art image bank (www.servier.com/Powerpoint-image-bank) and review articles (Harris et al., 2011; Lopes & Elliott, 2014).

2.2.5 Early development of the heart

The heart is the first functional organ that develops during embryogenesis. It develops from the mesoderm, although signals from adjacent cell populations, especially from the endoderm, have a significant role in cardiogenesis. The entirety of the development of the human heart is not yet fully understood; however, many molecular events and factors taking part in the early stages of cardiomyogenesis have been identified. The three main growth factor families thought to participate in early mesodermal induction and cardiomyogenesis are the bone morphogenetic proteins (BMPs) (subfamily in the TGFβ superfamily), the wingless/INT proteins (WNTs) and the fibroblast growth factors (FGFs). The expression of these factors or their inhibitors in the adjacent endoderm occurs at different times, and their combination eventually leads to the induction of the cardiac mesoderm. After receiving these initial signals, development is directed to more specific and highly conserved cardiogenesis. (Mummery et al., 2012; Rajala et al., 2011; Verma et al., 2013; Xin et al., 2013.)

2.2.6 *In vitro* differentiation of cardiomyocytes

In vitro differentiation methods mimic the phases of heart development, from the mesoderm to the cardiac mesoderm, cardiac progenitors and, finally, cardiomyocytes (Mummery et al., 2012). The current model for the stages of the cardiac differentiation of hPSCs and the most important transcription factors involved in these events are presented in Figure 6.

Current cardiac differentiation methods are based on EB differentiation in suspension, co-culturing the cells with END-2 cells or inducing cardiac differentiation with different growth factors on a monolayer. The first hESC-derived cardiomyocytes were isolated from spontaneously formed EBs (Itskovitz-Eldor et al., 2000; Kehat et al., 2001). In more recent versions of EB differentiation protocols, the aim has been to generate more uniformly-sized EBs, for example, via forced-aggregation using centrifugation (Burridge et al., 2007) or by culturing hPSCs in microwells coated with Matrigel™ prior to EB formation (Mohr et al., 2010). More guided EB differentiation methods using different growth factors have also been developed. Yang and co-workers were able to generate a population of cardiac progenitor cells by inducing EB differentiation with Activin A, BMP4, bFGF, vascular endothelial growth factor (VEGF) and Dickkopf homolog 1 (Dkk-1). After

plating down the EBs, they were able to generate populations with greater than 50% beating cardiomyocytes. (Yang et al., 2008.)

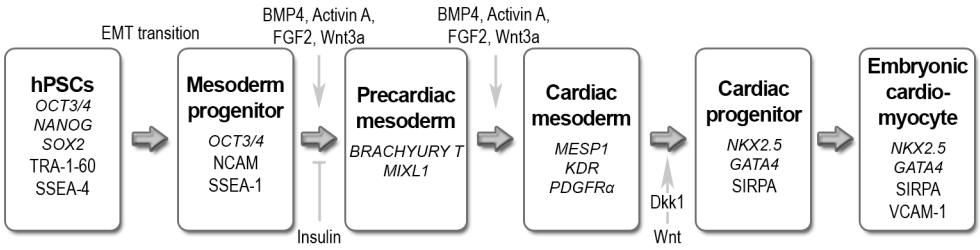

Figure 6. Model of different stages in cardiac differentiation. Transcription factors are presented in cursive and cell surface markers in normal text. The first precardiac mesoderm cells express the T-box factor Brachyury (*BRACHYURY T*) and the homeodomain protein Mixl1 (*MIXL1*). These cells subsequently activate the mesoderm posterior 1 protein (*MESP-1*), and the cardiac mesoderm is formed. NK2 transcription factor-related gene, locus 5 (*NKX2.5*) and GATA-binding protein 4 (*GATA4*) direct the development of embryonic cardiomyocytes. Finally, *NKX2.5*, together with certain other growth factors, activates cardiac structural genes, including actin, myosins and troponins. By activating and inhibiting signaling pathways, hPSCs can be directed toward cardiac differentiation *in vitro*. The removal of insulin enhances cardiac differentiation. Dickkopf homolog 1 (Dkk-1) can be used as a WNT antagonist to inhibit the WNT-pathway. (Mummery et al., 2012). EMT = epithelial to mesenchymal transformation.

In the END-2 differentiation method, the hPSCs are plated on top of mitotically inactivated END-2 cells (Mummery et al., 2003; Passier et al., 2005). END-2 cells are derived from mouse P19 embryonal carcinoma cells, and they provide cell-to-cell contacts and produce factors that induce cardiac differentiation. Thus, medium conditioned on END-2 cells has also been used in cardiac differentiation (Graichen et al., 2008; Xu et al., 2008a).

Monolayer methods begin with the feeder cell-free culture of hPSCs. The advantage of monolayer differentiation methods is that the cells are in uniform monolayers and there are no diffusional barriers, which would prevent the function of growth factors. Thus, differentiation should be easier to control and reproduce, as in EB or in co-culture methods. (Mummery et al., 2012.) In the first monolayer method published in 2007 by Laflamme and co-workers, cells were directed toward cardiac differentiation by a combination of Activin A and BMP4 (Laflamme et al., 2007). One of the more recent methods, the so-called sandwich method, is based on the combination of ECM with growth factor signaling (Zhang et al., 2012). Cells were seeded on Matrigel™, and after reaching 90% confluence, Matrigel™ was added on top of the cells. The sequential application of Activin A, BMP4 and bFGF

on the matrix sandwich resulted in 40-90% pure cardiomyocyte populations (Zhang et al., 2012).

As in the case of hPSC culture development, cardiac differentiation is also moving toward easily scalable, chemically defined and xeno-free conditions. A group of small molecules has been identified to replace the recombinant cytokines and unknown factors in the serum to activate and inhibit the WNT and TGFβ-signaling pathways. Two recent publications are based on the sequential activation and inhibition of the WNT signaling pathway. At first, the formation of the mesoderm is induced using small molecules, such as CHIR99021 and BIO for WNT signaling activation (Lian et al., 2012; Minami et al., 2012). After that, more specific cardiac differentiation is induced by inhibiting the WNT signaling pathway using small molecules, such as KY02111 and IWP2 (Lian et al., 2012; Minami et al., 2012).

In 2014, Burridge and co-workers published a chemically defined cardiac differentiation method (Burridge et al., 2014). The medium consisted of Roswell Park Memorial Institute (RPMI) basal medium supplemented with HSA and L-ascorbic acid. Cardiac differentiation was further induced by the sequential activation and inhibition of WNT signaling by CHIR99021 and WNT-C59, respectively. They also tested various defined matrices (E-cadherin, vitronectin, vitronectin peptide, laminin-521, laminin-511, fibronectin and fibronectin peptide) in combination with differentiation medium. Laminins were the most promising, but because they are extremely expensive for large-scale applications, vitronectin was selected for further studies. The final protocol resulted in 80-90% pure cardiomyocyte populations for the multiple hPSC lines tested (Burridge et al., 2014).

2.2.7 Selection and characterization of human pluripotent stem cell-derived cardiomyocytes

Although the differentiation methods for hPSC-derived cardiomyocytes have developed greatly, the efficiency of differentiation varies to a large degree when using different methods and cell lines and none of the methods result in a homogenous population of cardiomyocytes (Burridge et al., 2014; Mummery et al., 2012; Osafune et al., 2008). Homogenous cell populations would be needed, for example, to obtain reliable results from drug-screening assays (Mummery et al., 2012). Thus, there is a need for purification of the cardiomyocyte population.

Manual dissection (Mummery et al., 2003) and Percoll gradient separation (Xu et al., 2002) were the first published methods for cardiomyocyte purification. However,

the yield of pure cardiomyocytes with these methods was quite low. There are a few cell surfer markers that can be used for fluorescence activated cell sorting (FACS)-based purification methods for cardiomyocytes. These markers include signal regulatory protein alpha (SIRPA), which is expressed both in cardiac progenitor cells and in hPSC-derived cardiomyocytes (Dubois et al., 2011), and vascular cell adhesion molecule 1 (VCAM1), which functions in leukocyte-endothelial cell adhesion but is also expressed in hPSC-derived cardiomyocytes (Uosaki et al., 2011). However, the most efficient purification methods are based on genetic selection. In these methods, the hPSCs are genetically modified by adding a fluorescent reporter (Kolossov et al., 2005) or an antibiotic resistance selection gene (Xu et al., 2008b) downstream of a cardiac-specific promoter. After differentiation, the resulting cardiomyocytes can be purified based on fluorescence or by adding a specific antibiotic.

hPSC-derived cardiomyocytes can be characterized by their functional, structural and biochemical features. The most apparent characteristic of hPSC-derived cardiomyocytes is their ability to contract spontaneously in culture (Kehat et al., 2001; Mummery et al., 2003). Their functional characteristics can be further defined by studying the electrical properties of hPSC-derived cardiomyocytes on a cell cluster level using the MEA-platform approach or on the single-cell level using the patch clamp-method. The expression of cardiac genes can be studied by RT-PCR and of proteins by immunocytochemistry and western blotting. By immunolabeling the sarcomeric proteins the organization of the internal structures can be studied. The ultrastructural features of hPSC-derived cardiomyocytes can be studied in more detail using electron microscopy (EM). (Mummery et al., 2012.) However, the cardiomyocytes obtained from hPSCs still resemble more immature fetal cardiomyocytes than mature adult cardiomyocytes (Yang et al., 2014).

2.3 Hypertrophic cardiomyopathy

Cardiomyopathies are diseases that affect the heart muscle and can lead to progressive heart failure and cardiovascular death. Cardiomyopathies can either be genetic or acquired, and they can be divided into groups based on their morphological and functional characteristics. Cardiomyopathies include, among others, HCM, dilated cardiomyopathy (DCM) and arrhythmogenic cardiomyopathy (ARVC). (Elliott et al., 2008.) HCM is one of the most common genetic cardiac diseases, with a worldwide prevalence of 1:500, and is the most common cause of SCD among young competing athletes. HCM is inherited in an autosomal dominant

pattern, and the mutations are mainly located in the sarcomeric proteins, which, as discussed above, are responsible for the contraction and relaxation of the cardiomyocyte. The clinical manifestation of the disease is extremely variable: it has age-related penetrance, and the clinical symptoms can vary within the same family having the same gene mutation. Together, these facts indicate that there might be other factors in addition to the actual gene mutation, for example, epigenetic and environmental factors, that determine the clinical outcomes of the disease. Although a large number of mutations have now been identified and related to HCM, the pathophysiological mechanisms of the disease are still largely unknown. (Maron et al., 2014.)

2.3.1 Disease and mutations

In HCM the cardiac muscle is thickened (≥ 15 mm) in the free wall of the left ventricle or most commonly in the IVS separating the right and left ventricles. This thickening, i.e., hypertrophy, can lead to outflow tract obstruction, which indicates that the passage to the aorta from the left ventricle becomes narrow, disturbing the blood flow. This narrowed outflow leads to progressive heart failure. Other severe complications related to HCM include arrhythmias and SCD. However, most individuals remain asymptomatic for their whole lives, and it has been estimated that the actual prevalence of the disease might even be 1:200 in the general population. (Maron et al., 2014.) Penetrance indicates the percentage of mutation carriers who experience the phenotype of the disease. In HCM, the penetrance is highly variable: it can be age-related or even incomplete and related to gender. (Ho et al., 2015.)

There is no specific cure for this disease, but all the complications related to HCM can be treated individually. Patients are typically asymptomatic for a long time. Often the first sign is diastolic heart failure, while systolic heart failure can develop later. Treatments include beta-blockers and Ca^{2+}-channel blockers for relieving symptoms such as chest pain and shortness of breath and implantable cardioverter defibrillators (ICDs) for those patients who survive cardiac arrest. The actual hypertrophy can be treated by surgical myectomy, which indicates removing a small portion of the thickened cardiac tissue; via ethanol ablation, in which a myocardial infarction is induced in the septal area; or at the end-stage via heart transplantation. (Maron et al., 2014.) One of the issues that clinicians face with HCM is how to treat patients who carry the mutation leading to HCM but do not have clinical symptoms. Another problematic group is young competing athletes who might have a risk of SCD during

exercise. Histologically, HCM is characterized by myocyte hypertrophy (diameter > 40 μm); disorganization of myocyte bundles, individual myocytes and sarcomeres; and fibrosis of heart tissue. Nuclei are hyperchromatic (contain an abundance of chromatin), pleomorphic (vary in size and shape) and often enlarged. (Kocovski & Fernandes, 2015.)

The primary cause of HCM is a mutation in a sarcomeric gene, while changes in Ca^{2+} handling properties, energy deficiency, ion channel remodeling and microvascular dysfunction are thought to be the earliest pathophysiological mechanisms that play a role in disease progression. Novel HCM treatment strategies aim to prevent disease progression before irreversible changes in heart function occur by targeting either the gene mutation itself, sarcomeric proteins or the early mechanisms of the disease. (Tardiff et al., 2015.)

HCM is inherited in an autosomal dominant pattern and is caused by over 1400 mutations found in eleven or more genes coding primarily for sarcomeric proteins. Approximately 70% of patients have a gene mutation either in the MYH7 or MYBPC3 genes while mutations in other genes are far less common. (Maron et al., 2014; Roma-Rodrigues & Fernandes, 2014.) More rare mutations are located in Z-disc genes or calcium handling and regulation genes. Some of the most prevalent sarcomeric genes associated with HCM are presented in Table 2.

Table 2. Locations and frequencies of the most prevalent gene HCM mutations (Ho et al., 2015).

Protein	Location or function in the cell	Gene	Frequency
β-myosin heavy chain	sarcomere (thick filament)	*MYH7*	20-30%
cardiac myosin-binding protein C	sarcomere (thick filament)	*MYBPC3*	30-40%
regulatory myosin light chain	sarcomere (thick filament)	*MYL2*	2-4%
essential myosin light chain	sarcomere (thick filament)	*MYL3*	1-2%
α-myosin heavy chain	sarcomere (thick filament)	*MYH6*	rare
cardiac troponin T	sarcomere (thin filament)	*TNNT2*	10%
cardiac troponin I	sarcomere (thin filament)	*TNNI3*	7%
α-tropomyosin	sarcomere (thin filament)	*TPM1*	<1%
α-cardiac actin	sarcomere (thin filament)	*ACTC1*	<1%
α-actinin 2	sarcomere (Z-disc)	*ACTN2*	<1%
phospholamban	Ca^{2+} handling gene	*PLN*	rare
calsequestrin	Ca^{2+} handling gene	*CASQ2*	rare

One interesting feature of HCM mutations is that they are almost all identified only in one or a few families (Ho et al., 2015). Normally, a patient carries one

heterozygous mutation in a single allele. However, lately, double or even greater numbers of mutations have been reported to be found in one patient, which might affect the clinical variance related to the disease. (Ho et al., 2015; Maron et al., 2012.) Most pathogenic mutations are missense mutations in which a single nucleotide is changed, resulting in an amino acid substitution. Missense mutations are thought to act in a dominant negative manner. Thus, the mutated protein is produced and interferes with the normal function of the sarcomere. Nonsense mutations, in contrast, lead to a premature stop codon and truncated proteins. These mutations are thought to result in haploinsufficiency, in which the mutated protein is either degraded or not produced at all. The majority of the gene mutations in MYBPC3 are thought to act through this mechanism. (Ho et al., 2015; Lopes & Elliott, 2014.)

2.3.2 Finnish founder mutations for hypertrophic cardiomyopathy

Due to the historical isolation of Finland, the Finnish population descends primarily from a small number of ancestors, and the genetic background for many inherited diseases is very small. Three mutations have been found to account for approximately 24% of Finnish HCM cases: MYBPC (*MYBPC3-Gln1061X*, 11.4%), TPM1 (*TPM1-Asp175Asn*, 6.5%), and β-MHC (*MYH7-Arg1053Gln*, 5.6%) (Jääskeläinen et al., 2014, 2013). A gene mutation in *MYH*7 was found in 2014, but the founder effect of the gene mutation has not been confirmed (Jääskeläinen et al., 2014).

MYBPC3-Gln1061X and *TPM1-Asp175Asn* founder mutations, which are studied in this thesis, are relatively uncommon in other countries besides Finland (Jääskeläinen et al., 2013). *MYBPC3-Gln1061X* is a nonsense mutation leading to a premature stop-codon and a truncated MYBPC protein lacking the binding sites for both myosin and titin (Jääskeläinen et al., 2002). This mutation, similar to other mutations in *MYBPC3*, is characterized by age-related penetrance and late onset of the disease (Jääskeläinen et al., 2002; Maron et al., 2001; Niimura et al., 1998). *TPM1-Asp175Asn* is a missense mutation that leads to the substitution of aspartic acid with asparagine in codon 175 (Thierfelder et al., 1994). Originally, *MYBPC3-Gln1061X* was associated with a clinically mild phenotype, and *TPM1-Asp175Asn* was associated with a clinically intermediate phenotype with a substantial risk for SCD. Additionally, patients with *MYBPC3-Gln1061X* were suggested to be more prone to cardiac dilation and heart failure. (Jääskeläinen et al., 2004.) However, in the most recent studies, all three mutations were associated with variable left ventricular

hypertrophy, and no clear genotype-phenotype correlations could be verified in clinical studies (Jääskeläinen et al., 2014, 2013).

2.3.3 Modeling hypertrophic cardiomyopathy *in vitro*

Different animal models have been used to study HCM *in vitro*. These animals include cats, which have certain naturally occurring HCM mutations, and genetically engineered mice, rats, rabbits and Drosophila. (Reviewd in Duncker et al., 2015.) Additionally, HCM patient tissues obtained from myectomy samples have been studied (Marston et al., 2009). *In vitro* models for studying mutations in genes coding for the TPM1 and MYBPC proteins, more specifically *MYBPC3-Gln1061X* and *TPM1-Asp175Asn* mutations, are presented below.

The MYBPC protein is 1274 amino acids long and 140.7 kDa in size. MYBPC is incorporated into thick filament at its C-terminus through interactions with myosin and titin. The N-terminal portion, in contrast, is thought to function in a regulatory role for contraction, affecting cross-bridge cycling kinetics. The exact mechanism by which MYBPC acts and binds to myosin and actin filaments is not yet fully known. (Sequeira et al., 2014.) The *MYBPC3-Gln1061X* mutation is located in domain C8 (Figure 5). This mutation leads to a premature stop codon and thus a truncated protein lacking both myosin and titin binding sites (Harris et al., 2011).

Given that the *MYBPC3-Gln1061X* mutation is very rare worldwide, no functional studies with this particular mutation have been conducted. However, similar nonsense mutations, leading to truncated MYBPC lacking both the myosin and the titin binding sites, have been studied both in mouse models and in human cardiac samples. The first transgenic mouse models showed that the protein is translated but not correctly localized to the sarcomere. In addition, isolated fibers exhibited reduced power output and increased Ca^{2+} sensitivity, which indicates that less Ca^{2+} is needed for thin filament activation, and conversely, more Ca^{2+} must be released before relaxation occurs. (Van Dijk et al., 2012; Yang et al., 1998.) However, in later studies with a transgenic mouse model lacking only the myosin binding site, only a low amount of truncated protein was found (Yang et al., 1999). In human cardiac samples, the mechanical properties of the fibers were similar to those of mouse fibers; however, truncated forms of the MYBPC protein were not detected (Marston et al., 2009; Rottbauer et al., 1997; Van Dijk et al., 2009). Thus, it was believed that the truncated protein is misfolded and degraded via the ubiquitin proteasome system (UPS) (Van Dijk et al., 2012). This haploinsufficiency is thought

to be unique for the truncating MYBPC mutations, while other HCM mutations probably act as poison polypeptides, interfering with the normal function of the sarcomere. Lower force-generating capacity and higher Ca^{2+}-sensitivity, however, are believed to be common features of HCM, despite mutation (Van Dijk et al., 2012).

TPM1 is a coiled-coil dimer that lies along the actin filament and participates in the regulation of cardiac contraction as discussed above. TPM1 and the Tn complex together form the principal mechanism by which contractility is regulated in response to the Ca^{2+} concentration. The *TPM1-Asp175Asn* mutation is more common than the *MYBPC3-Gln1061X* mutation and was one of the first HCM-causing mutations found in the *TPM1* gene (Thierfelder et al., 1994). Thus, it has been studied more than the *MYBPC3-Gln1061X* mutation, including in transfected cardiomyocytes, animal models, single fibers extracted from patient tissues or fibers composed of recombinant proteins (Reviewed in Redwood & Robinson, 2013). The *TPM1* gene is also expressed in skeletal muscle, which represents a more easily obtained source of patient tissue. The expression of mutated and wildtype genes was found to be equivalent in the skeletal muscles of two patients carrying the *TPM1-Asp175Asn* mutation (Bottinelli et al., 1998). This mutation resides in the region that contains TnT interaction sites (Jagatheesan et al., 2004) and is thought to act via a dominant negative, poison polypeptide mechanism. Additionally, the *TPM1-Asp175Asn* mutation has been linked to increased thin filament Ca^{2+}-sensitivity. A recombinant protein was used in this experiment (Bing et al., 2000). The results from animal models have been controversial, and the *TPM1-Asp175Asn* mutation has behaved differently in different species. For example, in *TPM1-Asp175Asn* rat cardiac fibers, the Ca^{2+} sensitivity was decreased (Wernicke et al., 2004), while in a mouse model, increased Ca^{2+} sensitivity was observed at a fiber level; furthermore, on a tissue level, this mutation led to a moderate phenotype with mild ventricular myocyte disorganization and hypertrophy (Muthuchamy et al., 1999). Human skeletal muscle fibers with the *TPM1-Asp175Asn* mutation, in contrast, demonstrate the increased Ca^{2+} sensitivity (Bottinelli et al., 1998).

One of the major difficulties in studying the pathophysiological mechanisms of HCM has been the lack of tissue samples at early stages of disease development. While animal models have provided valuable insight into disease mechanisms, they contain only the mutated gene and not the rest of the genome, which might have effects on disease phenotype and progression. Thus, given that they contain the whole genomes of HCM patients, in addition to the fact that they are cell of human origin, hiPSC-derived cardiomyocytes represent a valuable new tool for modeling HCM *in vitro*.

3 Aims of the study

The main aims of the present thesis were as follows:

- **I** To compare the cardiac differentiation potential of hESC and hiPSC lines.
- **II** To determine the optimal culture method for hPSCs, evaluated according to their cardiac differentiation potential after long-term culture.
- **III** To develop cell models for HCM from patient-specific hiPSCs.

The specific aims of the substudies were as follows:

The aim of the first study (I) was to compare the differentiation potential of hESC and hiPSC lines derived in two separate laboratories using different methods and cell sources. hPSCs were differentiated toward endodermal hepatocyte-like cells, beating cardiomyocytes (mesoderm), pigmented mature RPE cells (ectoderm) and active neuronal networks forming neurons (ectoderm). Each differentiation protocol was performed by researchers dedicated to that differentiation and this thesis focuses on the cardiac differentiation.

The aim in the second study (II) was to optimize a cell culture method for the undifferentiated hPSCs, evaluated according to their cardiac differentiation potential. Feeder cell based methods were compared to one feeder cell -free culture method. The efficiency of cardiac differentiation for each culture method was evaluated at various timepoints during differentiation.

The aim of the third study (III) was to develop cell models for HCM using patient-specific hiPSCs. The aim was to examine and compare both the electrophysiological aandmorphological characteristics of patient-specific hiPSC-derived cardiomyocytes with two different HCM mutations (*MYBPC3-Gln1061* and *TPM1-Asp175Asn*) that are predominant in Finland.

4 Materials and methods

4.1 Ethical considerations

BioMediTech (formerly Regea) has approval from the National Authority for Medicolegal Affairs, Finland to conduct research with human embryos (1426/32/300/05), and permissions from Ethics Committee of Pirkanmaa Hospital District to establish, culture and differentiate both hESC (R05116) and hiPSC (R08070) lines. Skin biopsies for hiPSC establishment in study III were received from the Heart Hospital, Tampere University Hospital and patients donating the biopsies signed an informed consent form after receiving both an oral and written description of the study. FES29, FiPS5-7 and A116 hPSC lines were generated at the University of Helsinki with the permission of the Ethics Committee of the University of Helsinki.

4.2 Human pluripotent stem cell lines (I-III)

All hPSC lines used in Studies I-III and their details are listed in Table 3.

Table 3. hPSC lines used in this thesis.

Cell line	Origin	Induction method	Original culture method	Publication
H7	embryo	–	MEF	I, II, III
UTA.00112.hFF	foreskin fibroblast	retrovirus	MEF	I, II
UTA.04602.WT	adult skin fibroblast	retrovirus	MEF	II
UTA.00525.LQT2	adult skin fibroblast	retrovirus	MEF	II
UTA.00106.hFF	foreskin fibroblast	retrovirus	MEF	II
FES29	embryo	–	MEF	I
Regea 08/023	embryo	–	hFF	I
FiPS5-7	foreskin fibroblast	retrovirus	MEF	I
A116	adult skin fibroblast	retrovirus	MEF	I
UTA.01006.WT	adult skin fibroblast	retrovirus	MEF	I
UTA.04511.WT	adult skin fibroblast	Sendai virus	MEF	III
UTA.07801.HCMM	adult skin fibroblast	retrovirus (Cre-LoxP)	MEF	III
UTA.06108.HCMM	adult skin fibroblast	retrovirus (Cre-LoxP)	MEF	III
UTA.13602.HCMT	adult skin fibroblast	Sendai virus	MEF	III
UTA.02912.HCMT	adult skin fibroblast	Sendai virus	MEF	III

MEF mouse embryonic fibroblast; **hFF** human foreskin fibroblast; **WT** wildtype; **LQT2** long QT syndrome type 2; **HCMM** hypertrophic cardiomyopathy with *MYBPC3-Gln1061X* mutation; **HCMT** hypertrophic cardiomyopathy with *TPM1-Asp175Asn* mutation

4.3 Experimental design

4.3.1 Evaluating the efficiency of cardiac differentiation (I, II)

The cardiac differentiation potentials of four hiPSC lines and three hESC lines were evaluated in Study I. Each hPSC line was differentiated into cardiomyocytes 4-5 times in separate differentiation experiments. The effects of the culture method on the differentiation potential of one hESC line and four hiPSC lines were evaluated in Study II. Each hPSC line cultured with each culture method was differentiated into cardiomyocytes 2-6 times in separate differentiation experiments. The experimental design for the characterization and evaluation of cardiac differentiation in END-2 co-cultures was similar in both studies (Figure 7). Briefly, cardiac differentiation in END-2 co-cultures was characterized by studying the gene expression of pluripotency genes and genes from different germ layers by quantitative real-time PCR (qRT-PCR). Differentiation efficiency was evaluated by quantitative immunocytochemical analysis of TnT-positive cells in cytospin samples on day 20 and by counting the number of beating areas at the end of differentiation. The experimental design is presented in Figure 7, and more detailed methods can be found in the original publications.

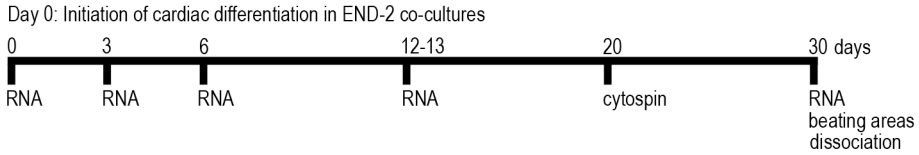

Figure 7. Schematic presentation of the experimental design for characterizing and evaluating the efficiency of cardiac differentiation.

4.3.2 Developing cell models for hypertrophic cardiomyopathy (III)

hiPSCs were derived from two patients carrying *TPM1-Aps175Asn* and from two patients carrying the *MYBPC3-Gln1061X* mutation. hiPSCs derived from HCM patients and control individuals were differentiated into cardiomyocytes via the END-2 co-culture method. Morphological (cell size) and biochemical (gene and protein expression), as well as functional (Ca^{2+} imaging, patch clamp), properties of the hiPSC-derived cardiomyocytes were studied, and the differences between *TPM1-*

Asp175Asn, *MYBPC3-Gln1061X* and control cells were evaluated. To study the effects of culture time on the properties of the cells, hiPSC-derived cardiomyocytes were dissociated and cultured for 1, 3 and 6 weeks as single cells or small clusters before analyzing the sizes of the cardiomyocytes.

4.3.3 Detailed experimental procedures

The methods used in this thesis are shown in Table 4. More details regarding the experimental procedures can be found in the original publications and their electronic supplements online.

Table 4. Methods used in this thesis and their original publications.

Method	Original publication
In vitro culture of hPSCs	
MEF + conventional hPSC culture medium	I, II, III
SNL + conventional hPSC culture medium	II
Matrigel™ + mTeSR™1	II
Generation of hiPSCs	III
Cardiac differentiation of hPSCs	I, II, III
Characterization of hPSCs	
Karyotype analysis	III
Mutation analysis	III
Study of protein expression	
Immunocytochemical staining	II, III
Flow cytometry	II
Study of gene expression	
RT-PCR	III
qRT-PCR	I, II, III
Pluripotency analysis	
in vitro EB assay	II, III
in vivo teratoma assay	III
Characterization of hPSC-derived cardiomyocytes	
Estimation of differentiation efficiency	I, II
Studying of protein expression	
Immunocytochemical staining	I, II, III
Western blot	III
Study of gene expression	
qRT-PCR	I, II
Fluidigm qRT-PCR	III
Functional analysis	
Ca^{2+} imaging	III
Patch clamp	III
Statistical analysis	I, II, III

hPSC human pluripotent stem cell; **MEF** mouse embryonic fibroblast; **SNL** feeder cells expressing neomycin-resistance and LIF genes; **hiPSC** human induced pluripotent stem cell; **EB** embryoid body

5 Results

5.1 Culture of human pluripotent stem cells (II)

In study II, one hESC line (H7) and four hiPSC lines (UTA.00112.hFF, UTA.04602.WT, UTA.00525.LQT2 and UTA.00106.hFF) were cultured under three different culture conditions, a MEF or SNL feeder cell layer combined with conventional hPSC culture medium and a Matrigel™ attachment matrix combined with mTeSR™1 culture medium, prior to cardiac differentiation in END-2 co-cultures. All tested hPSC lines expressed markers typical of pluripotent hPSCs (Nanog, OCT3/4, SSEA-4) after longterm culture (>14 passages, Figure 8, Study II). In addition, H7, UTA.00106.hFF and UTA.00525.LQT2 cell lines formed EBs expressing markers from all three germ layers (ectodermal paired box protein 6 (*PAX6*) and *SOX1*, endodermal α-fetoprotein (*AFP*) and *SOX17*, mesodermal α-cardiac actin (*ACTC1*) and kinase insert domain receptor (*KDR*)) (Study II).

However, the hPSCs cultured in mTeSR™1 medium on the Matrigel™ attachment matrix had the propensity to form neural cells in culture. These cells were further analyzed by immunocytochemical staining for microtubule-associated protein 2 (MAP-2). The amount of MAP-2-expressing cells was more abundant in the culture with the Matrigel™ attachment matrix combined with mTeSR™1 medium than on the MEF or SNL feeder cell layer combined with conventional hPSC culture medium (Study II). Variation with this propensity between the different hPSC lines was detected, and adaptation of the H7 and UTA.00112.hFF hiPSC lines from the original MEF feeder cell layer culture to Matrigel™ was hindered because of this phenomenon. Recently, similar problems have been observed when adapting hiPSC lines from a MEF feeder cell layer to a Matrigel™ or Geltrex® attachment matrix in combination with mTeSR™1 medium (unpublished results).

hPSCs cultured under different conditions were further characterized by flow cytometry analysis of the pluripotency marker TRA-1-81 and polysialylated-neural cell adhesion molecule (PSA-NCAM), which is mainly expressed in embryonic and neonatal neural tissue. The amount of TRA-1-81-expressing hPSCs was higher in MEF feeder cell layer cultures (86.53% ± 2.23%, n = 16) than in SNL feeder cell

layer cultures (60.53% ± 3.53%, n = 20) or on Matrigel™ (59.54% ± 3.09%, n = 15) (Study II). Furthermore, the amount of PSA-NCAM-expressing hPSCs was higher on Matrigel™ (11.61% ± 3.67, n = 15) and SNL feeder cell layer cultures (10.95% ± 1.67, n = 20) than on MEF feeder cell layer cultures (2.51% ± 0.36, n = 16) (Study II).

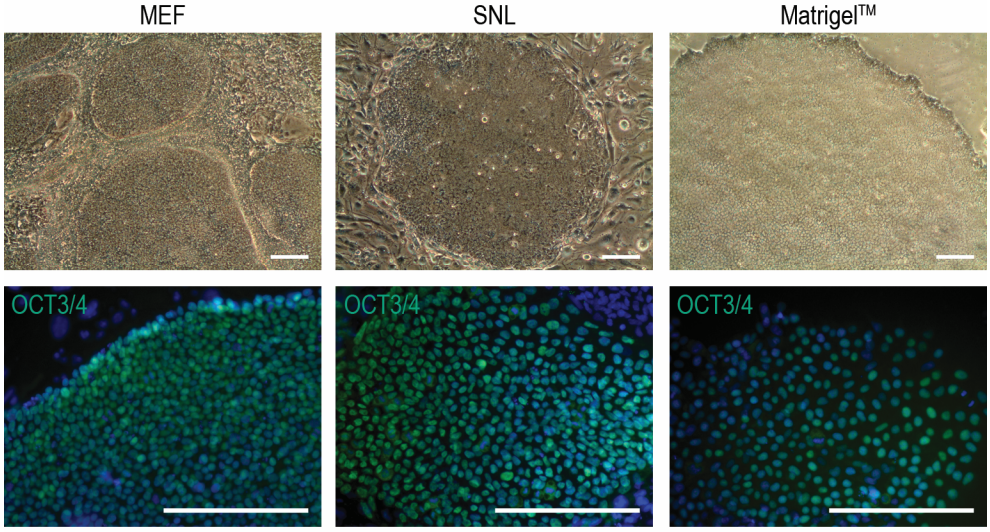

Figure 8. The undifferentiated and pluripotent growth of hPSCs under different culture conditions. Representative images of the UTA.00112.hFF (phase contrast microscope images) and H7 (immunofluorescence images) hPSC lines. Scale bars 200 µm.

5.2 Differentiation potential of human pluripotent stem cells (I and II)

In study I, three hESC lines (H7, FES29 and Regea 08/023) and four hiPSC lines (FiPS5-7, UTA.00112.hFF, A116 and UTA.01006.WT) were differentiated toward endodermal hepatocytes and mesodermal cardiomyocytes as well as ectodermal neural and RPE cells. The differentiation potential toward each lineage was evaluated by researchers dedicated to their respective line of differentiation. The general differentiation potentials of each individual hPSC line toward different lineages are presented in Table 5. The results from the cardiac differentiation in Study I are presented in more detail in Chapter 5.2.2.

Table 5. Differentiation potential of individual hPSC lines toward derivatives from all three germ layers.

hPSC line	Endoderm	Mesoderm	Ectoderm	
	hepatocyte	cardiomyocyte	neuronal	RPE
H7	++	+++	+	+
FES29	++	++	++	++
Regea 08/023	+++	+	+++	+++
FiPS5-7	++	+	++	+
UTA.00112.hFF	+++	++	++	+++
A116	++	++	+++	++
UTA.01006.WT	+	+	+	+

5.2.1 Expression of transgenes in human induced pluripotent stem cell lines (I)

The expression of the transgenes used in the hiPSC induction were studied by qRT-PCR before and at the end of each differentiation (hepatocytes, cardiomyocytes, neural and RPE cells) in Study I. *KLF4* was constantly expressed before differentiation in the UTA.01006.WT hiPSC line, which was inferior in differentiating toward all cell lineages (Table 5). In all other hiPSC lines, transgenes were completely silenced before the initiation of differentiation (Study I). All transgenes were silenced at the end of differentiation toward most of the lineages, including cardiomyocytes. However, the expression of exogenous *OCT3/4* was increased during long-term RPE differentiation of each hiPSC line (Study I).

5.2.2 Cardiac differentiation potential of individual human pluripotent stem cell lines (I)

Three hESC lines (H7, FES29 and Regea 08/023) and four hiPSC lines (FiPS5-7, UTA.00112.hFF, A116 and UTA.01006.WT) were differentiated into cardiomyocytes using the END-2 co-culture method in Study I. All hPSC lines differentiated into cardiomyocytes expressing α-actinin, TnT, connexin-43 and MHC proteins, and their functionality was confirmed by MEA analysis (Study I). The UTA.01006.WT cell line formed cystic structures, while the other hPSC lines formed compact beating areas in END-2 co-culture.

The cardiac differentiation efficiency of individual hPSC lines was evaluated by quantitative immunocytochemical analysis of TnT-positive cells in cytospin samples and by counting the beating areas (Table 6). The efficiency varied between individual

hPSC lines (Table 6) as well as between separate differentiation experiments with the same hPSC line (data not shown). H7 was the most potent cell line, while FiPS5-7 and UTA.01006.WT were the weakest cell lines (Table 6). When grouping the hESC and hiPSC cell lines, the amount of beating areas was significantly higher ($p < 0.005$) for hESCs (approximately 6 beating areas/well, n = 187) than for hiPSCs (approximately 2 beating areas/well, n = 263). The number of TnT-positive cells/well analyzed by cytospin assay was in accordance with the number of beating areas observed for all hPSC lines, except the H7 cell line, which produced beating areas of small size (Table 6).

Table 6. Cardiac differentiation efficiency of individual hPSC lines (Study I).

Cell line	Beating areas/well (n) (n of wells/n of experiments)	TnT^+ cells/well (n) (n of samples/n of experiments)
H7	9.74 ± 0.88 (78/5)	4761 ± 1892 (4/2)
FES29	4.68 ± 0.89 (56/5)	7386 ± 3331 (4/2)
Regea 08/023	1.06 ± 0.25 (53/4)	1531 ± 508 (4/2)
FiPS5-7	0.31 ± 0.11 (54/4)	1818 ± 785 (4/2)
UTA.00112.hFF	3.86 ± 0.51 (66/5)	3453 ± 1711 (4/2)
A116	3.17 ± 0.68 (72/5)	5539 ± 1675 (4/2)
UTA.01006.WT	0.32 ± 0.16 (71/5)	416 ± 251 (4/2)

5.2.3 Cardiac differentiation potential of human pluripotent stem cells cultured under different conditions (II)

In study II, one hESC line and four hiPSC lines cultured under three different culture conditions were differentiated into cardiomyocytes using the END-2 co-culture method. The hPSCs cultured on SNL feeder cell layers formed irregular, cystic structures on top of the END-2 cells, while the hPSCs cultured on MEF feeder cell layers or Matrigel™ formed more uniform structures. Occasionally, MAP-2-expressing neural cells and bundles of nerve fibers were detected in END-2 co-cultures of hPSCs cultured on Matrigel™ prior to differentiation (Study II).

Cardiomyocytes derived from all hPSC lines cultured under all three culture methods expressed α-actinin, TnT, connexin-43 and MHC proteins (Study II). The differentiation efficiency of hPSC lines cultured under different conditions was evaluated by quantitative immunocytochemical analysis of TnT-positive cells in cytospin samples and by counting the beating areas (Table 7). As in study I, considerable variation among the different hPSC lines was observed in Study II. The

H7 cell line produced the highest number of beating areas (9.42) when cultured on MEF feeder cell layers prior to differentiation, and this amount was similar to that in study I (9.74), whereas UTA.00112.hFF behaved differently in study II than in study I, producing 0.35 beating areas/well in study II when cultured on MEF feeder cell layers prior to differentiation and 3.86 beating areas/well in study I.

Table 7. Differentiation efficiency of hPSC lines cultured under different culture conditions. The optimal culture conditions for each cell line are bolded (* represents MEF or SNL vs. Matrigel, $ represents SNL vs. MEF, ** or $$ $p < 0.005$, * $p < 0.05$).

Cell line	Culture method	Beating areas/well (n of wells/n of experiments)	TnT+ cells/well (n of samples/n of experiments)
H7	**MEF**	9.42 ± 1.56 (105/6)**	3503 ± 859 (8/4)
H7	**SNL**	7.46 ± 0.87(67/5)**	3720 ± 835 (8/4)
H7	Matrigel™	1.36 ± 0.23 (89/5)	1913 ± 552 (8/4)
UTA.00525.LQT2	**MEF**	1.31 ± 0.34 (36/3)*	928 ± 313 (2/1)
UTA.00525.LQT2	SNL	0.61 ± 0.30 (18/2)	109 ± 109 (2/1)
UTA.00525.LQT2	Matrigel™	0.23 ± 0.11 (30/2)	111 ± 28 (2/1)
UTA.00106.hFF	MEF	1.13 ± 0.21 (40/3)	3153 ± 1300 (2/1)
UTA.00106.hFF	**SNL**	13.04 ± 2.00 (25/2)**,$$	5348 ± 1832 (2/1)
UTA.00106.hFF	Matrigel™	0.87 ± 0.18 (31/2)	853 ± 80 (2/1)
UTA.00112.hFF	MEF	0.35 ± 0.12 (48/3)	4274 ± 1021 (6/3)
UTA.00112.hFF	SNL	0.55 ± 0.17 (42/3)	2265 ± 725 (6/3)
UTA.00112.hFF	Matrigel™	0.30 ± 0.08 (54/3)	2013 ± 389 (6/3)
UTA.04602.WT	MEF	0.37 ± 0.10 (51/3)*	3010 ± 1003 (6/3)
UTA.04602.WT	SNL	0.70 ± 0.32 (46/3)	1785 ± 603 (6/3)
UTA.04602.WT	**Matrigel™**	1.22 ± 0.32 (45/3)	1722 ± 666 (6/3)

Three cell lines produced the highest numbers of beating areas when cultured on feeder cell layer prior to differentiation: H7 and UTA.0052.LQT2 cell lines when cultured on MEF feeder cell layers and UTA.00106.hFF when cultured on SNL feeder cell layers (Table 7). For the H7 cell line, the number of beating areas was significantly higher on MEF and SNL feeder cell layers compared to Matrigel™ attachment matrix ($p < 0.005$ in both cases, Table 6). The UTA.00525.LQT2 cell line had a significantly higher amount of beating areas when cultured on MEF feeder cell layers than on Matrigel™ ($p < 0.05$, Table 7). For the UTA.00106.hFF cell line, the number of beating areas was significantly higher when cultured on SNL than on MEF feeder cell layers or on Matrigel™ ($p < 0.005$ in both cases, Table 7). The UTA.04602.WT cell line was an exception and produced the highest number of

beating areas when cultured on Matrigel™; this number was significantly higher than when cultured on MEF feeder cell layers ($p < 0.05$, Table 7). The overall differentiation efficiency of the UTA.00112.hFF cell line was poor, and the amount of beating areas was low under all culture conditions (Table 7). When considering all hPSC lines under different conditions, the number of beating areas was significantly higher on MEF ($p < 0.05$) and SNL ($p < 0.05$) feeder cell layers compared to Matrigel™ (Study II). The number of TnT-positive cells for each hPSC line cultured under different conditions was consistent with the amount of beating areas (Table 7).

5.3 Gene expression profiles during END-2 co-culture (I, II)

Cardiac differentiation in END-2 co-cultures was characterized by studying the gene expression of pluripotency markers, as well as markers from different germ layers, on days 0, 3, 6, 12-13 and 30 by qRT-PCR in Studies I and II.

5.3.1 Gene expression profiles in END-2 co-cultures for human embryonic stem cells and human induced pluripotent stem cells (I)

The gene expression profiles of *NANOG*, *OCT3/4*, *BRACHYURY T*, NK2 transcription factor related gene, locus 5 (*NKX2.5*) and *SOX17* in END-2 co-cultures were examined for three hESC (H7, FES29 and Regea 08/023) and four hiPSC (FiPS5-7, UTA.00112.hFF, A116 and UTA.01006.WT) lines in Study I. Samples were collected in two different passages for each hPSC line. The expression of the pluripotency factors *NANOG* (Study I) and *OCT3/4* (Figure 9A) was highest on day 0 and decreased during END-2 co-culture for both hESC and hiPSC lines. The expression of mesodermal *BRACHYURY T* was highest on day 3 in hESC lines and on day 6 in hiPSC lines (Figure 9B), which produced smaller numbers of beating areas/well than the hESC lines (Table 6). Conversely, the expression of endodermal *SOX17* was highest on day 3 for both hPSC types (Study I). On day 6, the expression of *BRACHYURY T* was almost two times higher in hiPSC lines compared to hESC lines ($p < 0.005$, Figure 9B). The expression of mesodermal *NKX2.5* increased evenly during END-2 co-culture in the hESC and hiPSC lines (Study I).

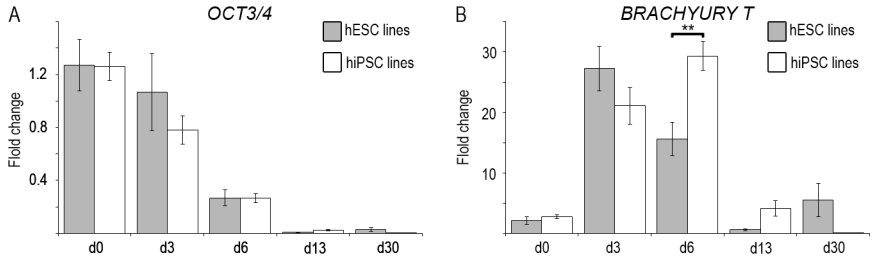

Figure 9. The expression profiles of *OCT3/4* (A) and *BRACHYURY T* (B) during END-2 co-culture for hESC and hiPSC lines. The standard error of the mean (SEM) is presented as error bars. The expression of genes was compared between hESC and hiPSC lines at each timepoint (* $p < 0.005$, n = 18 for all hESC columns, except the d30 timepoint (n = 9); n = 24 for all hiPSC columns, except in d30 timepoint (n =12)).

5.3.2 Gene expression profiles for END-2 co-cultures of human pluripotent stem cells cultured under different conditions (II)

The expression profiles of pluripotency factor *OCT3/4*, endodermal *SOX17*, mesodermal *BRACHYURY T* and *NKX2.5*, as well as ectodermal *PAX6*, *MUSASHI* and Neurofilament 68 (*NF-68*), were studied in END-2 co-cultures with the H7, UTA.00112.hFF and UTA.04602.WT cell lines in Study II. Samples were collected from two different passages for each of the three hPSC lines cultured under all three culture conditions. The expression of *OCT3/4* was 2.5 times higher on Matrigel™ than on MEF ($p < 0.005$) or SNL ($p < 0.05$) feeder cell layer on day 0 (Figure 10A). During differentiation, the expression of *OCT3/4* decreased in all hPSC lines cultured under all three culture methods. However, the expression of *OCT3/4* endured longer on Matrigel™ and was slightly but significantly higher than on MEF ($p < 0.005$) or SNL ($p < 0.05$) feeder cell layers on day 3 and MEF feeder cell layers ($p < 0.05$) on day 6 (Figure 10A).

The peak in *BRACHYURY T* expression was observed on day 3 with END-2 co-cultures originating from MEF and SNL feeder cell layers, while the peak was detected on day 6 on Matrigel™, in which the overall cardiac differentiation potential was lower than on MEF and SNL feeder cell layers (Figure 10B, Table 7). The highest *BRACHYURY T* expression was detected in END-2 co-cultures from MEF feeder cell layers on day 3, and the expression was approximately two times higher than on Matrigel ($p < 0.005$) and 1.5 times higher than on SNL feeder cell layers ($p < 0.005$, Figure 10B). On day 6, the expression of *BRACHYURY T* was approximately 1.3 times higher on Matrigel™ than on MEF or SNL feeder cell layers

($p < 0.05$ in both cases, Figure 10B). The expression of *SOX17* followed the same pattern as the expression of *BRACHYURY T* (Study II). Moreover, the expression of *NKX2.5* varied between different timepoints and culture conditions, being the highest on MEF feeder cell layers on day 30 (Study II).

The expression of *PAX6* increased in END-2 co-cultures originating from all three culture methods. However, on day 3, 6, 12 and 30 the expression was higher on Matrigel™ than on MEF or SNL feeder cell layers (Figure 10C). On day 30, the expression was approximately 6 times higher on Matrigel™ than on MEF or SNL feeder cell layers ($p < 0.005$ in both cases, Figure 10C). The expression of *MUSASHI* remained quite stable during END-2 co-culture under all three culture conditions. However, its expression was higher on Matrigel™ than on MEF and SNL feeder cell layer at all timepoints (Study II). Furthermore, the expression of *NF-68* remained stable in END-2 co-cultures originating from MEF or SNL feeder cell layers, but the expression increased steadily on Matrigel™ (Figure 10D). Finally, on day 30, the expression was over four times higher on Matrigel™ than on MEF or SNL feeder cell layers ($p < 0.005$ in both cases, Figure 10D).

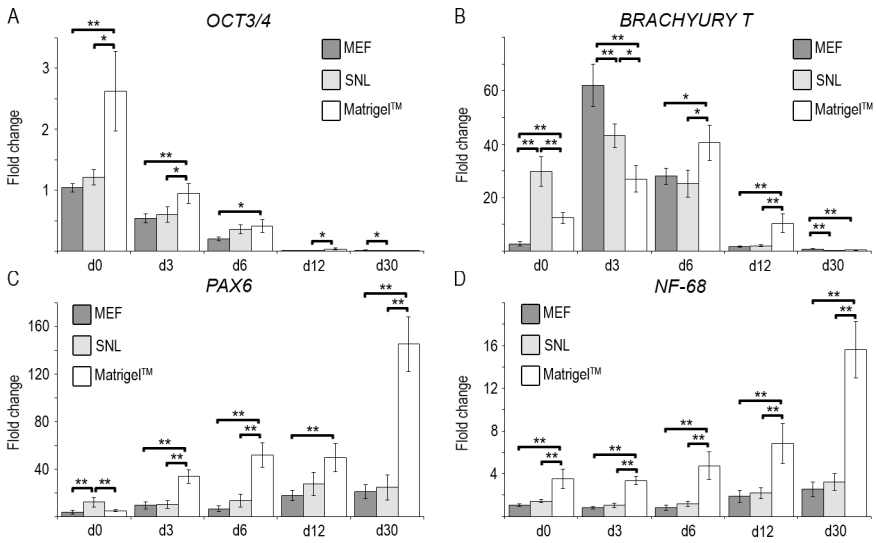

Figure 10. Gene expression profiles of *OCT3/4* (A), *BRACHYURY T* (B), *PAX6* (C) and *NF-68* (D) in END-2 co-cultures for hPSCs cultured under different culture conditions. The SEM is presented as error bars. The expression was compared between hPSCs cultured under different culture conditions at each timepoint (* $p < 0.05$, ** $p < 0.005$, n = 17-18 for *OCT3/4*, n = 17-18 for *BRACHYURY T*, n = 15-18 for *PAX6*, n = 17-18 for *NF-68* in each column).

5.4 Developing cell models for hypertrophic cardiomyopathy (III)

5.4.1 Characteristics of hypertrophic cardiomyopathy patients (III)

hiPSC lines were derived from two healthy volunteers and four individuals carrying the Finnish founder mutations in the *TPM1* or *MYBPC3* gene. Two hiPSC lines from patients carrying the *TPM1-Asp175Asn* mutation and two from patients carrying the *MYBP3-Gln1061X* mutation were analyzed. hiPSC lines, mutations and data on the tissue donors (clinical symptoms and treatments, SCDs in the family) are presented in Table 8. Additionally, two hiPSC lines from healthy control individuals are described in Table 8.

Table 8. hiPSC lines, mutations and details of the individuals from which they are derived.

Cell line	Mutation	Sex	Age	IVS (mm)	Other symptoms	SCDs in family	Treatment
UTA.04602.WT	–	F	56	–	–	–	–
UTA.04511.WT	–	M	34	–	–	–	–
UTA.13602.HCMT	*TPM1-Asp175Asn*	F	48	16	collapsed when 20 years old (normal heart structure)	mother at age of 51	none
UTA.02912.HCMT	*TPM1-Asp175Asn*	M	33	26	asymptomatic	one member at age of 21	β-blocker
UTA.06108.HCMM	*MYBPC3-Gln1061X*	M	55	22	asymptomatic	father at age of 36 uncle at age of 38	none
UTA.07801.HCMM	*MYBPC3-Gln1061X*	M	61	25	atrial fibrillation	none	β-blocker, ICD

IVS interventricular septum; **SCD** sudden cardiac death; **F** female; **M** male; **ICD** implantable cardioverter defibrillator

5.4.2 Human pluripotent stem cells derived from hypertrophic cardiomyopathy patients (III)

All hiPSCs, derived both from healthy control individuals and from HCM patients, formed colonies expressing proteins (Nanog, OCT3/4, SOX2, TRA-1-60 and TRA-1-80) and genes (*NANOG*, *OCT3/4*, *REX1*, *SOX2* and *C-MYC*) typical of hPSCs. The viral exogenous genes used in reprogramming were silenced, and karyotypes were normal. The pluripotency of the hiPSC lines was studied *in vitro* by EB formation and *in vivo* by teratoma assay (Figure 11). The presence of the *TPM1-Asp175Asn* or *MYBP3-Gln1061X* mutation in hiPSCs was studied by custom TaqMan SNP Genotyping Assays (Study III).

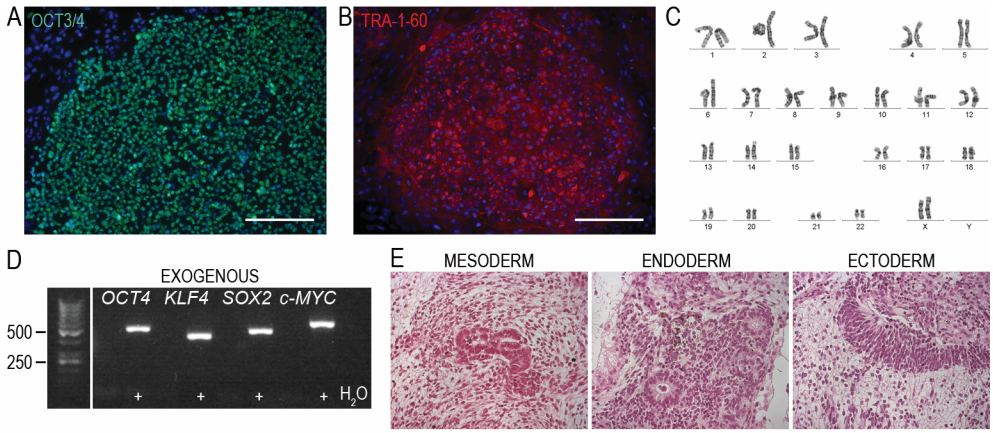

Figure 11. Characterization of hiPSC lines. hiPSC colonies expressed the OCT3/4 (A) and TRA-1-60 (B) proteins, and the karyotypes of tthe hiPSC lines were normal (C). The virally transferred exogenes *OCT3/4* (483 bp), *KLF4* (410 bp), *SOX2* (451 bp) and *C-MYC* (352 bp) were silenced (D), and hiPSCs formed tissue types from all three germ layers *in vivo* (E). Representative images from the UTA.07801.HCMM and UTA.13602.HCMT cell lines. Scale bars 200 µm.

5.4.3 Size of human induced pluripotent stem cell-derived cardiomyocytes (III)

All four HCM hiPSC lines and two hiPSC lines derived from healthy control individuals were differentiated into cardiomyocytes in END-2 co-cultures. The beating aggregates were dissociated into single cells or small clusters and cultured for 1, 3 and 6 weeks. After culturing, differences between the cell sizes of hiPSC-derived control cardiomyocytes and cardiomyocytes carrying the *TPM1-Asp175Asn* or *MYBP3-Gln1061X* mutations were analyzed.

The hiPSC-derived cardiomyocytes carrying the *MYBPC3-Gln1061X* mutation (HCMM) were significantly larger than cardiomyocytes carrying the *TPM1-Asp175Asn* mutation (HCMT) and hiPSC-derived control cardiomyocytes (WT) at all three timepoints (Figure 12A, $p < 0.005$ in all cases). The enlargement of cardiomyocytes carrying the *TPM1-Asp175Asn* mutation (HCMT) was observed after 3 weeks of culture at which point the cardiomyocytes were significantly larger (Figure 12A, $p < 0.005$) than the hiPSC-derived control cardiomyocytes.

The proportion of multinucleated cells was higher in cardiomyocytes carrying either of the two HCM mutations than in control cardiomyocytes. However, the proportion of multinucleated cardiomyocytes was significantly higher in hiPSC-

derived cardiomyocytes with the *TPM1-Asp175Asn* (HCMT) mutation compared to those with the *MYBPC3-Gln1061X* mutation (HCMM) or hiPSC-derived control cardiomyocytes (WT) (Figure 12B).

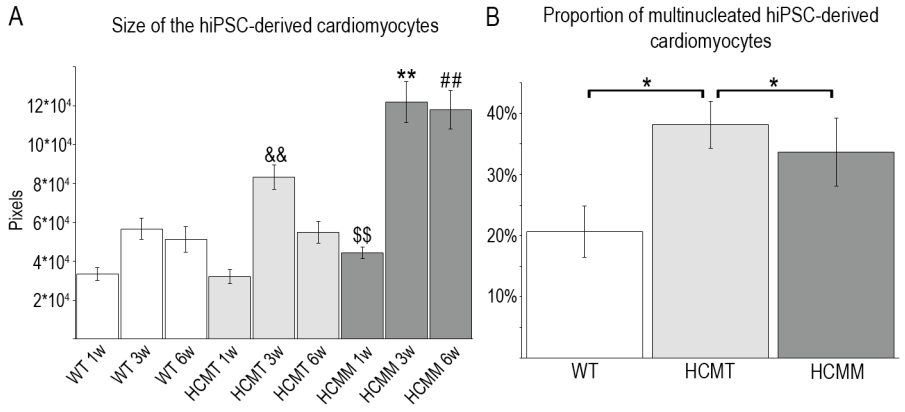

Figure 12. Mutation-specific differences between hiPSC-derived cardiomyocytes. A) Size of hiPSC-derived WT, HCMT and HCMM cardiomyocytes were compared at each timepoint separately (n = 100 in each column, except for HCMT 6w, for which n = 96, $^{\$\$}$ $p < 0.005$ compared to WT and HCMT cells at the 1-week timepoint, ** $p < 0.005$ compared to WT and HCMT cells at the 3-week timepoint, $^{\#\#}$ $p < 0.005$ compared to WT and HCMT cells at the 6-week timepoint, $^{\&\&}$ $p < 0.005$ compared to WT at the 3-week timepoint). B) Proportion of multinucleated cardiomyocytes in the WT, HCMT and HCMM groups (n = 6 in each column, * $p < 0.05$).

5.4.4 Ca^{2+} handling properties of human induced pluripotent stem cell-derived cardiomyocytes (III)

The Ca^{2+} handling properties of hiPSC-derived cardiomyocytes were studied via Ca^{2+} imaging. The percentages for each cell line were determined from hiPSC-derived cardiomyocytes cultured for 1, 3 and 6 weeks. For statistical analysis, the results were grouped as WT, HCMT and HCMM cardiomyocytes. Representative images of normal and abnormal Ca^{2+} transients are presented in Figure 13A. hiPSC-derived cardiomyocytes with the *TPM1-Asp175Asn* (HCMT) mutation had significantly more abnormalities compared to cardiomyocytes with the *MYBPC3-Gln1061X* mutation (HCMM) or hiPSC-derived control cardiomyocytes (WT) (Figure 13B, $p < 0.05$ in both cases).

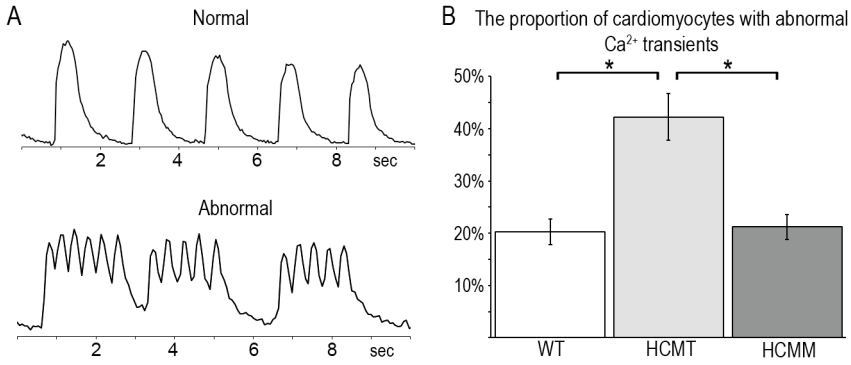

Figure 13. A) Representative images of normal and abnormal Ca^{2+} cycling observed in Ca^{2+} imaging experiments. B) The proportion of hiPSC-derived cardiomyocytes with abnormal Ca^{2+} transients in the WT, HCMT and HCMM groups (n = 6 in each column, * $p < 0.05$).

5.4.5 Electrophysiological properties of human induced pluripotent stem cell -derived cardiomyocytes (III)

The electrophysiological properties of hiPSC-derived cardiomyocytes carrying the *MYBPC3-Gln1061X* (HCMM) or *TPM1-Asp175Asn* (HCMT) mutation were studied in single-cell patch clamp experiments (Study III). Compared to control hiPSC-derived cardiomyocytes (WT), the amounts of cardiomyocytes with arrhythmic events were higher for both mutations (Figure 14A). In addition, the DAD rate was almost six times higher in hiPSC-derived cardiomyocytes carrying the *MYBPC3-Gln1061X* mutation (HCMM) than in control cardiomyocytes (WT) ($p < 0.005$, Figure 14B). Similarly, the DAD rate in hiPSC-derived cardiomyocytes carrying the *TPM1-Asp175Asn* mutation was almost three times higher than in hiPSC-derived control cardiomyocytes (WT), but the difference was not statistically significant (Figure 14B).

The beating rates of HCM hiPSC-derived cardiomyocytes were significantly lower than those of hiPSC-derived control cardiomyocytes ($p < 0.005$ in both cases, Table 8). In addition, the average action potential duration (APD) at 90% repolarization (APD_{90}) was significantly longer in HCM hiPSC-derived cardiomyocytes ($p < 0.005$ in both cases, Table 9). Furthermore, the APD_{90} was significantly longer in hiPSC-derived cardiomyocytes carrying the *TPM1-Asp175Asn* mutation than in cardiomyocytes carrying the *MYBPC3-Gln1061X* mutation ($p < 0.05$, Table 9).

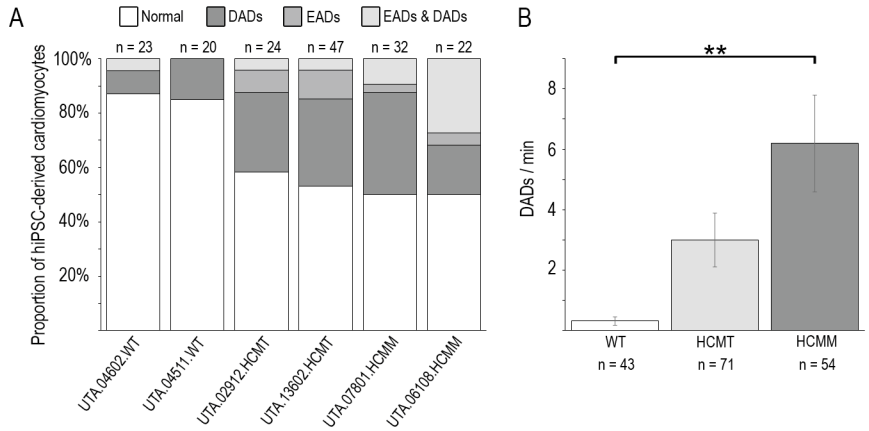

Figure 14. Electrophysiological properties of hiPSC-derived cardiomyocytes. A) The proportion of hiPSC-derived cardiomyocytes exhibiting arrhythmic events (EADs and DADs) for each hiPSC line. B) DAD rates for hiPSC-derived control cardiomyocytes (WT) and for cardiomyocytes carrying the *TPM1-Asp715Asn* (HCMT) or *MYBPC3-Gln1061X* (HCMM) mutation (** $p < 0.005$).

Table 9. Properties of action potentials for cardiomyocytes derived from control cardiomyocytes (WT) and cardiomyocytes carrying the *TPM1-Asp175Asn* (HCMT) or *MYBPC3-Gln1061X* (HCMM) mutation (* represents HCMT or HCMM vs. WT, $ represents HCMT vs. HCMM, ** $p < 0.005$, * or $ $p < 0.05$).

Cell line (baselines)	n	Beating rate (BPM)	ADP_{90}
WT	43	58.1 ± 2.3	323.6 ± 13.9
HCMT	71	48.4 ± 1.5**	433.1 ± 14.0**,$
HCMM	54	47.1 ± 1.8**	377.6 ± 15.0*

5.4.6 The expression of sarcomeric proteins in human induced pluripotent stem cell-derived cardiomyocytes (III)

All hiPSC-derived cardiomyocytes in Study III expressed the TnT, MYBPC and TPM1 proteins (Figure 15). The amounts of MYBPC, TnT and TPM1 proteins were determined by western blot analysis of each cell line in one differentiation experiment (Figure 15B-F). Due to a lack of replicates, statistical analysis was not performed. The truncated MYBPC protein (predicted size of 117 kDa) was not detected in hiPSC-derived cardiomyocytes with the *MYBPC3-Gln1061X* mutation (Figure 15C). However, the amount of MYBPC protein was slightly reduced in

hiPSC-derived cardiomyocytes carrying the *MYBPC3-Gln1061X* mutation (Figure 14D). The amounts of both TnT (Figure 15E) and TPM1 (Figure 15F) were elevated in hiPSC-derived cardiomyocytes carrying the *TPM1-Asp175Asn* or *MYBPC3-Gln1061X* mutation.

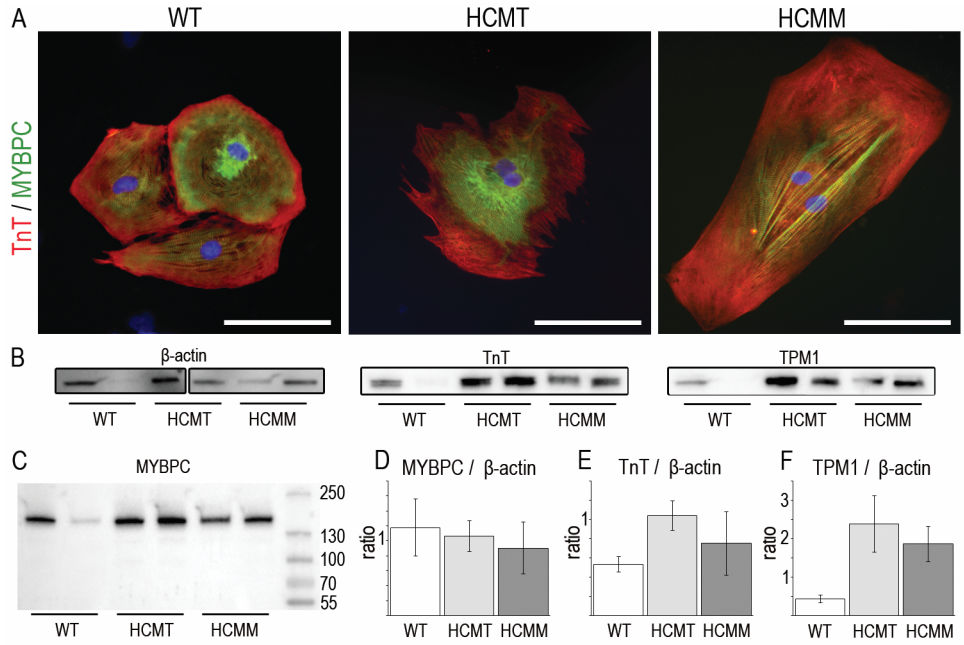

Figure 15. The expression of MYBPC, TnT and TPM1 in hiPSC-derived cardiomyocytes. A) hiPSC-derived control cardiomyocytes and cardiomyocytes carrying the *MYBPC3-Gln1061X* (HCMM) and *TPM1-Asp175Asn* (HCMT) mutations expressed TnT and MYBPC proteins according to immunocytochemical stainings. B-F) The expression of TnT, TPM1 and MYBPC was studied by western blot analysis. β-actin was used as a loading control. C) Expression of MYBPC in WT, HCMT and HCMM cardiomyocytes. The size of wildtype MYBPC was 141 kDa and the predicted size of truncated MYBPC was 117 kDa. Quantitative analysis of the expression of MYBPC (D), TnT (E) and TPM1 (F) by western blot analysis.

6 Discussion

The first two aims of this thesis were to compare the cardiac differentiation efficiencies of various hESC and hiPSC lines and to evaluate the effects of hPSC culture methods on the cardiac differentiation efficiencies of hPSCs. Not only were there differences between hESC and hiPSC differentiation potentials, but differences between individual experiments were also observed. Culture conditions had marked effects on the cardiac differentiation potentials of hPSCs, revealing the superiority of the mouse feeder cell layer-based methods over the tested feeder cell-free culture method. The third aim of this thesis was to develop cell models for studying HCM *in vitro* using patient-specific hiPSCs. hiPSC-derived HCM cardiomyocytes exhibited the HCM phenotype, at the same time revealing significant differences between cardiomyocytes carrying the *MYBPC3-Gln1061X* or *TPM1-Asp175Asn* mutation.

6.1 Differentiation potential between distinct human pluripotent stem cell lines (I)

The aim of the first study was to evaluate the differentiation potential of hESC and hiPSC lines into cell types derived from all three germ layers. hPSCs were differentiated into endodermal hepatocytes, mesodermal cardiomyocytes and ectodermal neural and RPE cells by researchers dedicated to their specific lineages of differentiation. This thesis concentrates on the cardiac differentiation potential of hPSCs. We found a marked variation in the cardiac differentiation potential of individual hPSC lines when using the END-2 co-culture method for differentiation. Further, the overall cardiac differentiation potential, evaluated by determining the number of beating aggregates and TnT positive cells, was higher in hESC than in hiPSC lines. Additionally, the highest peak of *BRACHYURY T* expression in END-2 co-cultures was detected on day 3 in hESC lines, while in hiPSC lines, the highest expression peak was shifted to day 6. The highest peak of *BRACHYURY T* expression in END-2 co-culture was normally detected on day 3 (Beqqali et al., 2006), while delayed *BRACHYURY T* expression has previously been associated

with poor cardiac differentiation efficiency (Bettiol et al., 2007; Pekkanen-Mattila et al., 2012).

Large variations in cardiomyocyte yield for the same method have also been observed in previous studies (Burridge et al., 2007; Osafune et al., 2008; Pekkanen-Mattila et al., 2009). In addition to the normal variation observed between hPSC lines, reprogramming can induce genomic changes, such as copy number variations (CNV) in hiPSCs (Hussein et al., 2011; Lund et al., 2012b). However, variations in the amounts of karyotypical abnormalities between integrating and non-integrating hiPSC reprogramming methods have not been detected (Taapken et al., 2011). Similar to every human, each hPSC line has a unique genotype and thus unique characteristics. It is therefore likely that individual cell lines endogenously produce different levels of growth factors and thus require different concentrations of external growth factors, including Activin A and BMP4, for optimal cardiac differentiation (Kattman et al., 2011). Therefore, in our study, the variations between the individual differentiation experiments for the same line might at least partially be explained by the rather spontaneous nature of the END-2 differentiation method, in which certain amounts of specific growth factors or small molecules are not used to induce cardiac differentiation.

Interestingly, one of the hiPSC lines was inferior in terms of differentiation toward all cell lineages, and *KLF4* was found to be incompletely silenced in this hiPSC line. This might partially explain the differences observed in the cardiac differentiation potential between hESC and hiPSC lines, as only four hiPSC lines were used in the study. Moreover, the expression of exogenous *OCT3/4* was increased during the long RPE differentiation protocol in each hiPSC line, suggesting a reactivation of retrovirally transferred genes during the long differentiation protocol, which lasted almost three months. This phenomenon was not detected with shorter differentiation protocols toward other lineages nor in one cell line produced with non-integrating Sendai virus. We hypothesized that the integrating hiPSC induction methods might be associated with the reactivation of transgenes, which could affect the differentiation potential of hiPSCs. Recently, the removal of integrated reprogramming factors has been found to improve the cardiogenesis of hiPSCs (Martinez-Fernandez et al., 2014). Together these data suggest that non-integrating or excisable vectors should be preferred in future studies.

6.2 Effects of culture conditions (II, III)

6.2.1 Effects of culture conditions on the cardiac differentiation potential of human pluripotent stem cells (II)

The second aim of this thesis was to optimize the culture method for hPSC lines, as determined by evaluating the cardiac differentiation of hPSCs. We discovered that culture conditions have a significant effect on the cardiac differentiation potential of hPSCs. hPSCs cultured on MEF or SNL mouse feeder cell layers in conventional hPSC culture medium produced more cardiomyocytes in END-2 co-cultures than hPSCs cultured on Matrigel™ in mTeSR™1 medium. Moreover, hPSCs cultured with the feeder cell-free method were more prone toward differentiating into neural cells. Thus, from among the hPSC culture methods studied here, the mouse feeder cell layers were found to be optimal for our purposes.

Previously, we have shown that hPSCs cultured on MEF feeder cell layers are more prone to differentiating into cardiomyocytes than hPSCs cultured on hFF feeder cell layers (Pekkanen-Mattila et al., 2012). Recently, consistent with our results, others have also demonstrated the enhancement of ectodermal and neural cell differentiation capacity in feeder cell-free cultures. In a recent report by Garitaonandia et al., the amount of ectodermal cells was significantly higher in teratomas derived from hPSCs cultured on a Geltrex® matrix in StemPro medium (27%) than in hPSCs cultured on MEF feeder cell layers (13%) (Garitaonandia et al., 2015). In another report, Lee et al. demonstrated the enhancement of neural differentiation at the expense of mesodermal hematopoietic differentiation when hESCs were cultured in mTeSR™1 medium on Matrigel™ (Lee et al., 2015). They cultured hESCs on Matrigel™ either in MEF-CM or mTeSR™1 medium. However, the effects appeared to be reversible, and when hESCs were transferred back to MEF-CM, the hematopoietic differentiation potential was retained. Interestingly, an optimal yield of hematopoietic cells was achieved after switching back to MEF-CM from mTeSR™1. (Lee et al., 2015.)

Although genetic alterations were not studied in this thesis, it is be important to consider the possible effects of culture conditions on the genetic and epigenetic properties of hPSCs when optimizing the best culture method. The results from studies investigating the effects of culture conditions on the genetic and epigenetic stability of hPSCs are quite controversial. Initial studies involving the long-term *in vitro* culture of hPSCs and enzymatic passaging have shown an increased

susceptibility to genetic and epigenetic alterations (Allegrucci et al., 2007; Mitalipova et al., 2005). However, in more recent and comprehensive reports studying various hESC and hiPSC lines from several laboratories, the culture method or passaging method has not been associated with the levels of abnormalities (Laurent et al., 2011; Taapken et al., 2011). Recently, Garitaonandia and co-workers cultured both hiPSCs and hESCs on MEF feeder cell layers in conventional hPSC culture medium or on Geltrex® matrix in StemPro medium (Garitaonandia et al., 2015). They compared both the genetic and epigenetic changes in hPSCs cultured on MEF feeder cell layers or on Geltrex® when the hPSCs were passaged either manually or enzymatically using the accutase enzyme. Inconsistent with their previous results (Laurent et al., 2011), the use of a feeder cell-free culture method, as well as the enzymatic passaging, resulted in increased genetic and epigenetic instability. (Garitaonandia et al., 2015.) This was explained by the differences in the design of the two studies. While the first study concentrated on the differences between the hESC lines established and cultured via different methods around the world, the second study concentrated on studying the differences between passages. Therefore, culture conditions might indeed have an effect on the differentiation potential of hPSCs, although the inhibitory effects might be reversible. However, more comprehensive studies are necessary to discover the actual cellular mechanisms that are affected.

6.2.2 Effects of culture conditions on the phenotype of human pluripotent stem cell-derived cardiomyocytes (III)

The third aim of this thesis was to develop cell models for HCM using hiPSC-derived cardiomyocytes carrying either the *MYBPC3-Gln1061X* or *TMP1-Asp175Asn* mutation. In our study, the size of the hiPSC-derived cardiomyocytes with the *MYBPC3-Gln1061X* mutation was significantly larger than that of hiPSC-derived cardiomyocytes with *TPM1-Asp175Asn* or hiPSC-derived control cardiomyocytes. Furthermore, the cellular enlargement of cardiomyocytes was increased during the long-term culture of cells at the single-cell level, which appeared to stimulate cell growth. Recently, serum has been found to mask the hypertrophic phenotype of hiPSC-derived cardiomyocytes with the *MYBPC3* mutation (Dambrot et al., 2014). Serum was found to increase the cell size of neonatal rat cardiomyocytes as well as cardiomyocytes derived from hESCs and control hiPSCs. However, the size of the hiPSC-derived cardiomyocytes with the *MYBPC3* mutation was smaller than that of hiPSC-derived control cardiomyocytes in the presence of serum. Under serum-free

conditions, hiPSC-derived cardiomyocytes with the *MYBPC3* mutation were significantly larger than hiPSC-derived control cardiomyocytes. (Dambrot et al., 2014.) In our study, our cardiomyocytes carrying the *MYBPC3-Gln1061X* mutation were enlarged, despite the 20% FBS used in the culture medium. Thus, we could not confirm the inhibitory effects of FBS on the enlargement of hiPSC-derived HCM cardiomyocytes.

Furthermore, hPSC-derived cardiomyocytes have been shown to more closely resemble fetal rather than adult cardiomyocytes (Van den Heuvel et al., 2014). The differences are discussed in more detail below, but culture conditions have been observed to effect the maturity of hPSC-derived cardiomyocytes. For example, when EBs were cultured over three months, both the molecular and electrophysiological properties of the cardiomyocytes started to resemble those of more adult cardiomyocytes (Sartiani et al., 2007). Additionally, other research groups have observed changes toward the adult phenotype not only in terms of molecular or electrophysiological properties but also morphological properties when culturing hPSC-derived cardiomyocytes for longer periods of time (Kamakura et al., 2013; Lundy et al., 2013; Otsuji et al., 2010).

Together, these data emphasize the importance of culture conditions at the pluripotent level and during the cardiac differentiation of hPSCs as well as when culturing hiPSC-derived cardiomyocytes. It is always important to consider whether the abnormal behavior observed in disease-specific hiPSC-derived cardiomyocytes is attributable to the actual disease or to technical artifacts originating from hiPSC induction, cardiac differentiation or culture conditions.

6.3 Modeling hypertrophic cardiomyopathy with human induced pluripotent stem cells (III)

The third aim of this thesis was to develop cell models for HCM using hiPSC-derived cardiomyocytes carrying either the *MYBPC3-Gln1061X* or *TMP1-Asp175Asn* mutation, which are the most prevalent HCM mutations in Finland. HCM is characterized by unexplained hypertrophy of the heart muscle in IVS or left ventricle, arrhythmias, and fibrosis as well as myocyte hypertrophy and myofibrillar disarray. HCM might lead to heart failure and SCD, and there are no specific therapies available for the prevention of HCM progression (Kocovski & Fernandes, 2015; Maron et al., 2014). The primary cause of the disease lies in the genes encoding for sarcomeric proteins, while on a cellular level, the earliest pathophysiological

mechanisms include disrupted Ca^{2+} handling properties, ion channel remodeling, increased energy consumption and reduced force generation (Eschenhagen et al., 2015; Tardiff et al., 2015). The clinical phenotype of HCM is impressively variable, ranging from individuals with severe hypertrophy or SCD to completely asymptomatic individuals. This indicates that other factors in addition to the identified gene mutation, such as additional mutations, genetic modifiers, epigenetic factors and environment, must have an impact on the development and progression of the disease. (Ho et al., 2015; Van der Velden et al., 2015.)

6.3.1 Comparison to other published reports

In our study, we derived karyotypically normal hiPSCs from HCM patients. All our hiPSC lines expressed genes and proteins typical of hPSCs. We differentiated both HCM patient-specific hiPSCs and hiPSCs derived from healthy control individuals into cardiomyocytes and compared their morphological and electrophysiological properties. Our HCM hiPSC-derived cardiomyocytes resembled the HCM phenotype *in vitro*, including enlarged cell size, multinuclearity, abnormal Ca^{2+} transients and increased number of arrhythmic events (both EADs and DADs) in electrophysiological recordings. Most importantly, we found major differences between hiPSC-derived cardiomyocytes carrying either the *MYBPC3-Gln1061X* or *TPM1-Asp715Asn* mutation. The enlargement of the cardiomyocytes carrying the *MYBPC3-Gln1061X* mutation was more significant and appeared earlier in culture than that of cardiomyocytes carrying the *TPM1-Asp715Asn* mutation. Conversely, cardiomyocytes carrying the latter mutation had significantly more abnormal Ca^{2+} transients and significantly more prolonged action potential durations compared to cardiomyocytes carrying the *MYBPC3-Gln1061X* mutation. However, both types of HCM cardiomyocytes demonstrated increased amounts of arrhythmic events, as determined by their electrophysiological recordings, compared to hiPSC-derived control cardiomyocytes.

Currently, there have been three reports published using HCM patient-specific hiPSCs (Han et al., 2014; Lan et al., 2013; Tanaka et al., 2014). The results presented in these three publications are shown in Table 9. In addition, HCM hiPSC-derived cardiomyocytes carrying *MYBPC3* mutations were used in one report, in which the effects of serum on hypertrophic phenotypes were studied (Dambrot et al., 2014). The results from this study have already been discussed above.

In this thesis, we derived hiPSC lines from two patients carrying the *MYBPC3-Gln1061X* mutation and from two patients carrying the *TPM1-Asp175Asn* mutation. The ages and clinical symptoms of our patients varied. Two unrelated hiPSC lines derived from healthy volunteers were used as control cells. hiPSCs were derived from fibroblasts using either retro- or Sendai viruses. All hiPSC-derived HCM cardiomyocytes were significantly larger than hiPSC-derived control cardiomyocytes in our study. In 2013, Lan et al. published the first report using HCM hiPSC-derived cardiomyocytes. In their publication hiPSCs were established via the lentiviral infection of fibroblasts derived from five patients carrying the *MYH7-Arg663His* mutation and from five related healthy individuals. Although the two youngest patients had not developed the clinical phenotype of HCM, the hiPSC-derived cardiomyocytes from all patients were significantly larger than the control cardiomyocytes (Lan et al., 2013). In 2014, Han et al. published a report in which hiPSCs were derived from a single patient carrying a *MYH7-Arg442Gly* mutation. Control hiPSCs were derived from two unrelated healthy individuals. Fibroblasts were used as a cell source for all established hiPSC lines, and the infection was performed using retroviruses (Han et al., 2014). In the latest paper by Tanaka et al. in 2014, hiPSCs were derived from three unrelated HCM patients and three healthy volunteers. One of the HCM patients carried the *MYBPC3-Gly999-Gln1004del* mutation, while in the two other patients, the mutations were unknown (Tanaka et al., 2014). Two control hiPSC lines were generated from dermal fibroblasts using retroviruses, while all patient hiPSC lines and one control hiPSC line were derived from T lymphocytes or peripheral blood with Sendai viruses. In the latest study, a mixture of EBs derived from all three patients was studied (Tanaka et al., 2014). Thus far, our report presented in this thesis is the first to compare two HCM mutations using hiPSC-derived cardiomyocytes in the same study with similar experimental settings.

Table 10. Summary of results from published reports using HCM patient-specific hiPSCs.

Patients and mutations	HCM phenotype in hiPSC-CMs	Drug treatments
Lan et al. 2013	**Morphological properties**	**Calcineurin-NFAT signaling**
Family with HCM	Cellular enlargement	Blockade by cyclosporin A and FK506 reduced hypertrophy
- 5 pers. with *MYH7-Arg663His*	Multinucleation	**β-adrenergic stimulation**
- 5 pers. without mutation	Increased myofibril content	Isoproterenol increased cell size and
(used as controls)	Disorganized sarcomeres	amount of irregular Ca^{2+} transients and arrhythmia
	Biochemical properties	
	Upregulation of *ANF*, *TNNT2*, *MYL2, MYH7*,	Propranolol abolished isoproterenol-induced
Timepoints:	*GATA4* and *MEF2c*	Ca^{2+} abnormalities, arrhythmia and hypertrophy
20, 30, 40 days	Elevation of *MYH7*/*MYH6* ratio	
	Nuclear translocation of NFAT	
	Ca^{2+} handling properties	**Blockade of L-type Ca^{2+} channel**
	Ca^{2+} transient irregularities	Treatment with verapamil for 5 days ameliorated HCM phenotype
	Elevation of intracellular [Ca^{2+}]	Diltiazem abolished Ca^{2+} abnormalities and arrhythmia
	Smaller SR Ca^{2+} release	
	Electrophysiological and mechanical properties	
	Arrhythmic waveforms including frequent DADs	
	Irregular beating observed in video recordings	
Han et al. 2014	**Morphological properties**	**β-adrenergic stimulation**
One patient:	Cellular enlargement	Isoproterenol elevated premature beats and irregular beating rates
- *MYH7*-Arg442Gly	Disorganized sarcomeres	Metoprolol decreased isoproterenol-induced beating irregularity
	Disorganized Z lines in EM	and arrhythmia
Two control hiPSC lines from	**Biochemical properties**	
unrelated healthy donors	Changes in (whole transcriptome sequencing):	**Blockade of L-type Ca^{2+} channel**
	WNT/β-catenin pathway	Treatment with verapamil for 4 days reduced arrhythmia and
	Notch signaling pathway	Ca^{2+} handling abnormalities
	FGF pathway	
	Nuclear translocation of NFAT	**K_{ATP} channel opener**
	Decreased level of *RYR2*, *SERCA2*	Antihypertensive drug pinacidil induced irregular interspike intervals
	Ca^{2+} handling properties	
	Ca^{2+} transient irregularities	**Inhibition of histone deacetylase activity**
	Elevation of intracellular [Ca^{2+}]	Treatment with trichostatin A for 3 days decreased cell size,
	Smaller SR Ca^{2+} release	led to nuclear translocation of NFAT, suppressed Ca^{2+}
	Delayed Ca^{2+} transient decay time	abnormalities and decreased resting [Ca^{2+}]
	Electrophysiological properties	
	Prolonged and dispersed interspike intervals and	
	increase of arrhythmogenic events in MEA	
	Irregular contractility in real-time cell analyzer	
	APD prolongation	
	Changes in the shape of AP	
	Increased Ca^{2+}, Na^{+} and outward K^{+} currents	
Tanaka et al. 2014	**Morphology without stimulation**	**Stimulation with hypertrophic factors**
Three patients:	Mildly but significantly larger cell size	Angiotensin II, IGF-1, phenylephrine
- *MYBPC3-GLY999-Gln1004del*	No time-dependent changes in cell size	no difference compared to non-stimulated cells
- In two of the patients,	Myofibrillar disarray in EM and cTnT staining	Endothelin 1 (ET-1)
mutation was unknown	Elevated cTnT and ANP levels	Increase in cell size and myofibrillar disarray
	Decreased MYBPC level in hiPSC-CMs with	Nuclear translocation of NFAT
Three control hiPSC lines from	*MYBPC3* mutation	Disorganized contractile form in video analysis
unrelated healthy donors	Mildly disorganized contractile form in video	Similar response in mouse $MYBPC^{+/-}$ cardiomyocytes
	recordings	**Blocking of ET-1 signaling**
Timepoints:		ETA receptor antagonist blocked ET-1-induced effects
30, 60, 90 days culture as EBs		ETB receptor antagonist had no effect

HCM hypertrophic cardiomyopathy; **hiPSC-CM** human induced pluripotent stem cell-derived cardiomyocyte; **SR** sarcoplasmic reticulum; **DAD** delayed after depolarization; **EM** electron microscopy; **MEA** microelectrode array; **APD** action potential duration; **AP** action potential

Myofibrillar disarray has been studied in most publications. However, in all publications, different methods and criteria have been used to quantify the disarray, and the results can be subjective. Han et al. showed that HCM hiPSC-derived cardiomyocytes have more disrupted sarcomeres than cardiomyocytes derived from control hiPSCs. However, the authors did not present any criteria to determine how the disruption was qualified (Han et al., 2014). In Tanaka et al., cardiomyocytes were qualified with myofibrillar disarray if over 50% of the myofibrils intersected with each other (Tanaka et al., 2014). In Lan et al., cardiomyocytes that had more than 25% of their cell area exhibiting punctate TnT distribution were considered disorganized. The overall morphology of hiPSC-derived cardiomyocytes is not mature, and their structure is often unorganized; this is also the case in cardiomyocytes derived from control hiPSCs. We did not report myofibrillar disarray due to the lack of proper quantitation criteria for this phenomenon. We have been developing software for the identification and characterization of the organization of myofibrils in a more automated and defined manner (Kartasalo et al., 2015, manuscript submitted).

In our study, the APD_{90} was significantly increased in hiPSC-derived cardiomyocytes carrying the *TMP1-Asp175Asn* mutation or the *MYBPC3-Gln1061X* mutation. However, the APD_{90} was significantly longer in cardiomyocytes carrying the *TMP1-Asp175Asn* mutation compared to cardiomyocytes carrying the *MYBPC3-Gln1061X* mutation. Although the numbers of cardiomyocytes exhibiting arrhythmias (DADs and EADs) were similar for both mutations, the DAD rate was higher in cardiomyocytes carrying the *MYBPC3-Gln1061X* mutation than in control cardiomyocytes. The electrophysiological properties of the HCM hiPSC-derived cardiomyocytes have been studied in two previous reports. Lan et al. observed more cardiomyocytes exhibiting DADs in hiPSC-derived HCM cell populations than in control cardiomyocyte populations. In addition, the DAD rate was significantly higher in these cells. Significant differences were observed only 30 days after the initiation of cardiac differentiation. (Lan et al., 2013.) Han and coworkers demonstrated a marked prolongation of APD in HCM hiPSC-derived cardiomyocytes carrying the *MYH7-Arg442Gly* mutation but no increased DAD ratio (Han et al., 2014). We are currently further studying the electrophysiological properties of our HCM hiPSC-derived cardiomyocytes.

In our study, the proportion of cardiomyocytes with abnormal Ca^{2+} transients was approximately 20% for hiPSC-derived control cardiomyocytes, 42% for cardiomyocytes carrying the *TPM1-Asp175Asn* mutation and 21% for cardiomyocytes carrying the *MYBPC3-Gln1061X* mutation. Lan and co-workers

reported that approximately 20% of hiPSC-derived HCM cardiomyocytes had irregularities in their Ca^{2+} handling properties on day 30 and approximately 30% on day 40 after initiating cardiac differentiation, while in control cardiomyocytes the proportion was approximately 5% at all timepoints (Lan et al., 2013). Han et al. reported that approximately 20% of hiPSC-derived cardiomyocytes had abnormal Ca^{2+} handling properties, while no control hiPSC-derived cardiomyocytes had abnormalities (Han et al., 2014). Similar to the characterization of disrupted sarcomeres, these data are also subjective, and the qualification criteria are rarely stated in publications. Thus, the results obtained in different publications are not directly comparable. For example, in the study presented in this thesis, approximately 20% of control hiPSC-derived cardiomyocytes had abnormalities in their Ca^{2+} handling properties, while in earlier studies, the proportions were 0-5%. Recently, we have been developing software to aid researchers in the visual characterization of Ca^{2+} signals to obtain more reliable and robust results (Penttinen et al., 2015, manuscript submitted).

6.3.2 Variable phenotype of hypertrophic cardiomyopathy

In Study III, we observed significant differences between hiPSC-derived cardiomyocytes carrying the *MYBPC3-Gln1061X* or *TPM1-Asp715Asn* mutation. Cardiomyocytes with the *MYBPC3-Gln1061X* mutation were significantly larger than cardiomyocytes carrying the *TPM1-Asp715Asn* mutation, while cardiomyocytes carrying the latter mutation had more abnormalities in their Ca^{2+} transients, and their APD_{90} was significantly longer than for cardiomyocytes carrying the *MYBPC3-Gln1061X* mutation. Originally, the *MYBPC3-Gln1061X* mutation was associated with a clinically mild phenotype, and *TPM1-Asp175Asn* was associated with a clinically intermediate phenotype with a substantial risk for SCD (Jääskeläinen et al., 2004). However, in the most recent clinical studies, as well as in the patient data analyzed in this thesis, hypertrophy has been in the same range in patients carrying either of these two mutations (Jääskeläinen et al., 2014, 2013). Therefore, the differences in cell size observed in this thesis do not correlate with the extent of clinical hypertrophy. However, our data demonstrate more abnormal Ca^{2+} transients and longer APD_{90} for *TPM1-Asp175Asn* cardiomyocytes than cardiomyocytes carrying the *MYBPC3-Gln1061X* mutation, which is in line with the clinical findings that patients with *TPM1-Asp175Asn* are more prone to arrhythmias than those with the *MYBPC3-Gln1061X* mutation.

It is known that the primary causes of genetic HCM are mutations in the sarcomeric genes. However, the reasons why progressive changes initiated by these primary mutations occur in one individual and not in others are still largely unknown. Many mechanisms related to the variable phenotype of HCM have been proposed (Figure 15). Conventionally, HCM has been studied with animal models or patient samples obtained from surgical myectomy. There are limitations to these models. Animal models carry only the mutated gene, and although they contain the entire genome of an HCM patient, myectomy samples are obtained from patients in the late stage of HCM development. While HCM leads to progressive heart failure, the major difficulty in studying the pathophysiological mechanisms leading to HCM has been the lack of tissue at the early stages of disease development. Thus, our hiPSC models represent a valuable tool to study HCM *in vitro*.

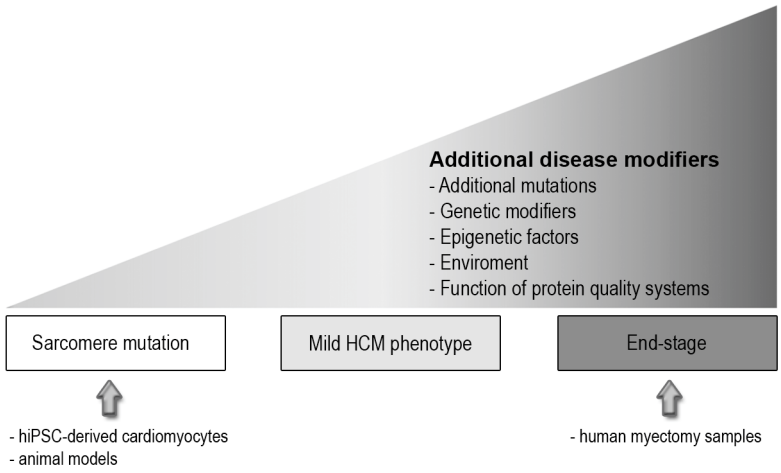

Figure 16. Factors related to the variable phenotype of HCM (figure modified from Van der Velden et al., 2015).

In our study, we could not detect the mutated MYBPC protein, which is in line with previous studies using human myectomy samples and hiPSC-derived cardiomyocytes (Marston et al., 2009; Rottbauer et al., 1997; Tanaka et al., 2014; Van Dijk et al., 2009). The total amount of the MYBPC protein was slightly reduced in our study in cardiomyocytes carrying the *MYBPC3-Gln1061X* mutation compared to hiPSC-derived control cardiomyocytes. The dosage of the mutated gene is one of the factors that has been proposed to affect the severity of the observed clinical phenotype. HCM is inherited in an autosomal dominant pattern, and thus, both mutated and wildtype proteins are expected to be incorporated into the sarcomere. (Van der

Velden et al., 2015.) However, the expression of the mutated protein can be regulated on many levels. In particular, the *MYBPC3* mutations leading to truncated proteins can be directed toward degradation by nonsense-mediated mRNA decay, UPS and the autophagy/lysosomal pathway, which leads to haploinsufficiency (Helms et al., 2014). The age-related decline of these protein quality systems has been suggested to effect the progression of HCM (Van der Velden et al., 2015). The amount of the wildtype MYBPC protein varies in patient tissue samples, which might correlate with the clinical phenotypes observed in patients (Helms et al., 2014; Van Dijk et al., 2009). Another mechanism affecting the dosage of the mutated gene and thus disease severity could be allelic imbalance, which indicates differences in the expression levels of mutated and wildtype alleles (Helms et al., 2014; Tripathi et al., 2011).

Other additional disease modifiers are thought to act later during life. Protein phosphorylation is one of the most important post-translational modifications, which has also been suggested to affect disease development. For example, the reduced phosphorylation of TnI and MYBPC has been related to increased myofilament Ca^{2+} sensitivity, which is a common feature of HCM. (Sequeira et al., 2013.) However, Ca^{2+} sensitivity has also been suggested to be a primary consequence of HCM. Additionally, Ca^{2+} sensitivity has been proposed to increase arrhythmia sensitivity either by increasing the Ca^{2+} binding affinity in the cytosol, which could lead to remodeling of action potentials and thus trigger arrhythmias, or by affecting energy consumption and increasing arrhythmia susceptibility via stress (Huke et al., 2013; Schober et al., 2012; Van der Velden et al., 2015).

Some HCM patients have been shown to carry more than just one mutation in their genotype, and patients carrying multiple mutations have been associated with more severe symptoms or earlier onset of disease (Ho et al., 2015; Maron et al., 2012). Other genetic mechanisms include genetic modifiers, which can be either near or distantly located DNA variants that influence the expression of the mutated gene (Ho et al., 2014). Additionally, epigenetic changes, which cannot be explained by the DNA sequence itself, have been suggested to contribute to the progression of HCM. These mechanisms include the methylation of GpC islands by DNA methyltransferases, histone modification, microRNAs (miRNAs) and long non-coding RNAs (lncRNAs), which can lead to the altered regulation of genes (Ho et al., 2015).

In this study, we were able to detect differences between the cellular phenotypes of the *MYBPC3-Gln1061X* and *TPM1-Asp175Asn* mutations, which are partially in line with clinical findings published previously (Jääskeläinen et al., 2014, 2013, 2004). The actual mechanism related to the differences between the *MYBPC3-Gln1061X*

and *TPM1-Asp175Asn* mutations observed in this thesis remains unknown, and further studies are necessary. However, the HCM hiPSC cell models developed in this thesis represent a valuable tool to study the pathophysiological mechanisms, including the effects of additional disease modifiers, which have been almost impossible to study before using animal models and human myectomy samples.

6.3.3 Limitations in the use of human induced pluripotent stem cell-derived cardiomyocytes as an *in vitro* model for hypertrophic cardiomyopathy

The major limitation when using hiPSC-derived cardiomyocytes in disease modeling is the immature nature of these cells. The characteristics of hPSC-derived cardiomyocytes and the differences between these and adult human cardiomyocytes have recently been reviewed (Van den Heuvel et al., 2014). Compared to adult cardiomyocytes, the sarcomeric structures of hPSC-derived cardiomyocytes are unorganized, they lack clear T tubules, they have different ion channel profiles, and their Ca^{2+} handling is immature. In addition, the shapes of hPSC-derived cardiomyocytes vary from circular to star-shaped, while adult human cardiomyocytes are rod-shaped *in vivo*. Overall, the phenotype of hPSC-derived cardiomyocytes is thought to more closely resemble that of fetal cardiomyocytes than adult cardiomyocytes. (Van den Heuvel et al., 2014.) At the moment, much effort is being expended to obtain more mature cardiomyocytes. In addition to culture conditions and the long-term culture of cardiomyocytes discussed above, other techniques such as electrical and mechanical stimulation, as well as engineered heart tissue (EHT) structures, have been developed (Kreutzer et al., 2014; Kujala et al., 2012b; Nunes et al., 2013; Stoehr et al., 2014).

Another issue related to the study of HCM with hiPSC-derived cardiomyocytes is related to the assumption that cell types other than cardiomyocytes might be directly involved in the progression of HCM. For example, microvascular dysfunction is thought to be the primary reason for replacement-type fibrosis observed in HCM patients (Van der Velden et al., 2015). Thus, it is important to consider whether studying HCM at the single cell level is sufficient to obtain an exact picture of the disease mechanisms. EHT structures and cardiovascular constructs, consisting of various cell types could be useful in this context (Stoehr et al., 2014; Vuorenpää et al., 2014).

As discussed above, in addition to primary HCM gene mutations, gene modifiers and epigenetic changes might also have an effect on disease development and

progression. In all published reports, including the results presented in this thesis, the phenotypes of HCM hiPSC-derived cardiomyocytes have been compared to control hiPSC-derived cardiomyocytes established from related or non-related healthy individuals (Han et al., 2014; Lan et al., 2013; Tanaka et al., 2014). Currently, useful gene-editing approaches, including clustered regularly interspaced short palindromic repeats (CRISPR) and transcription activator-like effector nuclease (TALEN) techniques, are available, and they can be used either to create mutations or correct existing mutations in an hiPSC line, thus generating genotype-matched isogenic control lines (Li et al., 2014). When considering the variable phenotypes of HCM patients, these isogenic control hiPSCs would be useful when further studying HCM disease mechanisms.

6.4 Future perspectives

In this thesis, we observed marked variations in the cardiac differentiation potential of individual hPSC lines, which has also been reported in earlier studies. Furthermore, hESC lines appeared to be more efficient in producing cardiomyocytes than hiPSC lines. Although a large number of cardiac differentiation methods have recently been developed, none of them appear to efficiently and robustly produce cardiomyocytes from every hPSC line. In addition to the actual cardiac differentiation method, hPSC line-specific differences have been related to the hiPSC induction method, culture conditions, and characteristics of individual hPSC lines. Regardless, the optimization and maintenance of the best differentiation method for each individual hPSC line is laborious, and more robust cardiac differentiation methods are still needed.

When studying the effects of hPSC culture methods on the cardiac differentiation potential of hPSCs, we observed that the hPSCs cultured on mouse feeder cell layers more efficiently produced cardiomyocytes in END-2 co-cultures than hPSCs cultured with a feeder cell-free method. Furthermore, the hPSCs cultured with the feeder cell-free method were more prone to differentiating toward neural cells. These data suggest that in addition to optimizing the differentiation method, culture conditions for hPSCs should also be optimized when differentiating hPSCs into specific lineages.

In this thesis, *KLF4* was incompletely silenced before differentiation in one of the hiPSC lines used. This particular cell line was inferior in terms of differentiation into cell derivatives from all three germ layers. In addition, exogenous *OCT3/4* was

expressed in all hiPSC lines at the end of RPE cell differentiation. The RPE differentiation protocol was the longest differentiation protocol used in our study, lasting almost three months. When considering the potential reactivation of transgenes in retrovirally induced hiPSCs, other reprogramming techniques employing non-integrating methods should be preferred in future studies.

To our knowledge, the study presented in this thesis is the first report in which hiPSC-derived cardiomyocytes have been used to compare two different HCM mutations in similar experimental settings. Due to a lack of standardized characterization methods and criteria, results from separate publications are hard to compare. Although the current methods for studying cardiomyopathies *in vitro* with patient-specific cardiomyocytes are far from optimal, we were able to create hiPSC models with the HCM phenotype and discover mutation-specific differences between hiPSC-derived cardiomyocytes carrying the *MYBPC3-Gln1061X* or *TPM1-Asp175Asn* mutation. When using isogenic controls in which the mutation is corrected with gene-editing techniques, hiPSC-derived cardiomyocytes also represent a valuable tool to study the effects of genetic modifiers and epigenetic factors on disease progression between different individuals, which has been difficult when using animal models or samples from surgical myectomy.

However, particularly in the case of HCM associated with highly variable phenotypes, it would be important to optimize cardiac differentiation and cell culture conditions. The study design becomes highly valuable, and the culture conditions should be similar for both control and disease-specific cardiomyocytes. When experiment are thoroughly designed, the results obtained from these studies would be more robust and reliable. However, we believe that the hiPSC-derived HCM *in vitro* models established in this thesis represent a valuable tool to further study the pathophysiological mechanisms of HCM as well as to test novel drug therapies developed to prevent disease progression and potentially optimize treatments in a mutation-specific manner.

7 Conclusions

The aim of this thesis was to compare the differentiation efficiencies of various hPSC lines and to study the effects of hPSC culture methods on the cardiac differentiation potential of hPSCs as well as to develop cell models for HCM with patient-specific hiPSCs. Based on the three studies presented here, the following conclusions can be drawn:

- Marked variation in the cardiac differentiation potential of different hPSC lines was observed. Overall, the hESC lines were more efficient in producing cardiomyocytes than hiPSCs. This phenomenon could partially be explained by the reprogramming method utilized.
- Culture conditions have a significant effect on the cardiac differentiation potential of hPSCs. hPSCs cultured on mouse MEF or SNL feeder cell layers in conventional stem cell culture medium were more potent in producing cardiomyocytes in END-2 co-cultures than hPSCs cultured on Matrigel™ in mTeSR™1 medium. Furthermore, hPSCs cultured on Matrigel™ in mTeSR™1 medium were more prone to neural lineages.
- Karyotypically normal hiPSCs expressing genes and proteins typical of hPSCs were derived from HCM patients, and hiPSCs were differentiated into cardiomyocytes, which resembled the HCM phenotype *in vitro*. These changes include enlarged cell size, abnormal Ca^{2+} transients and an increased number of arrhythmic events, as observed in electrophysiological recordings.
- Significant differences between hiPSC-derived cardiomyocytes carrying the *TPM1-Asp175Asn* or *MYBPC3-Gln1061X* mutation were detected. Greater disturbances in the Ca^{2+} handling properties of *TPM1-Asp175Asn* cardiomyocytes were detected, while the size of *MYBPC3-Gln1061X* cardiomyocytes was significantly larger.

Acknowledgements

The research for this thesis was conducted at the BioMediTech, University of Tampere during the years 2009-2015. I am grateful to the former and the present directors of our institute, Riitta Seppänen and Hannu Hanhijärvi, for providing the research facilities for my studies. I wish to thank Tampere Graduate Programme in Biomedicine and Biotechnology (TGPBB) for the education and financially supporting my journeys to international conferences around the world. I wish to thank the entire personnel of BioMediTech for the friendly and supportive atmosphere. I owe my gratitude to everyone who has helped and advised me in the lab during these years.

I express my deepest gratitude to my supervisor professor, MD, PhD Katriina Aalto-Setälä. You have been an excellent role model of determined and enthusiastic researcher. Thank you for all the pleasant and informative conversations and all the important scientific skills that you have taught me. I also thank my other supervisor PhD Kristiina Rajala. Our collaboration in the lab was seamless and it was a pleasure to work with you. You also adviced and supported me tremendously when I was finalizing my thesis even though you were on a maternity leave.

Next, I wish to acknowledge the members of my follow-up group, Professors Olli Silvennoinen and Timo Ylikomi. I owe my sincere gratitude to Professor Heikki Ruskoaho and Docent Riikka Lund for reviewing my thesis and providing critical comments and suggestions to improve the quality of my thesis.

I owe my gratitude to all my co-authors: Sanna Toivonen, Anu Hyysalo, Tanja Ilmarinen, Mari Pekkanen-Mattila, Riikka Äänismaa, Karolina Lundin, Jaan Palgi, Jere Weltner, Ras Trokovic, Olli Silvennoinen, Heli Skottman, Susanna Narkilahti, Timo Otonkoski, Marinka Miettinen, Heini Huhtala, Chandra Prajapati, Risto-Pekka Pölönen, Jyrki Rasku and Kim Larsson. Without your help, this work would not have been possible to accomplish.

I thank the following foundations for the financial support during my years as a PhD student: The Alfred Kordelin Foundation, Tampere University Foundation (The Kalle Kaihari Heart Research Fund), University of Tampere, The Finnish Concordia Fund, Aarne and Aili Turunen Foundation, The Finnish Cultural Foundation (Pirkanmaa Regional Fund), Maud Kuistila Memorial Foundation, Oskar Öflunds Stiftelse, Finnish Foundation for Cardiovascular Research, Aarne Koskelo Foundation and the City of Tampere.

I wish to thank the past and present members of the Heart group. We have had such a great time together! I owe special thanks to Markus Haponen, Merja Lehtinen and Henna Venäläinen for their excellent technical assistance. Henna, thank you for your friendship and all adventures that we have shared in- and outside the lab. I wish to thank Liisa Ikonen, Anna Kiviaho and Kirsi Penttinen for their friendship and support during these years. Special thanks to Kirsi for sharing an office and your expertise in Ca^{2+} imaging with me. Your support and friendship have been priceless.

I am grateful to all my friends for providing me time to relax. I wish to thank members of Priima, Piritta Laitakari, Katriina Pekkinen and Annika Sykkö, for the enjoyable musical moments. Special thanks to Katriina for your friendship and proofreading the Finnish parts of this thesis. Without my supportive and encouraging parents, Päivi and Tapio Ojala, I probably would never have even started my PhD. I thank you with all of my heart. I am grateful to my sisters Satu Ojala and Riitta Ojala-Korhonen and their families Nicolas and Tommi Alasuvanto; Noora, Erika and Petteri Korhonen, for all the cheerful moments along the way. I thank my grandmothers Aino Ojala and Bertta Pietilä for the support and encouragement. Thanks to our cats, non-stopping purring machine Chewie and Samu, who did not have HCM after all. Finally, yet importantly, I would like to thank Turkka Mannila for being such a supportive and loving person during these years. Not only do I thank you for the mental encouragement but also for helping me to manage huge amount of data by programming all the nice software for me.

Tampere, July 2015

Marisa

References

Allegrucci, C., Wu, Y.-Z., Thurston, A., Denning, C. N., Priddle, H., Mummery, C. L., Ward-van Oostwaard, D., Andrews, P. W., Stojkovic, M., Smith, N., Parkin, T., Jones, M. E., Warren, G., Yu, L., Brena, R. M., Plass, C. and Young, L. E. (2007). Restriction landmark genome scanning identifies culture-induced DNA methylation instability in the human embryonic stem cell epigenome. Human Molecular Genetics, 16(10), 1253–1268.

Amit, M., Carpenter, M. K., Inokuma, M. S., Chiu, C. P., Harris, C. P., Waknitz, M. A., Itskovitz-Eldor, J. and Thomson, J. A. (2000). Clonally derived human embryonic stem cell lines maintain pluripotency and proliferative potential for prolonged periods of culture. Developmental Biology, 227(2), 271–278.

Amit, M., Shariki, C., Margulets, V. and Itskovitz-Eldor, J. (2004). Feeder layer- and serum-free culture of human embryonic stem cells. Biology of Reproduction, 70(3), 837–845.

Bayart, E. and Cohen-Haguenauer, O. (2013). Technological overview of iPS induction from human adult somatic cells. Current Gene Therapy, 13(2), 73–92.

Beqqali, A., Kloots, J., Ward-van Oostwaard, D., Mummery, C. and Passier, R. (2006). Genome-wide transcriptional profiling of human embryonic stem cells differentiating to cardiomyocytes. Stem Cells, 24(8), 1956–1967.

Bers, D. M. (2008). Calcium cycling and signaling in cardiac myocytes. Annual Review of Physiology, 70, 23–49.

Bettiol, E., Sartiani, L., Chicha, L., Krause, K. H., Cerbai, E. and Jaconi, M. E. (2007). Fetal bovine serum enables cardiac differentiation of human embryonic stem cells. Differentiation; Research in Biological Diversity, 75(8), 669–681.

Bing, W., Knott, A., Redwood, C., Esposito, G., Purcell, I., Watkins, H. and Marston, S. (2000). Effect of hypertrophic cardiomyopathy mutations in human cardiac muscle α -tropomyosin (Asp175Asn and Glu180Gly) on the regulatory properties of human cardiac troponin determined by in vitro motility assay. Journal of Molecular and Cellular Cardiology, 32(8), 1489–1498.

Bottinelli, R., Coviello, D. a, Redwood, C. S., Pellegrino, M. a, Maron, B. J., Spirito, P., Watkins, H. and Reggiani, C. (1998). A mutant tropomyosin that causes hypertrophic cardiomyopathy is expressed in vivo and associated with an increased calcium sensitivity. Circulation Research, 82(1), 106–115.

Boyer, L. A., Lee, T. I., Cole, M. F., Johnstone, S. E., Levine, S. S., Zucker, J. P., Guenther, M. G., Kumar, R. M., Murray, H. L., Jenner, R. G., Gifford, D. K., Melton, D. A., Jaenisch, R. and Young, R. A. (2005). Core transcriptional regulatory circuitry in human embryonic stem cells. Cell, 122(6), 947–956.

Briggs, R. and King, T. J. (1952). Transplantation of living nuclei from blastula cells into enucleated frogs' eggs. Proceedings of the National Academy of Sciences of the United States of America, 38(5), 455–463.

Burridge, P. W., Anderson, D., Priddle, H., Barbadillo Muñoz, M. D., Chamberlain, S., Allegrucci, C., Young, L. E. and Denning, C. (2007). Improved human embryonic stem cell embryoid body homogeneity and cardiomyocyte differentiation from a novel V-96 plate aggregation system highlights interline variability. Stem Cells, 25(4), 929–938.

Burridge, P. W., Matsa, E., Shukla, P., Lin, Z. C., Churko, J. M., Ebert, A. D., Lan, F., Diecke, S., Huber, B., Mordwinkin, N. M., Plews, J. R., Abilez, O. J., Cui, B., Gold, J. D. and Wu, J. C. (2014). Chemically defined generation of human cardiomyocytes. Nature Methods, 11(8), 855–860.

Buta, C., David, R., Dressel, R., Emgård, M., Fuchs, C., Gross, U., Healy, L., Hescheler, J., Kolar, R., Martin, U., Mikkers, H., Müller, F.-J., Schneider, R. K., Seiler, A. E. M., Spielmann, H. and Weitzer, G. (2013). Reconsidering pluripotency tests: do we still need teratoma assays? Stem Cell Research, 11(1), 552–562.

Celiz, A. D., Smith, J. G. W., Langer, R., Anderson, D. G., Winkler, D. A., Barrett, D. A., Davies, M. C., Young, L. E., Denning, C. and Alexander, M. R. (2014). Materials for stem cell factories of the future. Nature Materials, 13(6), 570–579.

Chang, C.-W., Lai, Y.-S., Pawlik, K. M., Liu, K., Sun, C.-W., Li, C., Schoeb, T. R. and Townes, T. M. (2009). Polycistronic lentiviral vector for "hit and run" reprogramming of adult skin fibroblasts to induced pluripotent stem cells. Stem Cells, 27(5), 1042–1049.

Chen, G., Gulbranson, D. R., Hou, Z., Bolin, J. M., Ruotti, V., Probasco, M. D., Smuga-Otto, K., Howden, S. E., Diol, N. R., Propson, N. E., Wagner, R., Lee, G. O., Antosiewicz-Bourget, J., Teng, J. M. C. and Thomson, J. A. (2011). Chemically defined conditions for human iPSC derivation and culture. Nature Methods, 8(5), 424–429.

Dambrot, C., Braam, S. R., Tertoolen, L. G. J., Birket, M., Atsma, D. E. and Mummery, C. L. (2014). Serum supplemented culture medium masks hypertrophic phenotypes in human pluripotent stem cell derived cardiomyocytes. Journal of Cellular and Molecular Medicine, 18(8), 1509–1518.

Dubois, N. C., Craft, A. M., Sharma, P., Elliott, D. A., Stanley, E. G., Elefanty, A. G., Gramolini, A. and Keller, G. (2011). SIRPA is a specific cell-surface marker for isolating cardiomyocytes derived from human pluripotent stem cells. Nature Biotechnology, 29(11), 1011–1018.

Duncker, D. J., Bakkers, J., Brundel, B. J., Robbins, J., Tardiff, J. C. and Carrier, L. (2015). Animal- and in silico models for the study of sarcomeric cardiomyopathies. Cardiovascular Research, 105(4), 439–448.

Eiselleova, L., Peterkova, I., Neradil, J., Slaninova, I., Hampl, A. and Dvorak, P. (2008). Comparative study of mouse and human feeder cells for human embryonic stem cells. The International Journal of Developmental Biology, 52(4), 353–363.

Elliott, P., Andersson, B., Arbustini, E., Bilinska, Z., Cecchi, F., Charron, P., Dubourg, O., Kühl, U., Maisch, B., McKenna, W. J., Monserrat, L., Pankuweit, S., Rapezzi, C., Seferovic, P., Tavazzi, L. and Keren, A. (2008). Classification of the cardiomyopathies: a position statement from the European Society Of Cardiology Working Group on Myocardial and Pericardial Diseases. European Heart Journal, 29(2), 270–276.

Eschenhagen, T., Mummery, C. and Knollmann, B. C. (2015). Modelling sarcomeric cardiomyopathies in the dish: from human heart samples to iPSC cardiomyocytes. Cardiovascular Research, 105(4), 424–438.

Fatima, A., Xu, G., Shao, K., Papadopoulos, S., Lehmann, M., Arnáiz-Cot, J. J., Rosa, A. O., Nguemo, F., Matzkies, M., Dittmann, S., Stone, S. L., Linke, M., Zechner, U., Beyer, V., Hennies, H. C., Rosenkranz, S., Klauke, B., Parwani, A. S., Haverkamp, W., Pfitzer, G., Farr, M., Cleemann, L., Morad, M., Milting, H., Hescheler, J. and Saric, T. (2011). In vitro modeling of ryanodine receptor 2 dysfunction using human induced pluripotent stem cells. Cellular Physiology and Biochemistry, 28(4), 579–592.

Fusaki, N., Ban, H., Nishiyama, A., Saeki, K. and Hasegawa, M. (2009). Efficient induction of transgene-free human pluripotent stem cells using a vector based on Sendai virus, an RNA virus that does not integrate into the host genome. Proceedings of the Japan Academy. Series B, Physical and Biological Sciences, 85(8), 348–362.

Garitaonandia, I., Amir, H., Boscolo, F. S., Wambua, G. K., Schultheisz, H. L., Sabatini, K., Morey, R., Waltz, S., Wang, Y.-C., Tran, H., Leonardo, T. R., Nazor, K., Slavin, I., Lynch, C., Li, Y., Coleman, R., Gallego Romero, I., Altun, G., Reynolds, D., Dalton, S., Parast, M., Loring, J. F. and Laurent, L. C. (2015). Increased risk of genetic and epigenetic instability in human embryonic stem cells associated with specific culture conditions. PloS ONE, 10(2), e0118307.

George, A. L. (2013). Molecular and genetic basis of sudden cardiac death. The Journal of Clinical Investigation, 123(1), 75–83.

Graichen, R., Xu, X., Braam, S. R., Balakrishnan, T., Norfiza, S., Sieh, S., Soo, S. Y., Tham, S. C., Mummery, C., Colman, A., Zweigerdt, R. and Davidson, B. P. (2008). Enhanced cardiomyogenesis of human embryonic stem cells by a small molecular inhibitor of p38 MAPK. Differentiation, 76(4), 357–370.

Grynkiewicz, G., Poenie, M. and Tsien, R. Y. (1985). A new generation of Ca2+ indicators with greatly improved fluorescence properties. The Journal of Biological Chemistry, 260(6), 3440–3450.

Gurdon, J. B. (1962). The developmental capacity of nuclei taken from intestinal epithelium cells of feeding tadpoles. Journal of Embryology and Experimental Morphology, 10, 622–640.

Hamill, O., Marty, A., Neher, E., Sakmann, B. and Sigworth, F. (1981). Improved patch-clamp techniques for high-resolution current recording from cells and cell-free membrane patches. Pflügers Archiv : European Journal of Physiology, 2(391), 85–100.

Han, L., Li, Y., Tchao, J., Kaplan, A. D., Lin, B., Li, Y., Mich-Basso, J., Lis, A., Hassan, N., London, B., Bett, G. C. L., Tobita, K., Rasmusson, R. L. and Yang, L. (2014). Study familial hypertrophic cardiomyopathy using patient-specific induced pluripotent stem cells. Cardiovascular Research, 104(2), 258–269.

Harris, S. P., Lyons, R. G. and Bezold, K. L. (2011). In the thick of it: HCM-causing mutations in myosin binding proteins of the thick filament. Circulation Research, 108(6), 751–764.

Hay, D. C., Fletcher, J., Payne, C., Terrace, J. D., Gallagher, R. C. J., Snoeys, J., Black, J. R., Wojtacha, D., Samuel, K., Hannoun, Z., Pryde, A., Filippi, C., Currie, I. S., Forbes, S. J., Ross, J. A., Newsome, P. N. and Iredale, J. P. (2008). Highly efficient differentiation of hESCs to functional hepatic endoderm requires ActivinA and Wnt3a signaling. Proceedings of the National Academy of Sciences of the United States of America, 105(34), 12301–12306.

Helms, A. S., Davis, F. M., Coleman, D., Bartolone, S. N., Glazier, A. A., Pagani, F., Yob, J. M., Sadayappan, S., Pedersen, E., Lyons, R., Westfall, M. V, Jones, R., Russell, M. W.

and Day, S. M. (2014). Sarcomere mutation-specific expression patterns in human hypertrophic cardiomyopathy. Circulation. Cardiovascular Genetics, 7(4), 434–443.
Hendriks, S., Dancet, E. A. F., van Pelt, A. M. M., Hamer, G. and Repping, S. (2015). Artificial gametes: a systematic review of biological progress towards clinical application. Human Reproduction Update, 21(3), 285–296.
Hisamatsu-Sakamoto, M., Sakamoto, N. and Rosenberg, A. S. (2008). Embryonic stem cells cultured in serum-free medium acquire bovine apolipoprotein B-100 from feeder cell layers and serum replacement medium. Stem Cells, 26(1), 72–78.
Ho, C. Y., Charron, P., Richard, P., Girolami, F., van Spaendonck-Zwarts, K. Y. and Pinto, Y. (2015). Genetic advances in sarcomeric cardiomyopathies: state of the art. Cardiovascular Research, 105(4), 397–408.
Ho, C. Y., Lakdawala, N. K., Cirino, A. L., Lipshultz, S. E., Sparks, E., Abbasi, S. A., Kwong, R. Y., Antman, E. M., Semsarian, C., González, A., López, B., Diez, J., Orav, E. J., Colan, S. D. and Seidman, C. E. (2014). Diltiazem treatment for pre-clinical hypertrophic cardiomyopathy sarcomere Mutation carriers: a pilot randomized trial to modify disease expression. Journal of the American College of Cardiology; Heart Failure, 3(2), 180–188.
Hoffman, L. M. and Carpenter, M. K. (2005). Characterization and culture of human embryonic stem cells. Nature Biotechnology, 23(6), 699–708.
Hovatta, O., Mikkola, M., Gertow, K., Strömberg, A.-M., Inzunza, J., Hreinsson, J., Rozell, B., Blennow, E., Andäng, M. and Ahrlund-Richter, L. (2003). A culture system using human foreskin fibroblasts as feeder cells allows production of human embryonic stem cells. Human Reproduction, 18(7), 1404–1409.
Hu, K. (2014). All roads lead to induced pluripotent stem cells: the technologies of iPSC generation. Stem Cells and Development, 23(12), 1285–1300.
Huke, S., Venkataraman, R., Faggioni, M., Bennuri, S., Hwang, H. S., Baudenbacher, F. and Knollmann, B. C. (2013). Focal energy deprivation underlies arrhythmia susceptibility in mice with calcium-sensitized myofilaments. Circulation Research, 112(10), 1334–1344.
Hussein, S. M., Batada, N. N., Vuoristo, S., Ching, R. W., Autio, R., Närvä, E., Ng, S., Sourour, M., Hämäläinen, R., Olsson, C., Lundin, K., Mikkola, M., Trokovic, R., Peitz, M., Brüstle, O., Bazett-Jones, D. P., Alitalo, K., Lahesmaa, R., Nagy, A. and Otonkoski, T. (2011). Copy number variation and selection during reprogramming to pluripotency. Nature, 471(7336), 58–62.
Itskovitz-Eldor, J., Schuldiner, M., Karsenti, D., Eden, A., Yanuka, O., Amit, M., Soreq, H. and Benvenisty, N. (2000). Differentiation of human embryonic stem cells into embryoid bodies compromising the three embryonic germ layers. Molecular Medicine, 6(2), 88–95.
Jagatheesan, G., Rajan, S., Petrashevskaya, N., Schwartz, A., Boivin, G., Arteaga, G., de Tombe, P. P., Solaro, R. J. and Wieczorek, D. F. (2004). Physiological significance of troponin T binding domains in striated muscle tropomyosin. American Journal of Physiology. Heart and Circulatory Physiology, 287(4), H1484–1494.
Jääskeläinen, P., Heliö, T., Aalto-Setälä, K., Kaartinen, M., Ilveskoski, E., Hämäläinen, L., Melin, J., Kärkkäinen, S., Peuhkurinen, K., Nieminen, M. S., Laakso, M. and Kuusisto, J. (2014). A new common mutation in the cardiac beta-myosin heavy chain gene in Finnish patients with hypertrophic cardiomyopathy. Annals of Medicine, 46(6), 424–429.

Jääskeläinen, P., Heliö, T., Aalto-Setälä, K., Kaartinen, M., Ilveskoski, E., Hämäläinen, L., Melin, J., Nieminen, M. S., Laakso, M., Kuusisto, J., Kervinen, H., Mustonen, J., Juvonen, J., Niemi, M., Uusimaa, P., Huttunen, M., Kotila, M. and Pietilä, M. (2013). Two founder mutations in the alpha-tropomyosin and the cardiac myosin-binding protein C genes are common causes of hypertrophic cardiomyopathy in the Finnish population. Annals of Medicine, 45(1), 85–90.

Jääskeläinen, P., Kuusisto, J., Miettinen, R., Kärkkäinen, P., Kärkkäinen, S., Heikkinen, S., Peltola, P., Pihlajamäki, J., Vauhkonen, I. and Laakso, M. (2002). Mutations in the cardiac myosin-binding protein C gene are the predominant cause of familial hypertrophic cardiomyopathy in eastern Finland. Journal of Molecular Medicine, 80(7), 412–422.

Jääskeläinen, P., Miettinen, R., Kärkkäinen, P., Toivonen, L., Laakso, M. and Kuusisto, J. (2004). Genetics of hypertrophic cardiomyopathy in eastern Finland: few founder mutations with benign or intermediary phenotypes. Annals of Medicine, 36(1), 23–32.

Kaji, K., Norrby, K., Paca, A., Mileikovsky, M., Mohseni, P. and Woltjen, K. (2009). Virus-free induction of pluripotency and subsequent excision of reprogramming factors. Nature, 458(7239), 771–775.

Kamakura, T., Makiyama, T., Sasaki, K., Yoshida, Y., Wuriyanghai, Y., Chen, J., Hattori, T., Ohno, S., Kita, T., Horie, M., Yamanaka, S. and Kimura, T. (2013). Ultrastructural maturation of human-induced pluripotent stem cell-derived cardiomyocytes in a long-term culture. Circulation Journal, 77(5), 1307–1314.

Kattman, S. J., Witty, A. D., Gagliardi, M., Dubois, N. C., Niapour, M., Hotta, A., Ellis, J. and Keller, G. (2011). Stage-specific optimization of activin/nodal and BMP signaling promotes cardiac differentiation of mouse and human pluripotent stem cell lines. Cell Stem Cell, 8(2), 228–240.

Katz, A. M. (2001). Physiology of the Heart: 4th Edition.

Kehat, I., Gepstein, A., Spira, A., Itskovitz-Eldor, J. and Gepstein, L. (2002). High-resolution electrophysiological assessment of human embryonic stem cell-derived cardiomyocytes: a novel in vitro model for the study of conduction. Circulation Research, 91(8), 659–661.

Kehat, I., Kenyagin-Karsenti, D., Snir, M., Segev, H., Amit, M., Gepstein, A., Livne, E., Binah, O., Itskovitz-Eldor, J. and Gepstein, L. (2001). Human embryonic stem cells can differentiate into myocytes with structural and functional properties of cardiomyocytes. The Journal of Clinical Investigation, 108(3), 407–414.

Khan, M., Narayanan, K., Lu, H., Choo, Y., Du, C., Wiradharma, N., Yang, Y.-Y. and Wan, A. C. A. (2013). Delivery of reprogramming factors into fibroblasts for generation of non-genetic induced pluripotent stem cells using a cationic bolaamphiphile as a non-viral vector. Biomaterials, 34(21), 5336–5343.

Kleinman, H. K., McGarvey, M. L., Liotta, L. A., Robey, P. G., Tryggvason, K. and Martin, G. R. (1982). Isolation and characterization of type IV procollagen, laminin, and heparan sulfate proteoglycan from the EHS sarcoma. Biochemistry, 21(24), 6188–6193.

Klimanskaya, I., Chung, Y., Becker, S., Lu, S.-J. and Lanza, R. (2006). Human embryonic stem cell lines derived from single blastomeres. Nature, 444(7118), 481–485.

Kocovski, L. and Fernandes, J. (2015). Sudden cardiac death: a modern pathology approach to hypertrophic cardiomyopathy. Archives of Pathology & Laboratory Medicine, 139(3), 413–416.

Kolossov, E., Lu, Z., Drobinskaya, I., Gassanov, N., Duan, Y., Sauer, H., Manzke, O., Bloch, W., Bohlen, H., Hescheler, J. and Fleischmann, B. K. (2005). Identification and characterization of embryonic stem cell-derived pacemaker and atrial cardiomyocytes. The Journal of the Federation of American Societies for Experimental Biology, 19(6), 577–579.

Kreutzer, J., Ikonen, L., Hirvonen, J., Pekkanen-Mattila, M., Aalto-Setälä, K. and Kallio, P. (2014). Pneumatic cell stretching system for cardiac differentiation and culture. Medical Engineering & Physics, 36(4), 496–501.

Kujala, K., Ahola, A., Pekkanen-Mattila, M., Ikonen, L., Kerkelä, E., Hyttinen, J. and Aalto-Setälä, K. (2012b). Electrical field stimulation with a novel platform: effect on cardiomyocyte gene expression but not on orientation. International Journal of Biomedical Science : IJBS, 8(2), 109–120.

Kujala, K., Paavola, J., Lahti, A., Larsson, K., Pekkanen-Mattila, M., Viitasalo, M., Lahtinen, A. M., Toivonen, L., Kontula, K., Swan, H., Laine, M., Silvennoinen, O. and Aalto-Setälä, K. (2012a). Cell model of catecholaminergic polymorphic ventricular tachycardia reveals early and delayed afterdepolarizations. PLoS ONE, 7(9), e44660.

Laflamme, M. A., Chen, K. Y., Naumova, A. V, Muskheli, V., Fugate, J. A., Dupras, S. K., Reinecke, H., Xu, C., Hassanipour, M., Police, S., O'Sullivan, C., Collins, L., Chen, Y., Minami, E., Gill, E. A., Ueno, S., Yuan, C., Gold, J. and Murry, C. E. (2007). Cardiomyocytes derived from human embryonic stem cells in pro-survival factors enhance function of infarcted rat hearts. Nature Biotechnology, 25(9), 1015–1024.

Lahti, A. L., Kujala, V. J., Chapman, H., Koivisto, A.-P., Pekkanen-Mattila, M., Kerkelä, E., Hyttinen, J., Kontula, K., Swan, H., Conklin, B. R., Yamanaka, S., Silvennoinen, O. and Aalto-Setälä, K. (2012). Model for long QT syndrome type 2 using human iPS cells demonstrates arrhythmogenic characteristics in cell culture. Disease Models & Mechanisms, 5(2), 220–230.

Lan, F., Lee, A. S., Liang, P., Sanchez-Freire, V., Nguyen, P. K., Wang, L., Han, L., Yen, M., Wang, Y., Sun, N., Abilez, O. J., Hu, S., Ebert, A. D., Navarrete, E. G., Simmons, C. S., Wheeler, M., Pruitt, B., Lewis, R., Yamaguchi, Y., Ashley, E. a, Bers, D. M., Robbins, R. C., Longaker, M. T. and Wu, J. C. (2013). Abnormal calcium handling properties underlie familial hypertrophic cardiomyopathy pathology in patient-specific induced pluripotent stem cells. Cell Stem Cell, 12(1), 101–113.

Laurent, L. C., Ulitsky, I., Slavin, I., Tran, H., Schork, A., Morey, R., Lynch, C., Harness, J. V, Lee, S., Barrero, M. J., Ku, S., Martynova, M., Semechkin, R., Galat, V., Gottesfeld, J., Izpisua Belmonte, J. C., Murry, C., Keirstead, H. S., Park, H.-S., Schmidt, U., Laslett, A. L., Muller, F.-J., Nievergelt, C. M., Shamir, R. and Loring, J. F. (2011). Dynamic changes in the copy number of pluripotency and cell proliferation genes in human ESCs and iPSCs during reprogramming and time in culture. Cell Stem Cell, 8(1), 106–118.

Lee, C. H., Kim, J.-H., Lee, H. J., Jeon, K., Lim, H., Choi, H. yeon, Lee, E.-R., Park, S. H., Park, J.-Y., Hong, S., Kim, S. and Cho, S.-G. (2011). The generation of iPS cells using non-viral magnetic nanoparticle based transfection. Biomaterials, 32(28), 6683–6691.

Lee, J. B., Graham, M., Collins, T. J., Lee, J.-H., Hong, S.-H., Mcnicol, A. J., Shapovalova, Z. and Bhatia, M. (2015). Reversible lineage-specific priming of human embryonic stem cells can be exploited to optimize the yield of differentiated cells. Stem Cells, 33(4), 1142–1152.

Li, M., Suzuki, K., Kim, N. Y., Liu, G.-H. and Izpisua Belmonte, J. C. (2014). A cut above the rest: targeted genome editing technologies in human pluripotent stem cells. The Journal of Biological Chemistry, 289(8), 4594–4599.

Lian, X., Hsiao, C., Wilson, G., Zhu, K., Hazeltine, L. B., Azarin, S. M., Raval, K. K., Zhang, J., Kamp, T. J. and Palecek, S. P. (2012). Robust cardiomyocyte differentiation from human pluripotent stem cells via temporal modulation of canonical Wnt signaling. Proceedings of the National Academy of Sciences of the United States of America, 109(27), E1848–1857.

Lopes, L. R. and Elliott, P. M. (2014). A straightforward guide to the sarcomeric basis of cardiomyopathies. Heart, 100(24), 1916–1923.

Ludwig, T. E., Bergendahl, V., Levenstein, M. E., Yu, J., Probasco, M. D. and Thomson, J. A. (2006b). Feeder-independent culture of human embryonic stem cells. Nature Methods, 3(8), 637–646.

Ludwig, T. E., Levenstein, M. E., Jones, J. M., Berggren, W. T., Mitchen, E. R., Frane, J. L., Crandall, L. J., Daigh, C. A., Conard, K. R., Piekarczyk, M. S., Llanas, R. A. and Thomson, J. A. (2006a). Derivation of human embryonic stem cells in defined conditions. Nature Biotechnology, 24(2), 185–187.

Lund, R. J., Nikula, T., Rahkonen, N., Närvä, E., Baker, D., Harrison, N., Andrews, P., Otonkoski, T. and Lahesmaa, R. (2012a). High-throughput karyotyping of human pluripotent stem cells. Stem Cell Research, 9(3), 192–195.

Lund, R. J., Närvä, E. and Lahesmaa, R. (2012b). Genetic and epigenetic stability of human pluripotent stem cells. Nature Reviews. Genetics, 13(10), 732–744.

Lundy, S. D., Zhu, W.-Z., Regnier, M. and Laflamme, M. A. (2013). Structural and functional maturation of cardiomyocytes derived from human pluripotent stem cells. Stem Cells and Development, 22(14), 1991–2002.

Maron, B. J., Maron, M. S. and Semsarian, C. (2012). Double or compound sarcomere mutations in hypertrophic cardiomyopathy: a potential link to sudden death in the absence of conventional risk factors. Heart Rhythm, 9(1), 57–63.

Maron, B. J., Niimura, H., Casey, S. A., Soper, M. K., Wright, G. B., Seidman, J. G. and Seidman, C. E. (2001). Development of left ventricular hypertrophy in adults in hypertrophic cardiomyopathy caused by cardiac myosin-binding protein C gene mutations. Journal of the American College of Cardiology, 38(2), 315–321.

Maron, B. J., Ommen, S. R., Semsarian, C., Spirito, P., Olivotto, I. and Maron, M. S. (2014). Hypertrophic cardiomyopathy: present and future, with translation into contemporary cardiovascular medicine. Journal of the American College of Cardiology, 64(1), 83–99.

Marston, S., Copeland, O., Jacques, A., Livesey, K., Tsang, V., McKenna, W. J., Jalilzadeh, S., Carballo, S., Redwood, C. and Watkins, H. (2009). Evidence from human myectomy samples that MYBPC3 mutations cause hypertrophic cardiomyopathy through haploinsufficiency. Circulation Research, 105(3), 219–222.

Martin, M. J., Muotri, A., Gage, F. and Varki, A. (2005). Human embryonic stem cells express an immunogenic nonhuman sialic acid. Nature Medicine, 11(2), 228–232.

Martinez-Fernandez, A., Nelson, T. J., Reyes, S., Alekseev, A. E., Secreto, F., Perez-Terzic, C., Beraldi, R., Sung, H.-K., Nagy, A. and Terzic, A. (2014). iPS cell-derived cardiogenicity is hindered by sustained integration of reprogramming transgenes. Circulation. Cardiovascular Genetics, 7(5), 667–676.

Matsui, T., Leung, D., Miyashita, H., Maksakova, I. A., Miyachi, H., Kimura, H., Tachibana, M., Lorincz, M. C. and Shinkai, Y. (2010). Proviral silencing in embryonic stem cells requires the histone methyltransferase ESET. Nature, 464(7290), 927–931.

Mikkelsen, T. S., Hanna, J., Zhang, X., Ku, M., Wernig, M., Schorderet, P., Bernstein, B. E., Jaenisch, R., Lander, E. S. and Meissner, A. (2008). Dissecting direct reprogramming through integrative genomic analysis. Nature, 454(7200), 49–55.

Minami, I., Yamada, K., Otsuji, T. G., Yamamoto, T., Shen, Y., Otsuka, S., Kadota, S., Morone, N., Barve, M., Asai, Y., Tenkova-Heuser, T., Heuser, J. E., Uesugi, M., Aiba, K. and Nakatsuji, N. (2012). A small molecule that promotes cardiac differentiation of human pluripotent stem cells under defined, cytokine- and xeno-free conditions. Cell Reports, 2(5), 1448–1460.

Mitalipova, M. M., Rao, R. R., Hoyer, D. M., Johnson, J. A., Meisner, L. F., Jones, K. L., Dalton, S. and Stice, S. L. (2005). Preserving the genetic integrity of human embryonic stem cells. Nature Biotechnology, 23(1), 19–20.

Mohr, J. C., Zhang, J., Azarin, S. M., Soerens, A. G., de Pablo, J. J., Thomson, J. A., Lyons, G. E., Palecek, S. P. and Kamp, T. J. (2010). The microwell control of embryoid body size in order to regulate cardiac differentiation of human embryonic stem cells. Biomaterials, 31(7), 1885–1893.

Moretti, A., Bellin, M., Welling, A., Jung, C. B., Lam, J. T., Bott-Flügel, L., Dorn, T., Goedel, A., Höhnke, C., Hofmann, F., Seyfarth, M., Sinnecker, D., Schömig, A. and Laugwitz, K.-L. (2010). Patient-specific induced pluripotent stem-cell models for long-QT syndrome. The New England Journal of Medicine, 363(15), 1397–1409.

Mummery, C., Ward-van Oostwaard, D., Doevendans, P., Spijker, R., van den Brink, S., Hassink, R., van der Heyden, M., Opthof, T., Pera, M., de la Riviere, A. B., Passier, R. and Tertoolen, L. (2003). Differentiation of human embryonic stem cells to cardiomyocytes: role of coculture with visceral endoderm-like cells. Circulation, 107(21), 2733–2740.

Mummery, C., Zhang, J., Ng, E. S., Elliott, D. A., Elefanty, A. G. and Kamp, T. J. (2012). Differentiation of human embryonic stem cells and induced pluripotent stem cells to cardiomyocytes: a methods overview. Circulation Research, 111(3), 344–358.

Muthuchamy, M., Pieples, K., Rethinasamy, P., Hoit, B., Grupp, I. L., Boivin, G. P., Wolska, B., Evans, C., Solaro, R. J. and Wieczorek, D. F. (1999). Mouse model of a familial hypertrophic cardiomyopathy mutation in alpha-tropomyosin manifests cardiac dysfunction. Circulation Research, 85(1), 47–56.

Nandivada, H., Villa-Diaz, L. G., O'Shea, K. S., Smith, G. D., Krebsbach, P. H. and Lahann, J. (2011). Fabrication of synthetic polymer coatings and their use in feeder-free culture of human embryonic stem cells. Nature Protocols, 6(7), 1037–1043.

Nat, R., Nilbratt, M., Narkilahti, S., Winblad, B., Hovatta, O. and Nordberg, A. (2007). Neurogenic neuroepithelial and radial glial cells generated from six human embryonic stem cell lines in serum-free suspension and adherent cultures. Glia, 55(4), 385–399.

Nerbonne, J. M. and Kass, R. S. (2005). Molecular physiology of cardiac repolarization. Physiological Reviews, 85(4), 1205–1253.

Niimura, H., Bachinski, L. L., Sangwatanaroj, S., Watkins, H., Chudley, A. E., McKenna, W., Kristinsson, A., Roberts, R., Sole, M., Maron, B. J., Seidman, J. G. and Seidman, C. E. (1998). Mutations in the gene for cardiac myosin-binding protein C and late-onset familial hypertrophic cardiomyopathy. The New England Journal of Medicine, 338(18), 1248–1257.

Nunes, S. S., Miklas, J. W., Liu, J., Aschar-Sobbi, R., Xiao, Y., Zhang, B., Jiang, J., Massé, S., Gagliardi, M., Hsieh, A., Thavandiran, N., Laflamme, M. A., Nanthakumar, K., Gross, G. J., Backx, P. H., Keller, G. and Radisic, M. (2013). Biowire: a platform for maturation of human pluripotent stem cell-derived cardiomyocytes. Nature Methods, 10(8), 781–787.

Okita, K., Matsumura, Y., Sato, Y., Okada, A., Morizane, A., Okamoto, S., Hong, H., Nakagawa, M., Tanabe, K., Tezuka, K., Shibata, T., Kunisada, T., Takahashi, M., Takahashi, J., Saji, H. and Yamanaka, S. (2011). A more efficient method to generate integration-free human iPS cells. Nature Methods, 8(5), 409–412.

Osafune, K., Caron, L., Borowiak, M., Martinez, R. J., Fitz-Gerald, C. S., Sato, Y., Cowan, C. A., Chien, K. R. and Melton, D. A. (2008). Marked differences in differentiation propensity among human embryonic stem cell lines. Nature Biotechnology, 26(3), 313–315.

Otsuji, T. G., Minami, I., Kurose, Y., Yamauchi, K., Tada, M. and Nakatsuji, N. (2010). Progressive maturation in contracting cardiomyocytes derived from human embryonic stem cells: Qualitative effects on electrophysiological responses to drugs. Stem Cell Research, 4(3), 201–213.

Park, H.-J., Shin, J., Kim, J. and Cho, S.-W. (2014). Nonviral delivery for reprogramming to pluripotency and differentiation. Archives of Pharmacal Research, 37(1), 107–119.

Park, S.-P., Lee, Y. J., Lee, K. S., Ah Shin, H., Cho, H. Y., Chung, K. S., Kim, E. Y. and Lim, J. H. (2004). Establishment of human embryonic stem cell lines from frozen-thawed blastocysts using STO cell feeder layers. Human Reproduction, 19(3), 676–684.

Passier, R., Oostwaard, D. W., Snapper, J., Kloots, J., Hassink, R. J., Kuijk, E., Roelen, B., de la Riviere, A. B. and Mummery, C. (2005). Increased cardiomyocyte differentiation from human embryonic stem cells in serum-free cultures. Stem Cells, 23(6), 772–780.

Pekkanen-Mattila, M., Kerkelä, E., Tanskanen, J. M. A., Pietilä, M., Pelto-Huikko, M., Hyttinen, J., Skottman, H., Suuronen, R. and Aalto-Setälä, K. (2009). Substantial variation in the cardiac differentiation of human embryonic stem cell lines derived and propagated under the same conditions-a comparison of multiple cell lines. Annals of Medicine, 41(5), 360–370.

Pekkanen-Mattila, M., Ojala, M., Kerkelä, E., Rajala, K., Skottman, H. and Aalto-Setälä, K. (2012). The effect of human and mouse fibroblast feeder cells on cardiac differentiation of human pluripotent stem cells. Stem Cells International, Article ID 875059.

Pekkanen-Mattila, M., Pelto-Huikko, M., Kujala, V., Suuronen, R., Skottman, H., Aalto-Setälä, K. and Kerkelä, E. (2010). Spatial and temporal expression pattern of germ layer markers during human embryonic stem cell differentiation in embryoid bodies. Histochemistry and Cell Biology, 133(5), 595–606.

Price, P., Goldsborough, M. and Tilkins, M. (1998). Embryonic stem cell serum replacement. International Patent Application WO 98/30679.

Rajala, K., Pekkanen-Mattila, M. and Aalto-Setälä, K. (2011). Cardiac differentiation of pluripotent stem cells. Stem Cells International, Article ID 383709.

Redwood, C. and Robinson, P. (2013). Alpha-tropomyosin mutations in inherited cardiomyopathies. Journal of Muscle Research and Cell Motility, 34(3-4), 285–294.

Reppel, M., Pillekamp, F., Lu, Z. J., Halbach, M., Brockmeier, K., Fleischmann, B. K. and Hescheler, J. (2004). Microelectrode arrays: a new tool to measure embryonic heart activity. Journal of Electrocardiology, 37(supplement), 104–109.

Richards, M., Fong, C.-Y., Chan, W.-K., Wong, P.-C. and Bongso, A. (2002). Human feeders support prolonged undifferentiated growth of human inner cell masses and embryonic stem cells. Nature Biotechnology, 20(9), 933–936.

Richards, M., Tan, S.-P., Tan, J.-H., Chan, W.-K. and Bongso, A. (2004). The transcriptome profile of human embryonic stem cells as defined by SAGE. Stem Cells, 22(1), 51–64.

Rodin, S., Antonsson, L., Niaudet, C., Simonson, O. E., Salmela, E., Hansson, E. M., Domogatskaya, A., Xiao, Z., Damdimopoulou, P., Sheikhi, M., Inzunza, J., Nilsson, A.-S., Baker, D., Kuiper, R., Sun, Y., Blennow, E., Nordenskjöld, M., Grinnemo, K.-H., Kere, J., Betsholtz, C., Hovatta, O. and Tryggvason, K. (2014). Clonal culturing of human embryonic stem cells on laminin-521/E-cadherin matrix in defined and xeno-free environment. Nature Communications, 5, Article number 3195.

Rodin, S., Domogatskaya, A., Ström, S., Hansson, E. M., Chien, K. R., Inzunza, J., Hovatta, O. and Tryggvason, K. (2010). Long-term self-renewal of human pluripotent stem cells on human recombinant laminin-511. Nature Biotechnology, 28(6), 611–615.

Roma-Rodrigues, C. and Fernandes, A. R. (2014). Genetics of hypertrophic cardiomyopathy: advances and pitfalls in molecular diagnosis and therapy. The Application of Clinical Genetics, 7, 195–208.

Rottbauer, W., Gautel, M., Zehelein, J., Labeit, S., Franz, W. M., Fischer, C., Vollrath, B., Mall, G., Dietz, R., Kübler, W. and Katus, H. a. (1997). Novel splice donor site mutation in the cardiac myosin-binding protein-C gene in familial hypertrophic cardiomyopathy. Characterization Of cardiac transcript and protein. The Journal of Clinical Investigation, 100(2), 475–482.

Sakmann, B. and Neher, E. (1984). Patch clamp techniques for studying ionic channels in excitable membranes. Annual Review of Physiology, 46, 455–472.

Sarantitis, I., Papanastasopoulos, P., Manousi, M., Baikoussis, N. G. and Apostolakis, E. (2012). The cytoskeleton of the cardiac muscle cell. Hellenic Journal of Cardiology, 53(5), 367–379.

Sartiani, L., Bettiol, E., Stillitano, F., Mugelli, A., Cerbai, E. and Jaconi, M. E. (2007). Developmental changes in cardiomyocytes differentiated from human embryonic stem cells: a molecular and electrophysiological approach. Stem Cells, 25(5), 1136–1144.

Sato, N., Sanjuan, I. M., Heke, M., Uchida, M., Naef, F. and Brivanlou, A. H. (2003). Molecular signature of human embryonic stem cells and its comparison with the mouse. Developmental Biology, 260(2), 404–413.

Savla, J. J., Nelson, B. C., Perry, C. N. and Adler, E. D. (2014). Induced pluripotent stem cells for the study of cardiovascular disease. Journal of the American College of Cardiology, 64(5), 512–519.

Schober, T., Huke, S., Venkataraman, R., Gryshchenko, O., Kryshtal, D., Hwang, H. S., Baudenbacher, F. J. and Knollmann, B. C. (2012). Myofilament Ca sensitization increases cytosolic Ca binding affinity, alters intracellular Ca homeostasis, and causes pause-dependent Ca-triggered arrhythmia. Circulation Research, 111(2), 170–179.

Sequeira, V., Wijnker, P. J. M., Nijenkamp, L. L. a M., Kuster, D. W. D., Najafi, A., Witjas-Paalberends, E. R., Regan, J. a., Boontje, N., Ten Cate, F. J., Germans, T., Carrier, L., Sadayappan, S., Van Slegtenhorst, M. a., Zaremba, R., Foster, D. B., Murphy, A. M., Poggesi, C., Dos Remedios, C., Stienen, G. J. M., Ho, C. Y., Michels, M. and Van Der Velden, J. (2013). Perturbed length-dependent activation in human hypertrophic

cardiomyopathy with missense sarcomeric gene mutations. Circulation Research, 112(11), 1491–1505.

Sequeira, V., Witjas-Paalberends, E. R., Kuster, D. W. D. and van der Velden, J. (2014). Cardiac myosin-binding protein C: hypertrophic cardiomyopathy mutations and structure-function relationships. Pflügers Archiv : European Journal of Physiology, 466(2), 201–206.

Skottman, H. (2010). Derivation and characterization of three new human embryonic stem cell lines in Finland. In Vitro Cellular & Developmental Biology. Animal, 46(3-4), 206–209.

Soldner, F., Hockemeyer, D., Beard, C., Gao, Q., Bell, G. W., Cook, E. G., Hargus, G., Blak, A., Cooper, O., Mitalipova, M., Isacson, O. and Jaenisch, R. (2009). Parkinson's disease patient-derived induced pluripotent stem cells free of viral reprogramming factors. Cell, 136(5), 964–977.

Sridharan, R., Tchieu, J., Mason, M. J., Yachechko, R., Kuoy, E., Horvath, S., Zhou, Q. and Plath, K. (2009). Role of the murine reprogramming factors in the induction of pluripotency. Cell, 136(2), 364–377.

Stadtfeld, M., Nagaya, M., Utikal, J., Weir, G. and Hochedlinger, K. (2008). Induced pluripotent stem cells generated without viral integration. Science, 322(5903), 945–949.

Stoehr, A., Neuber, C., Baldauf, C., Vollert, I., Friedrich, F. W., Flenner, F., Carrier, L., Eder, A., Schaaf, S., Hirt, M. N., Aksehirlioglu, B., Tong, C. W., Moretti, A., Eschenhagen, T. and Hansen, A. (2014). Automated analysis of contractile force and Ca2+ transients in engineered heart tissue. AJP: Heart and Circulatory Physiology, 306(9), H1353–H1363.

Stojkovic, P., Lako, M., Stewart, R., Przyborski, S., Armstrong, L., Evans, J., Murdoch, A., Strachan, T. and Stojkovic, M. (2005). An autogeneic feeder cell system that efficiently supports growth of undifferentiated human embryonic stem cells. Stem Cells, 23(3), 306–314.

Strelchenko, N., Verlinsky, O., Kukharenko, V. and Verlinsky, Y. (2004). Morula-derived human embryonic stem cells. Reproductive Biomedicine Online, 9(6), 623–629.

Sun, N., Yazawa, M., Liu, J., Han, L., Sanchez-Freire, V., Abilez, O. J., Navarrete, E. G., Hu, S., Wang, L., Lee, a, Pavlovic, a, Lin, S., Chen, R., Hajjar, R. J., Snyder, M. P., Dolmetsch, R. E., Butte, M. J., Ashley, E. a, Longaker, M. T., Robbins, R. C. and Wu, J. C. (2012). Patient-specific induced pluripotent stem cells as a model for familial dilated cardiomyopathy. Science Translational Medicine, 4(130), 130ra47.

Taapken, S. M., Nisler, B. S., Newton, M. A., Sampsell-Barron, T. L., Leonhard, K. A., McIntire, E. M. and Montgomery, K. D. (2011). Karyotypic abnormalities in human induced pluripotent stem cells and embryonic stem cells. Nature Biotechnology, 29(4), 313–314.

Takahashi, K., Tanabe, K., Ohnuki, M., Narita, M., Ichisaka, T., Tomoda, K. and Yamanaka, S. (2007). Induction of pluripotent stem cells from adult human fibroblasts by defined factors. Cell, 131(5), 861–872.

Takahashi, K. and Yamanaka, S. (2006). Induction of pluripotent stem cells from mouse embryonic and adult fibroblast cultures by defined factors. Cell, 126(4), 663–676.

Tanaka, A., Yuasa, S., Mearini, G., Egashira, T., Seki, T., Kodaira, M., Kusumoto, D., Kuroda, Y., Okata, S., Suzuki, T., Inohara, T., Arimura, T., Makino, S., Kimura, K., Kimura, A., Furukawa, T., Carrier, L., Node, K. and Fukuda, K. (2014). Endothelin-

1 induces myofibrillar disarray and contractile vector variability in hypertrophic cardiomyopathy-induced pluripotent stem cell-derived cardiomyocytes. Journal of the American Heart Association, 3(6), e001263.

Tardiff, J. C., Carrier, L., Bers, D. M., Poggesi, C., Ferrantini, C., Coppini, R., Maier, L. S., Ashrafian, H., Huke, S. and van der Velden, J. (2015). Targets for therapy in sarcomeric cardiomyopathies. Cardiovascular Research, 105(4), 457–470.

Thierfelder, L., Watkins, H., MacRae, C., Lamas, R., McKenna, W., Vosberg, H. P., Seidman, J. G. and Seidman, C. E. (1994). Alpha-tropomyosin and cardiac troponin T mutations cause familial hypertrophic cardiomyopathy: a disease of the sarcomere. Cell, 77(5), 701–712.

Thomson, J. A., Itskovitz-Eldor, J., Shapiro, S. S., Waknitz, M. A., Swiergiel, J. J., Marshall, V. S. and Jones, J. M. (1998). Embryonic stem cell lines derived from human blastocysts. Science, 282(5391), 1145–1147.

Tortora, G. J. and Derrickson, B. (2011). Principles of Anatomy and Physiology: 13th Edition.

Tripathi, S., Schultz, I., Becker, E., Montag, J., Borchert, B., Francino, A., Navarro-Lopez, F., Perrot, A., Özcelik, C., Osterziel, K.-J., McKenna, W. J., Brenner, B. and Kraft, T. (2011). Unequal allelic expression of wild-type and mutated β-myosin in familial hypertrophic cardiomyopathy. Basic Research in Cardiology, 106(6), 1041–1055.

Uosaki, H., Fukushima, H., Takeuchi, A., Matsuoka, S., Nakatsuji, N., Yamanaka, S. and Yamashita, J. K. (2011). Efficient and scalable purification of cardiomyocytes from human embryonic and induced pluripotent stem cells by VCAM1 surface expression. PLoS ONE, 6(8), e23657.

Vaajasaari, H., Ilmarinen, T., Juuti-Uusitalo, K., Rajala, K., Onnela, N., Narkilahti, S., Suuronen, R., Hyttinen, J., Uusitalo, H. and Skottman, H. (2011). Toward the defined and xeno-free differentiation of functional human pluripotent stem cell-derived retinal pigment epithelial cells. Molecular Vision, 17, 558–575.

Van den Heuvel, N. H. L., van Veen, T. A. B., Lim, B. and Jonsson, M. K. B. (2014). Lessons from the heart: mirroring electrophysiological characteristics during cardiac development to in vitro differentiation of stem cell derived cardiomyocytes. Journal of Molecular and Cellular Cardiology, 67, 12–25.

Van der Velden, J., Ho, C. Y., Tardiff, J. C., Olivotto, I., Knollmann, B. C. and Carrier, L. (2015). Research priorities in sarcomeric cardiomyopathies. Cardiovascular Research, 105(4), 449–456.

Van Dijk, S. J., Dooijes, D., Remedios, C. Dos, Michels, M., Lamers, J. M. J., Winegrad, S., Schlossarek, S., Carrier, L., Cate, F. J. Ten, Stienen, G. J. M. and Van Velden, J. Der. (2009). Cardiac myosin-binding protein C mutations and hypertrophic ardiomyopathy haploinsufficiency, deranged phosphorylation, and cardiomyocyte dysfunction. Circulation, 119(11), 1473–1483.

Van Dijk, S. J., Paalberends, E. R., Najafi, A., Michels, M., Sadayappan, S., Carrier, L., Boontje, N. M., Kuster, D. W. D., van Slegtenhorst, M., Dooijes, D., dos Remedios, C., ten Cate, F. J., Stienen, G. J. M. and van der Velden, J. (2012). Contractile dysfunction irrespective of the mutant protein in human hypertrophic cardiomyopathy with normal systolic function. Circulation. Heart Failure, 5(1), 36–46.

Watanabe, K., Ueno, M., Kamiya, D., Nishiyama, A., Matsumura, M., Wataya, T., Takahashi, J. B., Nishikawa, S., Nishikawa, S., Muguruma, K. and Sasai, Y. (2007). A ROCK

inhibitor permits survival of dissociated human embryonic stem cells. Nature Biotechnology, 25(6), 681–686.

Verma, V., Purnamawati, K., Manasi and Shim, W. (2013). Steering signal transduction pathway towards cardiac lineage from human pluripotent stem cells: a review. Cellular Signalling, 25(5), 1096–1107.

Wernicke, D., Thiel, C., Duja-Isac, C. M., Essin, K. V, Spindler, M., Nunez, D. J. R., Plehm, R., Wessel, N., Hammes, A., Edwards, R.-J., Lippoldt, A., Zacharias, U., Strömer, H., Neubauer, S., Davies, M. J., Morano, I. and Thierfelder, L. (2004). alpha-Tropomyosin mutations Asp(175)Asn and Glu(180)Gly affect cardiac function in transgenic rats in different ways. American Journal of Physiology. Regulatory, Integrative and Comparative Physiology, 287(3), R685–695.

Villa-Diaz, L. G., Ross, A. M., Lahann, J. and Krebsbach, P. H. (2013). Concise review: The evolution of human pluripotent stem cell culture: from feeder cells to synthetic coatings. Stem Cells, 31(1), 1–7.

Wilmut, I., Schnieke, A. E., McWhir, J., Kind, A. J. and Campbell, K. H. (1997). Viable offspring derived from fetal and adult mammalian cells. Nature, 385(6619), 810–813.

Wobus, A. M. and Boheler, K. R. (2005). Embryonic stem cells: prospects for developmental biology and cell therapy. Physiological Reviews, 85(2), 635–678.

Wolpert, L., Jessel, T., Lawrence, P., Meyerowitz, E., Robertson, E. and Smith, J. (2007). Principles of Development: 3rd Edition.

Woltjen, K., Michael, I. P., Mohseni, P., Desai, R., Mileikovsky, M., Hämäläinen, R., Cowling, R., Wang, W., Liu, P., Gertsenstein, M., Kaji, K., Sung, H.-K. and Nagy, A. (2009). piggyBac transposition reprograms fibroblasts to induced pluripotent stem cells. Nature, 458(7239), 766–770.

Vuorenpää, H., Ikonen, L., Kujala, K., Huttala, O., Sarkanen, J.-R., Ylikomi, T., Aalto-Setälä, K. and Heinonen, T. (2014). Novel in vitro cardiovascular constructs composed of vascular-like networks and cardiomyocytes. In Vitro Cellular & Developmental Biology. Animal, 50(4), 275–286.

Xin, M., Olson, E. N. and Bassel-Duby, R. (2013). Mending broken hearts: cardiac development as a basis for adult heart regeneration and repair. Nature Reviews. Molecular Cell Biology, 14(8), 529–541.

Xu, C., Inokuma, M. S., Denham, J., Golds, K., Kundu, P., Gold, J. D. and Carpenter, M. K. (2001). Feeder-free growth of undifferentiated human embryonic stem cells. Nature Biotechnology, 19(10), 971–974.

Xu, C., Jiang, J., Sottile, V., McWhir, J., Lebkowski, J. and Carpenter, M. K. (2004). Immortalized fibroblast-like cells derived from human embryonic stem cells support undifferentiated cell growth. Stem Cells, 22(6), 972–980.

Xu, C., Police, S., Rao, N. and Carpenter, M. K. (2002). Characterization and enrichment of cardiomyocytes derived from human embryonic stem cells. Circulation Research, 91(6), 501–508.

Xu, X. Q., Graichen, R., Soo, S. Y., Balakrishnan, T., Rahmat, S. N. B., Sieh, S., Tham, S. C., Freund, C., Moore, J., Mummery, C., Colman, A., Zweigerdt, R. and Davidson, B. P. (2008a). Chemically defined medium supporting cardiomyocyte differentiation of human embryonic stem cells. Differentiation, 76(9), 958–970.

Xu, X., Zweigerdt, R., Soo, S. Y., Ngoh, Z. X., Tham, S. C., Wang, S. T., Graichen, R., Davidson, B., Colman, A. and Sun, W. (2008b). Highly enriched cardiomyocytes from human embryonic stem cells. Cytotherapy, 10(4), 376–389.

Yamanaka, S. (2008b). Pluripotency and nuclear reprogramming. Philosophical Transactions of the Royal Society of London. Series B, Biological Sciences, 363(1500), 2079–2087.

Yamanaka, S., Li, J., Kania, G., Elliott, S., Wersto, R. P., Van Eyk, J., Wobus, A. M. and Boheler, K. R. (2008a). Pluripotency of embryonic stem cells. Cell and Tissue Research, 331(1), 5–22.

Yang, L., Soonpaa, M. H., Adler, E. D., Roepke, T. K., Kattman, S. J., Kennedy, M., Henckaerts, E., Bonham, K., Abbott, G. W., Linden, R. M., Field, L. J. and Keller, G. M. (2008). Human cardiovascular progenitor cells develop from a KDR+ embryonic-stem-cell-derived population. Nature, 453(7194), 524–528.

Yang, Q., Sanbe, a, Osinska, H., Hewett, T. E., Klevitsky, R. and Robbins, J. (1998). A mouse model of myosin binding protein C human familial hypertrophic cardiomyopathy. The Journal of Clinical Investigation, 102(19), 1292–1300.

Yang, Q., Sanbe, A., Osinska, H., Hewett, T. E., Klevitsky, R. and Robbins, J. (1999). In vivo modeling of myosin binding protein C familial hypertrophic cardiomyopathy. Circulation Research, 85(9), 841–847.

Yang, X., Pabon, L. and Murry, C. E. (2014). Engineering adolescence: maturation of human pluripotent stem cell-derived cardiomyocytes. Circulation Research, 114(3), 511–523.

Yu, J., Hu, K., Smuga-Otto, K., Tian, S., Stewart, R., Slukvin, I. I. and Thomson, J. A. (2009). Human induced pluripotent stem cells free of vector and transgene sequences. Science, 324(5928), 797–801.

Yu, J., Vodyanik, M. A., Smuga-Otto, K., Antosiewicz-Bourget, J., Frane, J. L., Tian, S., Nie, J., Jonsdottir, G. A., Ruotti, V., Stewart, R., Slukvin, I. I. and Thomson, J. A. (2007). Induced pluripotent stem cell lines derived from human somatic cells. Science, 318(5858), 1917–1920.

Zhang, J., Klos, M., Wilson, G. F., Herman, A. M., Lian, X., Raval, K. K., Barron, M. R., Hou, L., Soerens, A. G., Yu, J., Palecek, S. P., Lyons, G. E., Thomson, J. A., Herron, T. J., Jalife, J. and Kamp, T. J. (2012). Extracellular matrix promotes highly efficient cardiac differentiation of human pluripotent stem cells: the matrix sandwich method. Circulation Research, 111(9), 1125–1136.

Zhao, W., Ji, X., Zhang, F., Li, L. and Ma, L. (2012). Embryonic stem cell markers. Molecules, 17(6), 6196–6236.

Zhou, W. and Freed, C. R. (2009). Adenoviral gene delivery can reprogram human fibroblasts to induced pluripotent stem cells. Stem Cells, 27(11), 2667–2674.

Zilberter, Y. I., Timin, E. N., Bendukidze, Z. A. and Burnashev, N. A. (1982). Patch-voltage-clamp method for measuring fast inward current in single rat heart muscle cells. Pflügers Archiv : European Journal of Physiology, 394(2), 150–155.

Original publications

STEM CELLS TRANSLATIONAL MEDICINE®

EMBRYONIC STEM CELLS/INDUCED PLURIPOTENT STEM (iPS) CELLS

Comparative Analysis of Targeted Differentiation of Human Induced Pluripotent Stem Cells (hiPSCs) and Human Embryonic Stem Cells Reveals Variability Associated With Incomplete Transgene Silencing in Retrovirally Derived hiPSC Lines

SANNA TOIVONEN,[a,*] MARISA OJALA,[b,c,*] ANU HYYSALO,[b,c,*] TANJA ILMARINEN,[b,c] KRISTIINA RAJALA,[b,c] MARI PEKKANEN-MATTILA,[b,c] RIIKKA ÄÄNISMAA,[b,c] KAROLINA LUNDIN,[a] JAAN PALGI,[a] JERE WELTNER,[a] RAS TROKOVIC,[a] OLLI SILVENNOINEN,[b,c] HELI SKOTTMAN,[b,c] SUSANNA NARKILAHTI,[b,c] KATRIINA AALTO-SETÄLÄ[b,c,d] TIMO OTONKOSKI[a,e]

Key Words. Embryonic stem cells • Pluripotent stem cells • Hepatocyte differentiation • Cardiac • Neural differentiation • Retinal pigmented epithelium • Differentiation

ABSTRACT

Functional hepatocytes, cardiomyocytes, neurons, and retinal pigment epithelial (RPE) cells derived from human embryonic stem cells (hESCs) or human induced pluripotent stem cells (hiPSCs) could provide a defined and renewable source of human cells relevant for cell replacement therapies, drug discovery, toxicology testing, and disease modeling. In this study, we investigated the differences between the differentiation potentials of three hESC lines, four retrovirally derived hiPSC lines, and one hiPSC line derived with the nonintegrating Sendai virus technology. Four independent protocols were used for hepatocyte, cardiomyocyte, neuronal, and RPE cell differentiation. Overall, cells differentiated from hESCs and hiPSCs showed functional similarities and similar expression of genes characteristic of specific cell types, and differences between individual cell lines were also detected. Reactivation of transgenic *OCT4* was detected specifically during RPE differentiation in the retrovirally derived lines, which may have affected the outcome of differentiation with these hiPSCs. One of the hiPSC lines was inferior in all directions, and it failed to produce hepatocytes. Exogenous *KLF4* was incompletely silenced in this cell line. No transgene expression was detected in the Sendai virus-derived hiPSC line. These findings highlight the problems related to transgene expression in retrovirally derived hiPSC lines. STEM CELLS TRANSLATIONAL MEDICINE *2013;2:83–93*

[a]Research Programs Unit, Molecular Neurology, Biomedicum Stem Cell Center, University of Helsinki, Helsinki, Finland; [b]Institute of Biomedical Technology and [c]BioMediTech, University of Tampere, Tampere, Finland; [d]Heart Center, Tampere University Hospital, Tampere, Finland; [e]Children's Hospital, Helsinki University Central Hospital, Helsinki, Finland

[*]Contributed equally as first authors.

Correspondence: Timo Otonkoski, M.D., Ph.D., Biomedicum Helsinki, Room C507b, P.O. Box 63, 00014 University of Helsinki, Helsinki, Finland. Telephone: 358-9-191-25692; Fax: 358-9-191-25610; E-Mail: timo.otonkoski@helsinki.fi

Received May 2, 2012; accepted for publication October 26, 2012; first published online in SCTM *EXPRESS* January 22, 2013.

1066-5099/2013/$20.00/0

http://dx.doi.org/10.5966/sctm.2012-0047

INTRODUCTION

Human embryonic stem cells (hESCs) and human induced pluripotent stem cells (hiPSCs), collectively termed human pluripotent stem cells (hPSCs), are considered a renewable source of cells for regenerative medicine because of their potential to differentiate into all cell types found in the adult human body [1]. hESCs are derived from the inner cell mass of developing embryos [2], whereas hiPSCs are reprogrammed from somatic cells [3, 4]. hiPSCs share several characteristics with hESCs, including similar morphology, expression of pluripotency markers, and the ability to differentiate into definitive cell lineages [5–8]. Initial studies have suggested that fully reprogrammed iPSCs are indistinguishable from ESCs [3, 4, 9]. More comprehensive studies have revealed that particularly early passage iPSCs show differences in their gene expression profile, but continued propagation tends to increase the similarity between hESCs and iPSCs [10, 11].

Recent studies have revealed that iPSCs maintain differential DNA methylation patterns as a sign of incomplete reprogramming [12, 13]. The possible consequences of this "epigenetic memory" still remain unknown. Some recent studies indicate that the origin of iPSCs is relevant for their differentiation capacity. iPSCs derived from retinal pigment epithelial (RPE) cells have a high tendency for pigmentation [14], and reprogramming of cardiac fibroblasts produces more cardiomyocytes than fibroblasts from other sources [15]. Although hiPSCs in general seem to differentiate into specific lineages as efficiently as hESCs, there are several examples of incomplete pluripotent differentiation capacity, possibly reflecting their epigenetic barriers [11, 16].

Most studies comparing the properties of hESCs and hiPSCs have focused on their undif-

ferentiated phenotype, their uncontrolled differentiation capacity in embryoid bodies or teratomas, or their differentiation toward a single specific lineage [6, 17–19]. However, many extended protocols have been developed for the differentiation of specific derivatives of all germ lines, such as hepatocytes (endoderm), cardiomyocytes (mesoderm), or neurons and retinal cells (ectoderm). The rationale of our study was to systematically compare the capability of the same hiPSC and hESC lines to develop into functional cell types following the protocols optimized by researchers dedicated to their respective line of differentiation. We studied four hiPSC and three hESC lines for their ability to differentiate into functional hepatocyte-like cells (HLCs), beating cardiomyocytes, neurons forming active neuronal networks, and highly pigmented mature RPE cells. Cell lines hiPSC1 to hiPSC4 were derived in two different laboratories, from neonatal and adult fibroblasts using retroviral vectors. One of the cell lines was derived using *NANOG, OCT4, SOX2*, and *LIN28*, whereas the other cell lines were derived by overexpressing *OCT4, SOX2, KLF4*, and *c-MYC*. In addition, the hiPSC5 line was derived with an integration-free Sendai-viral system. All of the cell lines were adapted in the same culture conditions prior to each differentiation protocol to avoid variation caused by different culture environments. Our results did not point to a systematic difference in the differentiation efficiency between hiPSC and hESC lines, except for one cell line with incomplete transgene silencing. Reactivation of transgenes was occasionally observed, especially with a long RPE differentiation protocol. These observations raise concerns related to the use of integrating reprogramming methods.

Materials and Methods

Ethical Issues

The Institute of Biomedical Technology has an approval of National Authority for Medicolegal Affairs Finland to study human embryos (Dnro1426/32/300/05), as well as the support of the Ethical Committee of Pirkanmaa Hospital District to derive, culture, and differentiate hESC lines from surplus human embryos (R05116) and to produce new hiPSC lines (R08070). The generation of hiPSC lines in Biomedicum Stem Cells Center Helsinki was approved by the Coordinating Ethics Committee of the Helsinki and Uusimaa Hospital District (Nro 423/13/03/00/08).

Cell Lines and Cell Culture

Three hESC lines (H7 [hESC1; WiCell Research Institute, Madison, WI, http://www.wicell.org], FES29 [hESC2] [20], and Regea 08/023 [hESC3] [21]) and five hiPSC lines (FiPS5-7 [hiPSC1] [22], UTA.00112.hFF [hiPSC2] [23], A116 [hiPSC3] [supplemental online Fig. 1], UTA.01006.WT [hiPSC4] [23], and Hel24.3 [hiPSC5] [supplemental online Fig. 1]) were used in this study. The hiPSC lines FiPS5-7 and UTA.00112.hFF were derived from human foreskin fibroblasts (hFFs) (CRL-2429; American Type Culture Collection, Manassas, VA, http://www.atcc.org), and the hiPSC lines A116, UTA.01006.WT, and Hel24.3 were derived from adult skin fibroblasts. FiPS5-7 (hiPSC1) was reprogrammed with *NANOG, OCT4, SOX2*, and *LIN28* and the other hiPSC lines with *OCT4, SOX2, KLF4*, and c-*MYC*. The cell lines used in this study are presented in supplemental online Table 1. Details of hiPSC reprogramming conditions are provided in the supplemental online Materials and Methods.

Differentiation Protocols

Pluripotent stem cell lines were differentiated into hepatocyte-like cells, cardiomyocytes, neural cells, and RPE cells. Detailed methods of differentiation and characterization are provided in the supplemental online Materials and Methods.

The efficiency of hepatic differentiation was evaluated by studying the expression of *OCT4, SOX17*, *FOXA2, AFP,* and *Albumin* at day (d) 7, d14, and d21 by quantitative polymerase chain reaction (qPCR) analysis and by studying the expression of OCT4, FOXA2, SOX17, AFP, and albumin with immunocytochemistry. The definitive endoderm induction was analyzed at d7 by flow cytometry for CXCR4+ cells, and the functionality of the differentiated hepatocyte-like cells was studied by albumin secretion measured with an enzyme-linked immunosorbent assay.

Cardiac differentiation was characterized by studying the expression of *Nanog, OCT4, SOX17*, *Brachyury T*, and *NKX2.5* at time points d0, d3, d6, d13, and d30 by qPCR and by studying the expression of α-actinin, Troponin T, connexin-43, and ventricular myosin heavy chain (MHC) with immunocytochemistry. The efficiency of cardiac differentiation was evaluated by immunocytochemical analysis of cytospin samples on day 20 and counting the number of beating areas in the end of differentiation on day 30. The functionality of the cardiomyocytes was analyzed using the microelectrode array (MEA) platform.

Neural differentiation was evaluated at the 4- and 8-week time points by studying the expression of *OCT4, Musashi, Neurofilament-68* (*NF-68*), and *glial fibrillary acidic protein* (*GFAP*) by qPCR and by studying the expression of OCT4, EpCAM, Nestin, microtubule-associated protein 2 (MAP-2), GFAP, brain lipid-binding protein (BLBP), chondroitin sulfate proteoglycan (NG2), and galactocerebroside (GalC) by immunocytochemistry. The morphological analysis was performed with time-lapse imaging. The spontaneous functionality of developing neuronal networks was characterized using MEA.

To evaluate putative RPE cell differentiation, the appearance of the first pigmented cells was followed daily and recorded. The percentage of pigment-containing cell aggregates from the total amount of aggregates was counted on day 28 $\pm$ 1 of the differentiation. The expression of *OCT4, MITF, BEST1*, and *RLBP1* was analyzed by qPCR from d0, d28, d52, and d82 of RPE differentiation. The expression of OCT4, MITF and bestrophin-1 proteins was quantified with cytospin analysis on day 82 or on day 116.

Statistical Analysis

Statistical analysis between two groups was performed with the unpaired Student's *t* test or Mann-Whitney *U* test according to the sample set. In the case of multiple groups, one-way analysis of variance and the Tukey post hoc test were used. A *p* value of $<.05$ was considered statistically significant.

Results

Transgene Silencing

hiPSC lines hiPSC1 [22], hiPSC2 [23], and hiPSC4 [23] were independently established by retroviral infection (*OCT4*, *SOX2*, *c-MYC*, and *KLF4* or *OCT4*, *SOX2*, *NANOG*, and *LIN28*) and characterized as described previously [22, 23]. hiPSC3 and hiPSC5 (supplemental online Fig. 1) lines were separately characterized

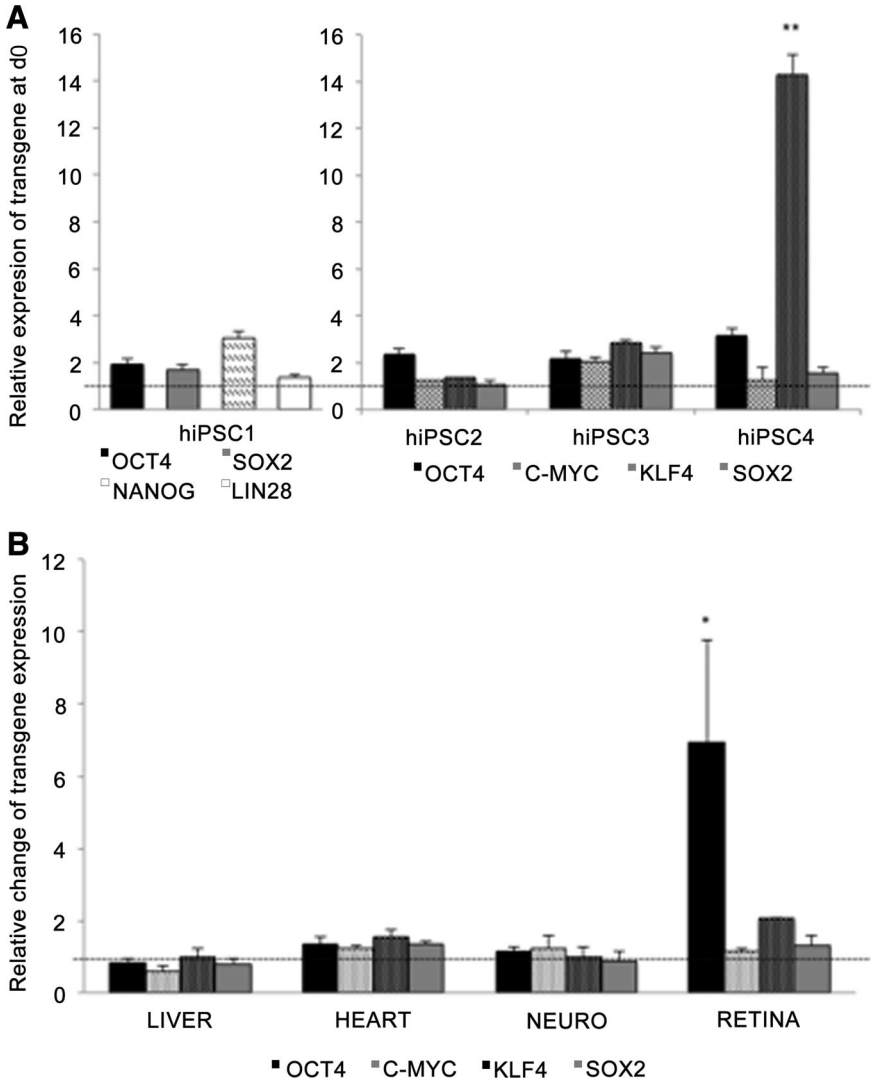

Figure 1. Transgene silencing. **(A):** Quantitative polymerase chain reaction (qPCR) analysis for expression of the transgenes *OCT4, SOX2, NANOG, LIN28, c-MYC*, and *KLF4* at the onset of differentiation (d0). The data are shown as the average (±SEM) relative value from four independent experiments. The value 1 indicates total silencing of transgenes. One-way analysis of variance with Tukey post hoc test was used for statistical analysis. **, $p < .01$. **(B):** qPCR analysis for activation of transgene expression during each differentiation protocol. The value 1 indicates no change in transgene expression. *, $p < .05$. Abbreviations: d, day; hiPSC, human induced pluripotent stem cell; NEURO, neural differentiation.

for this study. Relative transcriptional levels of the transgenes were studied by qPCR before and at the end of each differentiation protocol in lines hiPSC1–hiPSC4. The results revealed constant expression of exogenous *KLF4* in hiPSC4 at d0, whereas transgenes in other cell lines were silenced (Fig. 1A; supplemental online Fig. 2A). Transgene expression in general was not significantly induced by the differentiation protocols, with one remarkable exception. Levels of exogenous *OCT4* mRNA were systematically increased at the end of the long-term RPE differentiation protocol in all retrovirally derived hiPSC lines (Fig. 1B; supplemental online Fig. 2B), and OCT4+ cells could be detected by immunocytochemistry after 82 days of RPE differentiation (supplemental online Fig. 3B). In addition, exogenous *LIN28* and *NANOG* mRNA levels were markedly increased during the RPE differentiation in hiPSC1, the only cell line derived by overexpression of these factors (supplemental online Fig. 2B). When the Sendai-virally derived hiPSC5 line was differentiated into RPE cells, no reactivation of transgene expression was detected (supplemental online Fig. 3A, 3B).

Definitive Endoderm Differentiation

Hepatocyte differentiation protocol consists of three stages, slightly modified from that described by Hay et al. [24] (Fig. 2A). The first stage directs the cells from pluripotent cells into committed definitive endoderm (DE) cells. In this stage, after 7 days from the onset of induction, all the cell lines had lost their embryonic stem-like small, round, and dense morphology and the cells were growing as homogeneous monolayers. qPCR analysis showed marked upregulation of the anterior definitive endoderm genes *SOX17* and *Hhex* in all lines at day 7 (Fig. 2B; supplemental online Fig. 4A). During differentiation, the expression of *OCT4* decreased in all cell lines and became undetectable by day 14. The process was somewhat slower in hiPSCs than hESCs (Fig. 2D). There was no change in

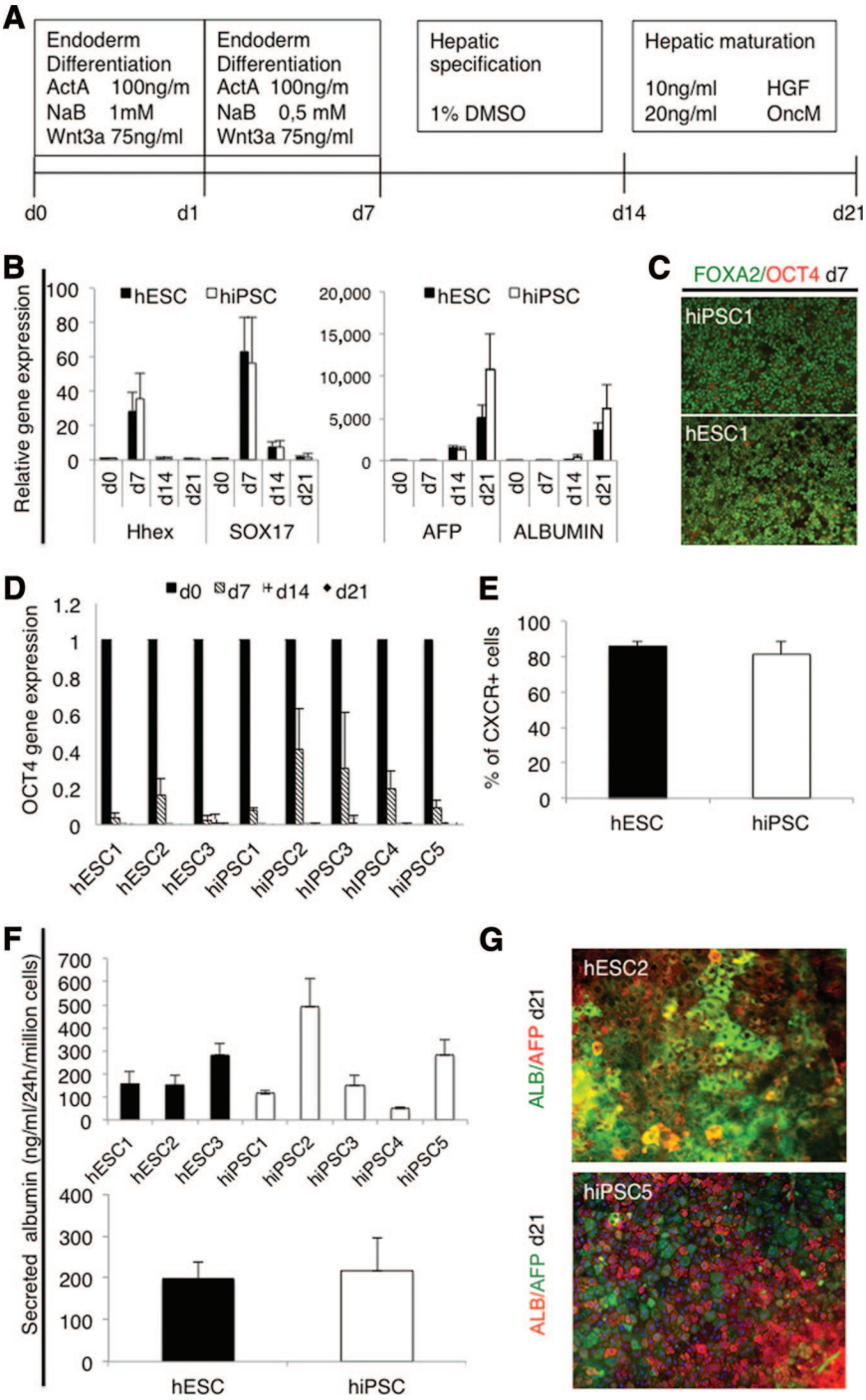

Figure 2. Hepatocyte differentiation. **(A):** Schematic presentation of the protocol used to differentiate human pluripotent stem cells into hepatocyte-like cells. **(B):** Quantitative polymerase chain reaction (qPCR) analysis for expression of the genes marking key stages of differentiation, first into definitive endoderm cells (*SOX17, Hhex*) and then into hepatocyte-like cells (*AFP, Albumin*). The columns show the average fold change from at least two independent experiments ± SEM for each line. **(C):** Representative immunostaining after 7 days of differentiation, demonstrating that almost all cells expressed nuclear FOXA2 as a sign of definitive endoderm differentiation and very few cells still expressed the pluripotency marker OCT4. **(D):** qPCR analysis for expression of the pluripotency gene *OCT4* at d0, d7, d14, and d21. The columns show the average fold change from at least two independent experiments ± SEM, demonstrating the rapid downregulation in both hESC and hiPSC lines. **(E):** Fluorescence-activated cell sorting analysis of cells expressing the endoderm marker CXCR4 at d7. Columns represent the average for hESCs ($n = 6$) and hiPSCs ($n = 8$). **(F):** Albumin secretion into the medium by the differentiated cells. In the upper graph, each cell line is presented separately (two or three repeated experiments). Lower graph shows the comparison between iPSCs ($n = 10$) and hESCs ($n = 6$). **(G):** Representative immunostaining after 21 days of differentiation of hESC2 and hiPSC5. Hepatocyte markers ALB and AFP are shown. Magnification, ×20. Abbreviations: AFP, α-fetoprotein; ALB, albumin; d, day; DMSO, dimethyl sulfoxide; hESC, human embryonic stem cell; HGF, hepatocyte growth factor; hiPSC, human induced pluripotent stem cell.

the expression level of the extraembryonic endoderm gene *SOX7* (data not shown). In immunocytochemical analysis more than 90% of the cells were positive for definitive endoderm marker FOXA2, and very few if any OCT4+ cells could be found (Fig. 2C; supplemental online Fig. 5A). The percentage of CXCR4+ cells as analyzed by flow cytometry varied between 65% and 96% between all the lines (supplemental online Fig. 5B), and there were no significant difference between hESC ($n = 3$) and hiPSC ($n = 4$) lines in group comparison (Fig. 2E). These results suggest that the hESC and hiPSC lines used in this study differentiated into definitive endoderm stage with equal efficiency.

Hepatocyte Differentiation

The resulting DE cells were then differentiated into HLCs by 7-day culture in medium supplemented with 1% dimethyl sulfoxide (stage 2) and by a final maturation step in medium supplemented with hepatocyte growth factor and Oncostatin M for a further 7 days [24] (Fig. 2A). During this time the cells displayed morphological changes from a spiky shape to a polygonal shape. On day 21, the cultures contained foci exhibiting features of human hepatocytes, including a typical polygonal shape with distinct round nuclei, and many of the cells were binuclear (supplemental online Fig. 5C). Only hiPSC4-derived cells failed to develop a

distinct hepatocyte-like morphology (supplemental online Fig. 5C). In qPCR analysis, *AFP* was highly upregulated at day 14 and *Albumin* at day 21 (Fig. 2B; supplemental online Fig. 4A).

The HLCs derived from hiPSC2 expressed the highest levels of *AFP* and *Albumin*, whereas the expression of these hepatocyte-specific markers was nearly undetectable with hiPSC4-derived cells. Variation in the differentiation efficiency, as measured by albumin expression, was detected between hESCs and iPSCs, but the differences were not statistically significant in a group comparison. The hepatocyte-specific functionality of the differentiated cells was analyzed by albumin secretion assay. The results correlated well with qPCR data; there was no overall difference in albumin secretion rate between the hESC1–hESC3 lines and the hiPSC1–hiPSC5 lines in a group comparison, although there was variation between the individual cell lines (Fig. 2F), particularly because hiPSC4 failed to develop into albumin-secreting cells. Taken together, both the highest and the lowest levels of differentiation were observed in the hiPSC lines, whereas there was less variation among the hESC lines.

Cardiomyocyte Differentiation

hPSC lines were differentiated into cardiomyocytes using the END-2 coculture method [25]. The progression of cardiac differentiation was monitored and cells analyzed as shown in Figure 3A. All four hiPSC and three hESC lines differentiated into beating cardiomyocytes, but the differentiation efficiency was variable. In addition, the cardiac differentiation efficiency varied between separate differentiation experiments within the same cell line. All cell lines formed compact structures in END-2 coculture except hiPSC4, which tended to form more cystic structures than the other cell lines. Cardiomyocytes derived from the cell lines expressed α-actinin, Troponin T, connexin-43, and MHC in immunocytochemical stainings (Fig. 3B). The electrical activity of cardiomyocytes was monitored with MEA measurements. The normal beating rate of the cell clusters was measured and the beating rate was increased by adding the β-adrenergic agonist isoprenaline to MEA chambers. All hESC- and hiPSC-derived cardiomyocytes beat and gave a signal on MEA and thus can be considered functional cardiomyocytes (Fig. 3C).

Quantitative immunocytochemical analysis was performed on cells cultured in END-2 cocultures on day 20, and beating areas were counted at the end of differentiation on day 30. The number of beating areas was highly variable between separate differentiation experiments within the same cell line. As a group, hESCs formed more beating areas than hiPSCs ($p < .001$, Fig. 3D). hESC1 had the most efficient cardiac differentiation efficiency, whereas hiPSC1 and hiPSC4 had the least efficient cardiac differentiation and the lowest number of beating areas (Fig. 3D). The results from the quantitative immunocytochemical analysis detecting cardiac Troponin T-positive cells were in accordance with the number of beating areas (Fig. 3E). In the hESC1 line, the beating areas were smaller than in other cell lines, but there were more beating areas. This may explain the difference between quantitative immunocytochemical results and the number of beating areas detected.

The expression of pluripotency markers *NANOG* and *OCT4* was highest on day 0 and descended during cardiac differentiation (supplemental online Fig. 6A, 6B). The expression of endodermal *SOX17* was the highest on day 3 in all hiPSC and hESC lines (supplemental online Fig. 6C). The expression of *Brachyury T* was also the highest on day 3 with the hESC lines (Fig. 3F). Interestingly, with hiPSC lines the highest expression of *Brachyury T* was detected on day 6, and it was significantly higher in hiPSC lines than in hESC lines ($p = .003$), suggesting a slower tempo of cardiac differentiation. The expression of *Nkx2.5* ascended evenly during differentiation in all hiPSC and hESC lines.

Neural Differentiation

The neural differentiation protocol and the analyses used in this study are summarized in Figure 4A. Cell lines displayed clear differences when differentiated and cultured as neurospheres in neural differentiation medium. Neurospheres usually develop into firm cell aggregates within 2 weeks. The hiPSC3-derived neurospheres, however, showed persistent growth of unwanted cystic structures up to 4 weeks of differentiation (supplemental online Fig. 7). When the cysts were repeatedly manually removed from the cultures, the cyst formation declined. In addition to hiPSC3, the hiPSC2 line produced relatively fast-growing and less firm neurospheres. The growth of hiPSC4-derived neurospheres was weaker than that in the other lines. Neurospheres derived from hESC lines showed less variation during differentiation and culture.

According to qPCR analysis, the expression of *OCT4* was strongly downregulated within every cell line during the neural differentiation at 8 weeks (Fig. 4B). The downregulation was, however, significantly stronger in neurospheres derived from hESC than from hiPSC lines ($p < .01$). The expression of neural precursor cell marker *Musashi* and neural marker *NF-68* increased during differentiation, and both were significantly higher in neurospheres derived from hESCs than from hiPSC lines (*Musashi* week 8, $p = .034$; *NF-68* weeks 4 and 8, $p = .002$ and $p = .01$, respectively) (Fig. 4B). Expression of glial marker *GFAP* was undetectable in 0 and 4 weeks, and it was expressed at a low level in every cell line after 8 weeks of differentiation. Line-specific expression of *OCT4*, *Musashi*, and *NF-68* is shown in supplemental online Figure 4.

The cells were monitored with time-lapse imaging at 4 and 8 weeks during the neural differentiation. Quantitative analysis of time-lapse imaging data was performed by Cell-IQ analysis software (Chip-Man Technologies Ltd., Tampere, Finland) [26], but the accurate neuronal cell number could not be reliably determined because of confluence of the cultures (supplemental online Fig. 7). Qualitative analysis of the imaged data showed that hESC3 and hiPSC3 produced very pure neuronal populations in 8 weeks, whereas hiPSC4 was clearly the weakest cell line for neural differentiation, producing a lot of flat epithelial-like cells (Fig. 4C). The cells in hiPSC1-derived cultures were also mostly neuronal, but more cells with non-neuronal morphology were detected compared with hESC3- and hiPSC3-derived cultures.

Immunocytochemical staining supported the results of the time-lapse imaging analysis (Fig. 4D). The highest levels of MAP-2-positive cells were detected within hESC3- and hiPSC3-derived cultures. In hiPSC4-derived cultures only single cells positive for MAP-2 could be detected. The number of Nestin-positive cells decreased in all lines from 4 weeks to 8 weeks. No OCT4, CD326, GFAP, or BLBP was detected in any cell lines, indicating that no undifferentiated cells, astrocytes, or radial glial cells were present in the cultures. Only single cells positive for NG2 or GalC could be detected at 8 weeks, indicating the presence of few oligodendrocyte precursor cells in the cultures (supplemental online Fig. 7).

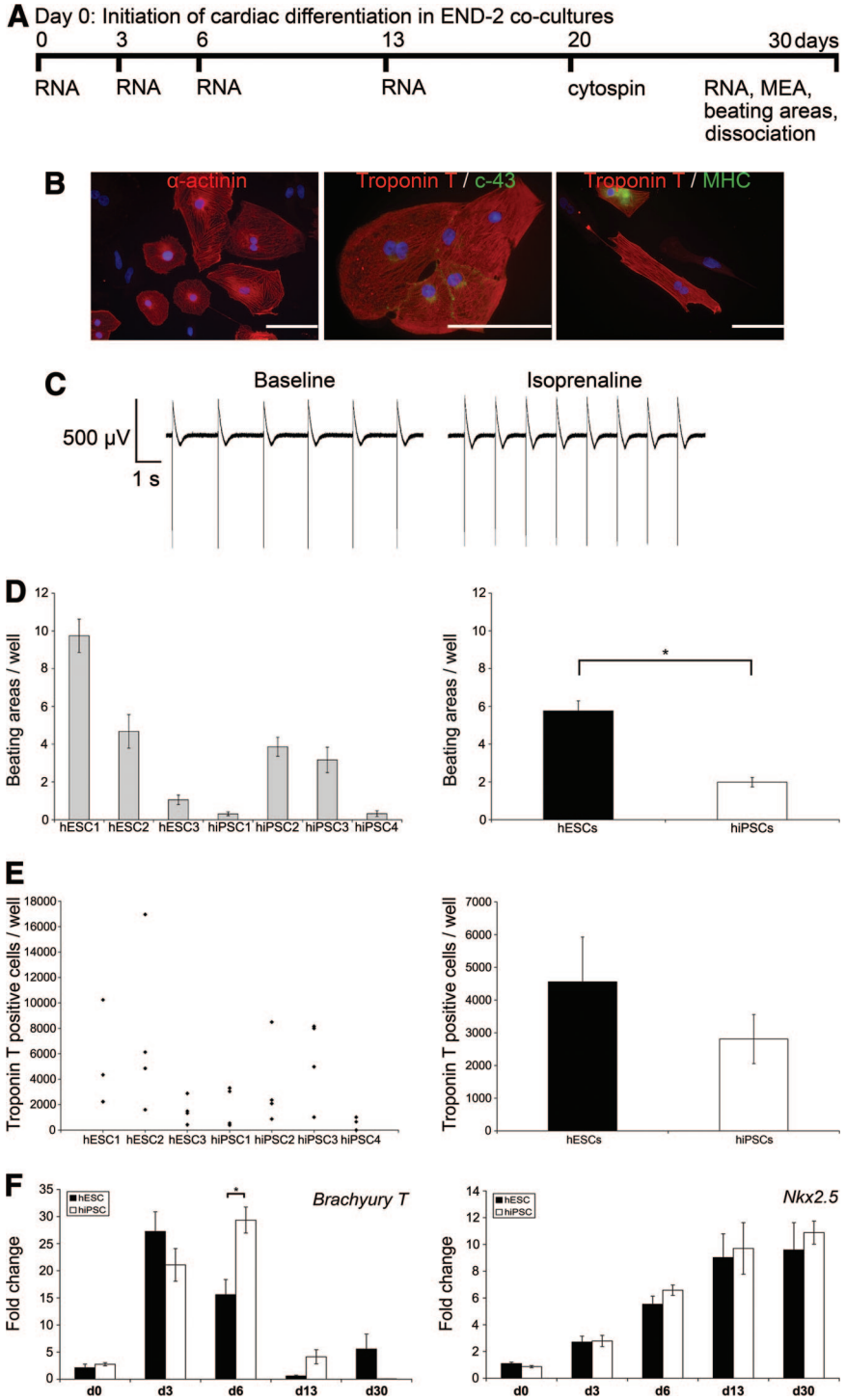

Figure 3. Cardiomyocyte differentiation. **(A):** Schematic presentation of the cardiac differentiation protocol and experimental design. **(B):** Cardiomyocytes derived from all human pluripotent stem cell (hPSC) lines expressed α-actinin, connexin-43, and ventricular myosin heavy chain proteins. Representative images of hiPSC2 line. Scale bars = 100 μm. **(C):** All hPSC lines gave a signal on the MEA platform, and the beating rate was increased by isoprenaline (80 nM). Shown are representative images of the hiPSC3 line. **(D):** The number of beating areas in one well with each hPSC line (left) and in hESC and hiPSC groups (right). Error bars show the SEM. $*$, $p < .001$. **(E):** Scatter plots (left) show the number of Troponin T-positive cells in one well, and the columns (right) show the Troponin T-positive cells found in the hESC and hiPSC groups. Error bars show the SEM. **(F):** Results of the gene expression analysis on *Brachyury T* and *Nkx2.5* genes at the d0, d3, d6, d13, and d30 time points during cardiac differentiation. The expression of genes was compared between hESC and hiPSC lines. In hiPSC lines the highest expression of *Brachyury T* was detected on day 6, and it was significantly higher in hiPSC lines than in hESC lines ($*$, $p < .003$). Error bars show the SEM. Abbreviations: c-43, connexin-43; d, day; hESC, human embryonic stem cell; hiPSC, human induced pluripotent stem cell; MEA, microelectrode array; MHC, myosin heavy chain; RNA, quantitative polymerase chain reaction samples.

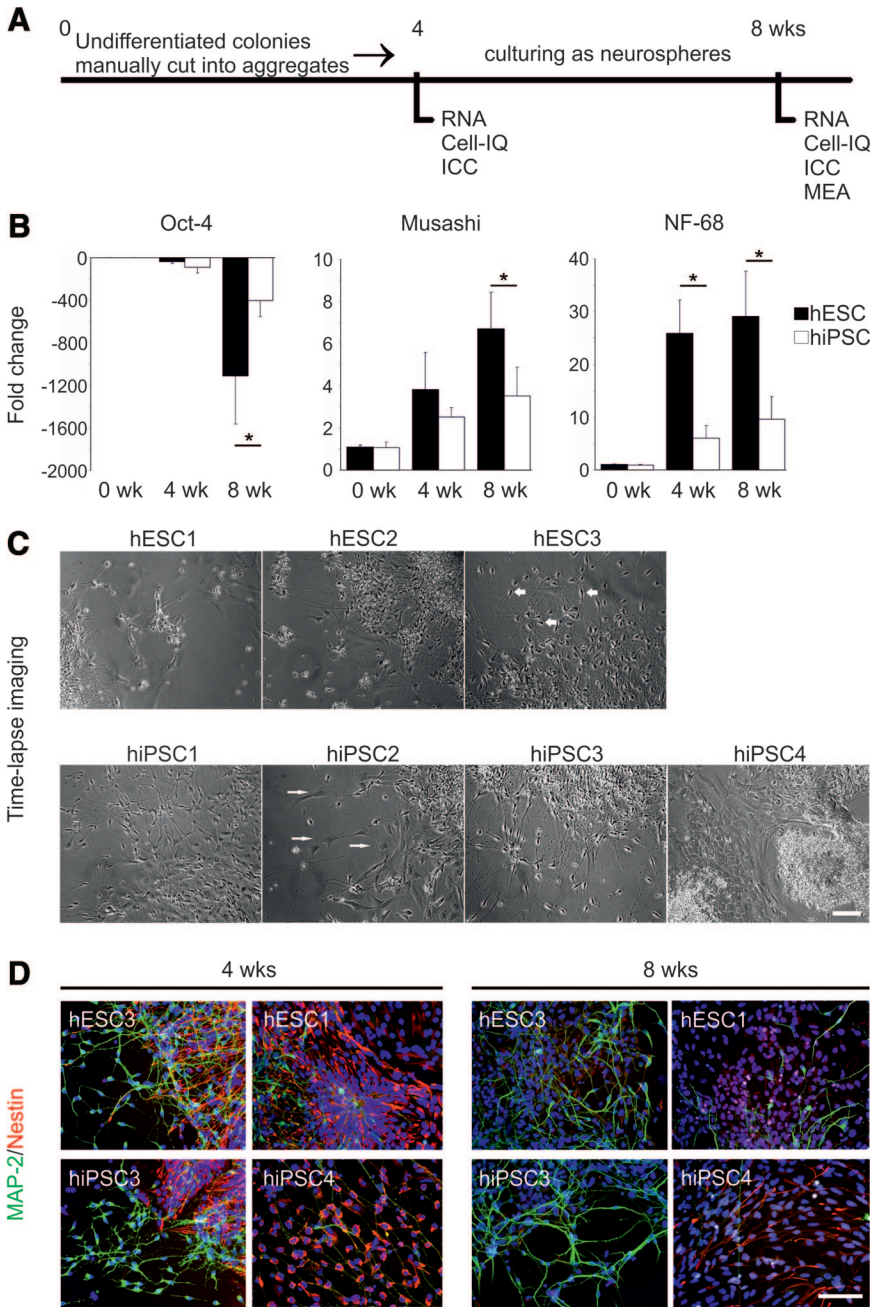

Figure 4. Neuronal differentiation. **(A):** Schematic presentation of the neural differentiation protocol and experimental design. **(B):** Results of the gene expression analysis of *OCT4*, *Musashi,* and *NF-68* at the 0-, 4-, and 8-week time points. The expressions of the genes were compared between hESC and hiPSC lines. Columns represent an average of hESC ($n = 3$) and hiPSC ($n = 4$) lines ± SEM. *Musashi* week 8, $p = .034$; *NF-68* weeks 4 and 8, $p = .002$ and $p = .01$, respectively. $*$, $p < .05$, Mann-Whitney *U* test. **(C):** Morphologies of the cells derived from different cell lines at the 8-week time point. hESC3-, hiPSC1-, and hiPSC3-derived cells displayed mostly neuronal morphology (thick arrows), whereas other cell lines produced cells with flat epithelial cell-like morphology (thin arrows). Scale bar = 100 μm. **(D):** Immunocytochemical characteristics of the differentiated cells. Neural precursor cell marker Nestin (red) and neural marker MAP-2 (green) were both detected in all the populations derived from hESC and hiPSC lines. Cell cultures derived from hESC3 and hiPSC3 lines were detected with high amounts of MAP-2-positive cells at both time points, whereas clearly fewer MAP-2-positive cells could be detected from the cultures of hESC1 and hiPSC4. The number of Nestin-positive cells decreased within all the cell lines from 4 to 8 weeks. Scale bar = 100 μm. Abbreviations: Cell-IQ, time-lapse imaging; hESC, human embryonic stem cell; hiPSC, human induced pluripotent stem cell; ICC, immunocytochemistry; MAP-2, microtubule-associated protein 2; MEA, microelectrode array; NF-68, Neurofilament-68; RNA, quantitative polymerase chain reaction samples; wk, week.

Electrophysiological Properties of Neuronal Networks

As previously described [27], the first form of electrical activity detected from the neuronal networks was single spikes, whereas the mature neuronal networks displayed bursts containing multiple spikes simultaneously on several electrodes (supplemental online Fig. 8). The cell lines with the highest neural differentiation efficiencies based on morphological and immunocytochemical characterizations (hESC3 and hiPSC3) displayed burst-activity within 3 weeks in MEA culture. The spontaneously active bursting neuronal networks were routinely recorded from hESC3- and hiPCS3-derived cultures. The neuronal networks formed by the other cell lines displayed activities varying from single spikes to bursts.

RPE Differentiation

The hESC and hiPSC1–hiPSC5 lines were differentiated into RPE cells according to a previously reported protocol, which is based on spontaneous differentiation in EB-like cultures [8]. The differentiation protocol and analyses are summarized in Figure 5A. The RPE differentiation potential of the cell lines was studied by monitoring the appearance of the first pigmented cells emerging in the cultures. In addition, the percentage of cell clusters containing pigmented cells was counted on day 28 after initiation of differentiation.

All the examined cell lines produced pigmented cells on average within 22 days after initiation of differentiation (Fig. 5B). hESC lines produced pigmented cells on average 2 days earlier than hiPSC lines. The first pigmented cells were detected on day

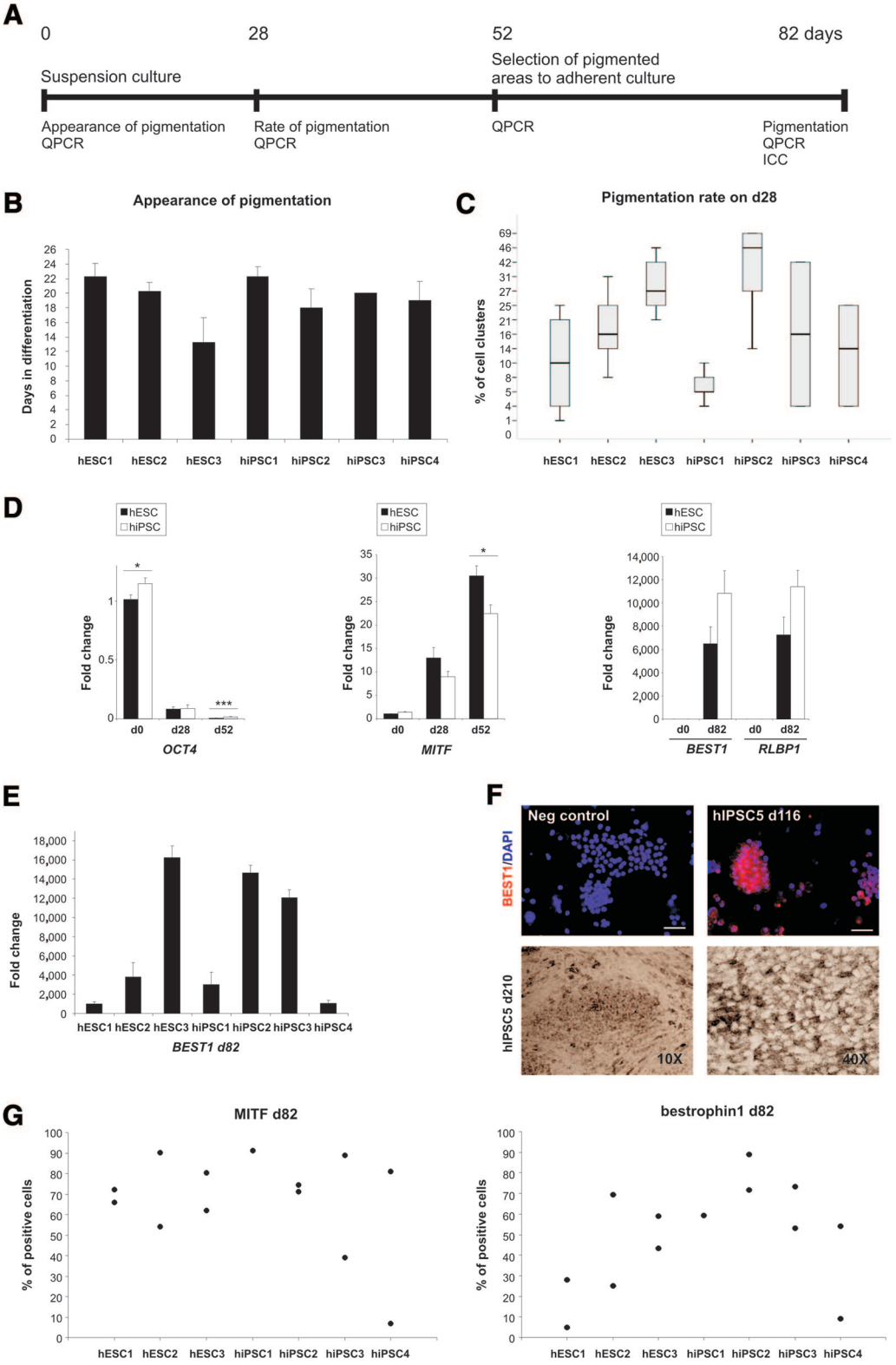

Figure 5. Retinal pigment epithelial (RPE) differentiation. **(A):** Schematic representation of the RPE differentiation protocol and experimental design. **(B):** Appearance of the first pigmented cells in the cultures at the beginning of RPE differentiation. Columns are representing an average of two to four independent experiments (n) ± SEM. Shown are hESC1 ($n = 4$), hESC2 ($n = 4$), hESC3 ($n = 3$), hiPSC1 ($n = 4$), hiPSC2 ($n = 3$), hiPSC3 ($n = 2$), and hiPSC4 ($n = 3$). **(C):** Rate of pigmentation on differentiation day 28. Box plots show the sample minimum, lower quartile, median, upper quartile, and sample maximum of two to four independent experiments. The number of experiments/total number of cell clusters counted were as follows: hESC1, 4/674; hESC2, 3/448; hESC3, 3/339; hiPSC1, 3/656; hiPSC2, 3/427; hiPSC3, 2/445; and hiPSC4, 2/704. **(D):** QPCR analysis for expression of genes marking key stages of human pluripotent stem cell differentiation (*OCT4*) into pigment-producing cells (*MITF*) and subsequently into RPE-like cells (*BEST1* and *RLBP1*). The columns show the average fold change from at least two

Table 1. Differentiation potential of individual human pluripotent stem cell lines

Cell line	Endodermal lineage: hepatocyte	Mesodermal lineage: cardiac	Ectodermal lineage: Neuronal	Ectodermal lineage: RPE
hESC1	++	+++	+	+
hESC2	++	++	++	++
hESC3	+++	+	+++	+++
hiPSC1	++	+	++	+
hiPSC2	+++	++	++	+++
hiPSC3	++	++	+++	++
hiPSC4	+	+	+	+
hiPSC5	+++			+++

Shown is the differentiation efficiency of the cell lines based on the rate of albumin secretion (hepatocyte), number of beating cardiomyocytes (cardiac), morphological and immunocytochemical criteria (neural), and rate of pigmentation (retinal pigment epithelial). + indicates lower differentiation potential than average, ++ indicates average differentiation capacity, and +++ indicates excellent differentiation capacity.
Abbreviations: hESC, human embryonic stem cell; hiPSC, human induced pluripotent stem cell; RPE, retinal pigment epithelial.

13 (hESC3). On day 28, the highest proportion of pigmented cell clusters in hESC lines was detected in hESC3 (31%) and the lowest in hESC1 (11%) (Fig. 5C). Of the hiPSC lines, the best performer was hiPSC2 (43%) and the weakest hiPSC1 (6%) (Fig. 5C). In a groupwise comparison, none of the differences between the hESC and hiPSC lines were statistically significant.

During differentiation, the expression of endogenous *OCT4* decreased in all cell lines. However, it was higher in the hiPSC than in the hESC lines on day 0 ($p = .03$) and day 52 ($p < .001$) (Fig. 5D). Expression of the selected differentiation markers *MITF*, *BEST1*, and *RLBP1* increased in all cell lines during differentiation. In a comparison of hESC and hiPSC lines, the pigment cell marker *MITF* was higher in hESC on day 52 ($p = .011$) (Fig. 5D). The more RPE-specific markers *BEST1* and *RLBP1* appeared higher on d82 in the hiPSC lines, but the differences were not statistically significant (Fig. 5D). The Sendai-virally derived hiPSC5 line was characterized only partially, but it also differentiated into pigmented epithelium with cobblestone morphology and bestrophin-1 immunoreactivity (Fig. 5F). At the protein level, all cell lines expressed MITF and bestrophin-1 proteins. The highest proportion of MITF-positive cells in hESC lines was detected in hESC2 (72%) and the lowest in hESC1 (69%). The results were less reproducible in the hiPSC lines (Fig. 5G). Bestrophin-1-positive cells tended to be more abundant in the hiPSC than the hESC lines (Fig. 5G), and the results correlated with *BEST1* gene expression and also with the rate of pigmentation.

When analyzed comprehensively, it appears that the hESC lines (particularly hESC1 and hESC3) displayed variable propensities for mesodermal versus ectodermal differentiation. The same cell lines differentiated consistently more efficiently in the ectodermal (neuronal and RPE) directions or mesodermal (cardiac) direction. However, none of the induced pluripotent stem cell (iPSC) lines showed such preferential differentiation capacity (Table 1).

Discussion

We studied the differentiation capacity of three hESC and five hiPSC lines. The four retrovirally derived hiPSC lines were characterized in detail using four well-established differentiation protocols and specific functional assays. Through this approach, we hope to elucidate the true variability between human pluripotent stem cell lines with respect to their most important characteristic: the ability to develop into physiologically functional cell types.

To our knowledge, our study is the first to use four separate extended differentiation protocols into derivatives of all germ layers in a systematic comparison of hPSC lines. In this study most of the cell lines showed no differentiation preference toward any specific cell lineages but rather showed more or less differentiation potential toward all different cell types produced. Only two of the cell lines (hESC1 and hESC3) had consistently more differentiation potential toward specific lineages. hESC1 differentiated well into beating cardiomyocytes and poorly into ectodermal lineages, and hESC3 had the best ectodermal differentiation capacity but produced few beating areas in cardiomyocyte differentiation. One reason for these differences may be the fact that the cardiac (END2 coculture) and neuronal (EB formation) protocols in this study are based more on the spontaneous differentiation of the cells than the hepatocyte protocol, which is based on guidance by specific growth factors. It is likely that the genetic background of the cells plays a more crucial role in the former than the latter situation.

Analysis of transgene expression showed that *KLF4* was incompletely silenced in hiPSC4 (Fig. 1A; supplemental online Fig. 2A), suggesting that this cell line was only partially reprogrammed. The retroviral transgenes are usually silenced as a late event of the reprogramming process [28] because of the activation of DNA [29] and histone methyltransferases [12]. This process, however, is often incomplete, resulting in partially reprogrammed cell lines [9, 30, 31]. This residual activity of viral transgenes in hiPSC-derived cells can affect their developmental potential [9]. Partially incomplete reprogramming may explain the poor differentiation capacity of hiPSC4, which was observed throughout this study.

All of the hESC and hiPSC lines differentiated efficiently into early DE progenitors. However, when the DE cells were further induced into HLCs some variability became evident. Although all the hESC lines differentiated with approximately equal efficiency, the iPSC lines were much more variable, ranging from very poor (hiPSC4) to excellent (hiPSC2). This variation was not correlated with the method used for hiPSC induction, and it is unlikely that it would be due to the different donor age (neonatal vs. adult). It has also been noted by others that there are differences in the timing of onset of expression of hepatocyte-specific genes between different cell lines [7].

The cardiomyocyte differentiation protocol used in this study produced beating areas from all the cell lines with variable efficiency. Overall, cardiac differentiation on END-2 cocultures is rather unspecific, and many other cell types besides cardiomyocytes are also induced [32]. Normally, the highest peak of

independent experiments ± SEM. *, $p < .05$; ***, $p < .001$. Statistical analyses were performed with independent samples *t* test or Mann-Whitney *U* test according to the sample set. **(E):** QPCR analysis for expression of BEST1 on d82 in each analyzed cell line. The columns show the average fold change from at least two independent experiments ± SEM. **(F):** Top row: Bestrophin-1 (BEST1) staining for cytospin samples collected from hiPSC5-derived RPE cells. Bottom row: pigmented cells derived from hiPSC5 at d210 in passage 2. **(G):** Expression of MITF and bestrophin-1 proteins on d82. Scatter plots show the percentage of positive cells from one or two independent experiments. The total number of cells counted were as follows for MITF/bestrophin-1: hESC1, 326/274; hESC2, 351/337; hESC3, 466/454; hiPSC1, 184/202; hiPSC2, 579/518; hiPSC3, 355/402; and hiPSC4, 288/269. Abbreviations: d, day; hESC, human embryonic stem cell; hiPSC, human induced pluripotent stem cell; ICC, immunocytochemistry; Neg, negative; QPCR, quantitative polymerase chain reaction.

Brachyury T expression is observed on day 3 in END-2 cocultures [32], and the delayed expression peak leads to poor cardiac differentiation efficiency [33, 34]. In this study, the expression peak of *Brachyury T* was extended up to day 6 with hiPSCs, which was associated with a lower lowest number of beating areas than in hESCs. However, high variation in cardiac differentiation efficiency was also detected between different passages/differentiation experiments within the same cell line, indicating that the cell line characteristics change over time in culture.

The neural differentiation protocol used here has been used routinely with several hESC lines previously [35, 36]. Both hESC and hiPSC lines were successfully differentiated toward neural cells regardless of their origin. Previous studies have, however, demonstrated the differences between the innate differentiation propensities within hESC and hiPSC lines [11, 16–18, 35] and between hESC and hiPSC lines [6]. In contrast, two other studies have suggested that in general, hESCs and hiPSCs have similar differentiation capacity toward neural cells, but line-specific variation can be detected in both groups [16, 17]. Our results were more compatible with the latter view.

Electrophysiological properties are an essential aspect of the characterization of neuronal cells. In the present study, all the cell lines differentiated into neuronal networks that were able to display some form of spontaneous electrical activity regarded as a feature of functional neuronal networks [27, 37]. However, obvious maturation stage-related functional variability was observed. None of the gene or protein level markers of neuronal differentiation directly correlated with the functional properties of the derived neuronal networks. Thus, it is difficult to predict the efficiency of a particular cell line to produce functional neuronal networks without electrophysiological analyses.

Lastly, we differentiated the hPSCs into another ectodermal cell type, RPE cells. During mammalian development, RPE is derived from optic neuroepithelium by approximately the seventh week of gestation [38], and RPE cell fate specification in vitro has been shown to follow a time course reminiscent of normal retinal development [39]. All the cell lines examined produced pigmented cells within 3 weeks after initiation of differentiation. On average, hiPSC lines produced pigmented cells slightly more slowly than hESC lines. This is compatible with the findings by Meyer et al., who also reported longer differentiation times with hiPSCs than hESCs [39]. hESC3 produced pigmented cells the fastest. This cell line also produced eventually mature RPE cells. Two hiPSC lines also produced mature RPE cells, suggesting that the time of pigment appearance is not a crucial factor for the later maturation of RPE cells.

Consistent reactivation of the *OCT4* transgene was observed in all retrovirally induced hiPSC lines during RPE differentiation (Fig. 1B; supplemental online Fig. 2B). The reactivation was most dramatic in hiPSC1. In addition, the *NANOG* and *LIN28* transgenes were also reactivated in hiPSC1 during the RPE differentiation. On the contrary, transgene reactivation was not observed with the Sendai virus-induced iPSC5 line (supplemental online Fig. 3). Interestingly, hiPSC1 was differentiated successfully into both HLCs and cardiomyocytes, and transgene reactivation was not seen during those experiments. During RPE differentiation, hiPSC1 appeared to produce a high number of MITF and bestrophin-1-positive cells. However, hiPSC1-derived RPE cells peeled off from the culture membranes easily, allowing only one successful experiment to be completed. The RPE differentiation protocol is much (almost 3 months) longer and more spontaneous than the other protocols, which could be one explanation for the difference. Obviously, these observations raise concerns about the safety of hiPSCs that have integrated transgenes in their genome.

Conclusion

Part of the variation in the differentiation efficiency between the individual hiPSCs could be explained by residual activity of viral transgene *KLF4* in hiPSC4 and the reactivation of several transgenes during RPE differentiation. In contrast, the hiPSC line that was derived through the nonintegrating Sendai virus technology differentiated well into both HLCs and RPE cells and did not show signs of transgene expression. Our study strongly suggests that many of the "first-generation" retrovirally derived iPSC lines are hampered by potential transgene reactivation, with specific effects on their further differentiation properties. These findings highlight the need for integration-free reprogramming technologies, resulting in transgene-free iPSCs, which could also be potentially therapeutically applicable, unlike the retrovirally derived cells used in this study. Several such technologies have been established, in addition to Sendai viruses [40]: polycistronic minicircle vectors [41], PiggyBac transposons [42], and modified mRNA-based [43] or protein transduction-based methods [44]. Future studies should focus on nontransgenic iPSC lines generated through these methods.

Acknowledgments

We are grateful to the following individuals for technical assistance: Markus Haponen, Maria af Hällström, Merja Lehtinen, Henna Venäläinen, Elina Konsén, Hanna Koskenaho, Outi Melin, Jarkko Ustinov, and Eila Korhonen. We thank Juha Heikkilä and Meeri Mäkinen for assistance with MEA measurements. This study was supported by funding from Biocenter Finland for the national platform on stem cells and biomaterials. Additional grant support was received from the Academy of Finland (to H.S., S.N., K.A.-S., T.O.), the Competitive Research Funding of the Pirkanmaa Hospital District (to H.S., S.N., K.A.-S.), the Alfred Kordelin Foundation (to K.A.-S.), the Finnish Foundation of Cardiovascular Research (to K.A.-S.), the Finnish Funding Agency for Technology and Innovation (to K.A.-S.), the Päivikki and Sakari Sohlberg Foundation (to H.S.), the Sigrid Jusélius Foundation (to T.O.), and the Competitive Research Funding of the Uusimaa Hospital District (to T.O.).

Author Contributions

S.T., M.O., A.H., T.I., K.R., and R.Ä.: conception and design, collection and assembly of data, data analysis and interpretation, manuscript writing; M.P.-M.: conception and design, data analysis and interpretation; K.L.: conception and design, collection and assembly of data; J.P.: collection and assembly of data, data analysis and interpretation; J.W. and R.T.: provision of study material, collection and assembly of data; O.S.: conception and design, financial support; H.S.: conception and design, financial support, data analysis and interpretation, final approval of manuscript; S.N.: conception and design, financial support, provision of study material, final approval of manuscript; K.A.-S. and T.O.: conception and design, financial support, provision of study material, data analysis and interpretation, manuscript writing, final approval of manuscript.

Disclosure of Potential Conflicts of Interest

The authors indicate no potential conflicts of interest.

References

1 Robinton DA, Daley GQ. The promise of induced pluripotent stem cells in research and therapy. Nature 2012;481:295–305.

2 Thomson JA, Itskovitz-Eldor J, Shapiro SS et al. Embryonic stem cell lines derived from human blastocysts. Science 1998;282:1145–1147.

3 Takahashi K, Tanabe K, Ohnuki M et al. Induction of pluripotent stem cells from adult human fibroblasts by defined factors. Cell 2007;131:861–872.

4 Yu J, Vodyanik MA, Smuga-Otto K et al. Induced pluripotent stem cell lines derived from human somatic cells. Science 2007;318:1917–1920.

5 Cao N, Liu Z, Chen Z et al. Ascorbic acid enhances the cardiac differentiation of induced pluripotent stem cells through promoting the proliferation of cardiac progenitor cells. Cell Res 2012;22:219–236.

6 Hu BY, Weick JP, Yu J et al. Neural differentiation of human induced pluripotent stem cells follows developmental principles but with variable potency. Proc Natl Acad Sci USA 2010;107:4335–4340.

7 Si-Tayeb K, Noto FK, Nagaoka M et al. Highly efficient generation of human hepatocyte-like cells from induced pluripotent stem cells. Hepatology 2010;51:297–305.

8 Vaajasaari H, Ilmarinen T, Juuti-Uusitalo K et al. Toward the defined and xeno-free differentiation of functional human pluripotent stem cell-derived retinal pigment epithelial cells. Mol Vis 2011;17:558–575.

9 Takahashi K, Yamanaka S. Induction of pluripotent stem cells from mouse embryonic and adult fibroblast cultures by defined factors. Cell 2006;126:663–676.

10 Chin MH, Mason MJ, Xie W et al. Induced pluripotent stem cells and embryonic stem cells are distinguished by gene expression signatures. Cell Stem Cell 2009;5:111–123.

11 Bock C, Kiskinis E, Verstappen G et al. Reference maps of human ES and iPS cell variation enable high-throughput characterization of pluripotent cell lines. Cell 2011;144:439–452.

12 Matsui T, Leung D, Miyashita H et al. Proviral silencing in embryonic stem cells requires the histone methyltransferase ESET. Nature 2010;464:927–931.

13 Lister R, Pelizzola M, Kida YS et al. Hotspots of aberrant epigenomic reprogramming in human induced pluripotent stem cells. Nature 2011;471:68–73.

14 Hu Q, Friedrich AM, Johnson LV et al. Memory in induced pluripotent stem cells: Reprogrammed human retinal-pigmented epithelial cells show tendency for spontaneous redifferentiation. Stem Cells 2010;28:1981–1991.

15 Ieda M, Fu JD, Delgado-Olguin P et al. Direct reprogramming of fibroblasts into functional cardiomyocytes by defined factors. Cell 2010;142:375–386.

16 Kim K, Zhao R, Doi A et al. Donor cell type can influence the epigenome and differentiation potential of human induced pluripotent stem cells. Nat Biotechnol 2011;29:1117–1119.

17 Boulting GL, Kiskinis E, Croft GF et al. A functionally characterized test set of human induced pluripotent stem cells. Nat Biotechnol 2011;29:279–286.

18 Osafune K, Caron L, Borowiak M et al. Marked differences in differentiation propensity among human embryonic stem cell lines. Nat Biotechnol 2008;26:313–315.

19 Zhang J, Wilson GF, Soerens AG et al. Functional cardiomyocytes derived from human induced pluripotent stem cells. Circ Res 2009;104:e30–e41.

20 Mikkola M, Olsson C, Palgi J et al. Distinct differentiation characteristics of individual human embryonic stem cell lines. BMC Dev Biol 2006;6:40.

21 Skottman H. Derivation and characterization of three new human embryonic stem cell lines in Finland. In Vitro Cell Dev Biol Anim 2010;46:206–209.

22 Hussein SM, Batada NN, Vuoristo S et al. Copy number variation and selection during reprogramming to pluripotency. Nature 2011;471:58–62.

23 Lahti AL, Kujala VJ, Chapman H et al. Model for long QT syndrome type 2 using human iPS cells demonstrates arrhythmogenic characteristics in cell culture. Dis Model Mech 2012;5:220–230.

24 Hay DC, Fletcher J, Payne C et al. Highly efficient differentiation of hESCs to functional hepatic endoderm requires ActivinA and Wnt3a signaling. Proc Natl Acad Sci USA 2008;105:12301–12306.

25 Passier R, Oostwaard DW, Snapper J et al. Increased cardiomyocyte differentiation from human embryonic stem cells in serum-free cultures. Stem Cells 2005;23:772–780.

26 Huttunen TT, Sundberg M, Pihlajamaki H et al. An automated continuous monitoring system: A useful tool for monitoring neuronal differentiation of human embryonic stem cells. Stem Cell Studies 2011;1:71–77.

27 Heikkilä TJ, Yla-Outinen L, Tanskanen JM et al. Human embryonic stem cell-derived neuronal cells form spontaneously active neuronal networks in vitro. Exp Neurol 2009;218:109–116.

28 Stadtfeld M, Maherali N, Breault DT et al. Defining molecular cornerstones during fibroblast to iPS cell reprogramming in mouse. Cell Stem Cell 2008;2:230–240.

29 Lei H, Oh SP, Okano M et al. De novo DNA cytosine methyltransferase activities in mouse embryonic stem cells. Development 1996;122:3195–3205.

30 Mikkelsen TS, Hanna J, Zhang X et al. Dissecting direct reprogramming through integrative genomic analysis. Nature 2008;454:49–55.

31 Sridharan R, Tchieu J, Mason MJ et al. Role of the murine reprogramming factors in the induction of pluripotency. Cell 2009;136:364–377.

32 Beqqali A, Kloots J, Ward-van Oostwaard D et al. Genome-wide transcriptional profiling of human embryonic stem cells differentiating to cardiomyocytes. Stem Cells 2006;24:1956–1967.

33 Bettiol E, Sartiani L, Chicha L et al. Fetal bovine serum enables cardiac differentiation of human embryonic stem cells. Differentiation 2007;75:669–681.

34 Pekkanen-Mattila M, Ojala M, Kerkela E et al. The effect of human and mouse fibroblast feeder cells on cardiac differentiation of human pluripotent stem cells. Stem Cells Int 2012;2012:875059.

35 Lappalainen RS, Salomaki M, Yla-Outinen L et al. Similarly derived and cultured hESC lines show variation in their developmental potential towards neuronal cells in long-term culture. Regen Med 2010;5:749–762.

36 Sundberg M, Jansson L, Ketolainen J et al. CD marker expression profiles of human embryonic stem cells and their neural derivatives, determined using flow-cytometric analysis, reveal a novel CD marker for exclusion of pluripotent stem cells. Stem Cell Res 2009;2:113–124.

37 Pine J. Recording action potentials from cultured neurons with extracellular microcircuit electrodes. J Neurosci Methods 1980;2:19–31.

38 Fuhrmann S. Eye morphogenesis and patterning of the optic vesicle. Curr Top Dev Biol 2010;93:61–84.

39 Meyer JS, Shearer RL, Capowski EE et al. Modeling early retinal development with human embryonic and induced pluripotent stem cells. Proc Natl Acad Sci USA 2009;106:16698–16703.

40 Fusaki N, Ban H, Nishiyama A et al. Efficient induction of transgene-free human pluripotent stem cells using a vector based on Sendai virus, an RNA virus that does not integrate into the host genome. Proc Jpn Acad Ser B Phys Biol Sci 2009;85:348–362.

41 Jia F, Wilson KD, Sun N et al. A nonviral minicircle vector for deriving human iPS cells. Nat Methods 2010;7:197–199.

42 Woltjen K, Michael IP, Mohseni P et al. piggyBac transposition reprograms fibroblasts to induced pluripotent stem cells. Nature 2009;458:766–770.

43 Warren L, Manos PD, Ahfeldt T et al. Highly efficient reprogramming to pluripotency and directed differentiation of human cells with synthetic modified mRNA. Cell Stem Cell 2010;7:618–630.

44 Kim D, Kim CH, Moon JI et al. Generation of human induced pluripotent stem cells by direct delivery of reprogramming proteins. Cell Stem Cell 2009;4:472–476.

See www.StemCellsTM.com for supporting information available online.

OPEN ACCESS Freely available online

PLOS ONE

Culture Conditions Affect Cardiac Differentiation Potential of Human Pluripotent Stem Cells

Marisa Ojala[1,2], Kristiina Rajala[1,2], Mari Pekkanen-Mattila[1,2], Marinka Miettinen[1,2], Heini Huhtala[3], Katriina Aalto-Setälä[1,2,4]*

1 Institute of Biomedical Technology, University of Tampere, Tampere, Finland, **2** BioMediTech, University of Tampere, Tampere, Finland, **3** School of Health Sciences, University of Tampere, Tampere, Finland, **4** Heart Center, Tampere University Hospital, Tampere, Finland

Abstract

Human pluripotent stem cells (hPSCs), including human embryonic stem cells (hESCs) and human induced pluripotent stem cells (hiPSCs), are capable of differentiating into any cell type in the human body and thus can be used in studies of early human development, as cell models for different diseases and eventually also in regenerative medicine applications. Since the first derivation of hESCs in 1998, a variety of culture conditions have been described for the undifferentiated growth of hPSCs. In this study, we cultured both hESCs and hiPSCs in three different culture conditions: on mouse embryonic fibroblast (MEF) and SNL feeder cell layers together with conventional stem cell culture medium containing knockout serum replacement and basic fibroblast growth factor (bFGF), as well as on a Matrigel matrix in mTeSR1 medium. hPSC lines were subjected to cardiac differentiation in mouse visceral endodermal-like (END-2) co-cultures and the cardiac differentiation efficiency was determined by counting both the beating areas and Troponin T positive cells, as well as studying the expression of *OCT-3/4*, mesodermal *Brachyury T* and *NKX2.5* and endodermal *SOX-17* at various time points during END-2 differentiation by q-RT-PCR analysis. The most efficient cardiac differentiation was observed with hPSCs cultured on MEF or SNL feeder cell layers in stem cell culture medium and the least efficient cardiac differentiation was observed on a Matrigel matrix in mTeSR1 medium. Further, hPSCs cultured on a Matrigel matrix in mTeSR1 medium were found to be more committed to neural lineage than hPSCs cultured on MEF or SNL feeder cell layers. In conclusion, culture conditions have a major impact on the propensity of the hPSCs to differentiate into a cardiac lineage.

Citation: Ojala M, Rajala K, Pekkanen-Mattila M, Miettinen M, Huhtala H, et al. (2012) Culture Conditions Affect Cardiac Differentiation Potential of Human Pluripotent Stem Cells. PLoS ONE 7(10): e48659. doi:10.1371/journal.pone.0048659

Editor: Martin Pera, University of Melbourne, Australia

Received April 4, 2012; **Accepted** September 28, 2012; **Published** October 31, 2012

Funding: This study was funded by the Academy of Finland, the Finnish Foundation for Cardiovascular Research, Biocenter Finland, the Finnish Funding Agency for Technology and Innovation, Competitive Research Funding of the Pirkanmaa Hospital District and the Alfred Kordelin Foundation. The funders had no role in study design, data collection and analysis, decision to publish, or preparation of the manuscript.

Competing Interests: Author Katriina Aalto- Setälä is a PLOS ONE Editorial Board member. This does not alter the authors' adherence to all the PLOS ONE policies on sharing data and materials.

* E-mail: katriina.aalto-setala@uta.fi

Introduction

Human pluripotent stem cells (hPSCs) include human embryonic stem cells (hESCs) and human induced pluripotent stem cells (hiPSCs). hPSCs are able to self-renew and to differentiate into any human cell type; therefore, they can be used as a cell model to study embryology and disease pathophysiology. hPSCs have additional utility in drug screening applications and as a cell source for regenerative medicine in the future. Since the first derivation of a hESC line in 1998 on a mouse embryonic fibroblast (MEF) feeder cell layer [1], many hPSC culture methods based on different human feeder cell layers [2,3], autologous feeder cells [4,5], feeder cell-free [6–10] and suspension culture techniques [11] have been developed and described. Feeder cells provide appropriate cell contacts, various growth factors and extracellular matrix (ECM) proteins that are required for the undifferentiated growth of hPSCs. Animal-derived feeder cells and other animal components used in hPSC culture conditions contain animal proteins and other nonhuman molecules which could be transmitted to hPSCs during culture [12,13]. Because the ultimate aim of hPSC research is to use the cells in regenerative medicine applications, culture conditions are being optimized in the xeno-free direction. In addition, culturing feeder cells is very laborious and time-consuming, and for the regenerative medicine applications, a large number of hPSCs are needed. Therefore the research is aiming at developing both xeno- and feeder cell-free cultures. In feeder cell-free culture methods, the feeder cells are replaced by Matrigel, which is a basement membrane extract from mouse tumor cells, or by ECM proteins such as laminin, collagen and fibronectin [6–10]. Despite the tremendous effort made to optimize hPSC culture conditions, a universal and reliable, xeno- and feeder-free culture method remains to be discovered.

Each individual hESC line has a unique gene expression profile [14,15] and thus the self-renewal and differentiation capabilities vary among the different cell lines [16,17]. According to recent reports, hiPSC lines are even more variable and more prone to genomic alterations than hESCs [18–21]. In addition to the differences among individual hPSC lines, differences in culture conditions also have a considerable influence on the gene expression profile and subsequent characteristics of hPSCs. For example, serum- and feeder cell-free culture conditions, as well as the processes of enzymatic passaging and culturing of hPSCs in physiological normoxia (2%), have been found to alter the gene expression profile and epigenome of hPSCs [22–24].

Efficient cardiac differentiation methods are needed to produce large numbers of human cardiomyocytes for research purposes and for future regenerative medicine applications. Due to the unique gene expression profile and variable differentiation potential of each individual hPSC line, it may be challenging to develop a universal cardiac differentiation protocol that is applicable and efficient for all or even the majority of hPSC lines. Thus, it has been proposed that individual hPSC lines may require optimization of the cardiac differentiation conditions [25]. We hypothesized that in addition to cardiac differentiation methods, the hPSC culture method, in which cell lines are cultured prior to differentiation, may also have a significant impact on the cardiac differentiation potential of individual hPSC lines. In this study, the impact of three different culture methods for cardiac differentiation of hPSCs were compared: MEF and SNL feeder cell layers combined with conventional stem cell culture medium containing knockout serum replacement (ko-SR) and basic fibroblast growth factor (bFGF), and a Matrigel matrix combined with commercial mTeSR1 medium.

Results

The morphology of the pluripotent stem cell colonies varies with the culture conditions

In this study, a single hESC line (H7) and four hiPSC lines (UTA.00112.hFF, UTA.04602.WT, UTA.00525.LQT2 and UTA.00106.hFF) were cultured with three different culture methods: MEF and SNL feeder cell layers combined with conventional stem cell culture medium and Matrigel matrix combined with mTeSR1 medium, and subjected into cardiac differentiation in mouse visceral endodermal-like cell (END-2) co-cultures. The experimental design is presented in Figure 1A. hPSC lines cultured in different conditions were characterized by the morphology of the colonies, immunocytochemical staining and embryoid body (EB) formation (Figure 1). All cell lines attached well to both MEF and SNL feeder cell layers and to Matrigel matrix after passaging, while the morphology of the colonies varied under different culture conditions. On MEF feeder cells, the colonies were thick and small, while on SNL feeders and on Matrigel the colonies were large and thin and thus needed to be passaged more often than hPSCs cultured on MEF feeders (Figure 1B). It was difficult to adapt the H7 and UTA.00112.hFF cell lines to the Matrigel matrix in mTeSR1 medium because of the spontaneous neural differentiation. The H7 cell line was lost once and the adaptation had to be started from the beginning, and the UTA.00112.hFF cell line had to be cultured for 12 passages on Matrigel before enough cells were generated for the cardiac differentiation. However, all hPSC lines cultured at least for 14 passages in all three conditions expressed markers typical of undifferentiated hPSCs (Nanog, octamer-binding transcription factor 3/4 (OCT-3/4) and stage-specific embryonic antigen 4 (SSEA-4)), which were detected by immunocytochemical staining (Figure 1B). The pluripotency of the H7, UTA.00106.hFF and UTA.00525.LQT2 cell lines, cultured in all three conditions, was verified by EB formation and the EBs expressed at least one marker from all three germ layers (Figure 1C).

Pluripotent stem cells from all culture conditions differentiate into cardiomyocytes

hPSC lines cultured in all three culture conditions were differentiated into cardiomyocytes at least twice in END-2 co-cultures (See Table 1 for the number of independent experiments). hPSCs from MEF feeder cell layers formed uniform structures on END-2 cells, while hPSCs from SNL feeder cells formed irregular structures consisting of both cystic structures and uniform areas. Cells, which were cultured on Matrigel in mTeSR1 medium prior the differentiation, formed large, thick and uniform structures on END-2 cells (data not shown). Interestingly, microtubule associated protein 2 (MAP-2) expressing neural-like cells and bundles of nerve fibers were occasionally observed in END-2 co-cultures of all cell lines previously cultured on Matrigel in mTeSR1 medium. These structures were not detected in hPSCs originally cultured on MEF or SNL feeder cell layers.

hPSC lines cultured in all three culture conditions differentiated into cardiomyocytes and expressed Troponin T, myosin ventricular heavy chain α/β (MHC) and α-actinin (Figure 2A). Differentiation efficiency was evaluated by determining the amount of Troponin T positive cells in cytospin experiments on day 20 and by determining the number of beating areas at the end of differentiation on day 30. There was considerable variability observed in cardiac differentiation efficiency among the different hPSC lines. The highest number of beating areas was found in the H7 and UTA.00106.hFF cell lines while UTA.04602.WT, UTA.00525.LQT2 and UTA.00112.hFF produced fewer beating areas (Figure 2B).

Two hPSC lines (H7 and UTA.00525.LQT2) produced the highest number of beating areas when they were cultured on a MEF feeder cell layer prior to differentiation and one hPSC line (UTA.00106.hFF) when cultured on an SNL feeder cell layer (Figure 2B). In the H7 cell line, the number of beating areas was significantly lower on Matrigel when compared to SNL ($p = 0.002$) or MEF ($p<0.001$) feeder cell layers. UTA.00525.LQT2 produced the highest number of beating areas when cultured on a MEF feeder cell layer, and the number was significantly higher that on Matrigel ($p = 0.017$) (Figure 2B). In the UTA.00106.hFF cell line, the number of beating areas was highest in cells cultured on an SNL feeder cell layer prior to differentiation ($p<0.001$). Taken together, three cell lines produced the highest number of beating areas when cultured on mouse feeder cell layers prior the differentiation. The UTA.04602.WT cell line was an exception, and the number of beating areas was significantly higher in cells taken from Matrigel cultures than from MEF feeder cell cultures ($p = 0.015$). The UTA.00112.hFF cell line had a very poor differentiation capacity and produced only a few beating areas overall, and there were no significant differences among the different culture conditions.

The highest number of Troponin T positive cells was found in cells originating on MEF feeder cell layers, while the number of Troponin T positive cells was lowest in cells originating on Matrigel ($p = 0.012$) (Figure 2C). The amount of Troponin T positive cells for each hPSC line is presented in Figure 2D. Although the total number of cytospin experiments was quite low, the results were consistent with the number of beating areas counted.

The expression of developmental markers varies in cells cultured in different conditions

RNA samples were collected from undifferentiated cells at the beginning of cardiac differentiation (day 0) and from END-2 co-cultures on days 3, 6, 12 and 30 during two individual differentiation experiments of the H7, UTA.00112.hFF and UTA.04602.WT cell lines. The expression of the marker for pluripotent stem cells (*OCT-3/4*), the mesodermal markers (*T, brachyury homolog* (*Brachyury T*) and *NK2 homeobox 5* (*NKX2.5*)), and the endodermal marker (*Sex determining region Y-box 17* (*SOX-17*)) were analyzed in the samples.

OCT-3/4 expression progressively declined during END-2 co-culture in all culture conditions (Figure 3A). On Matrigel, the

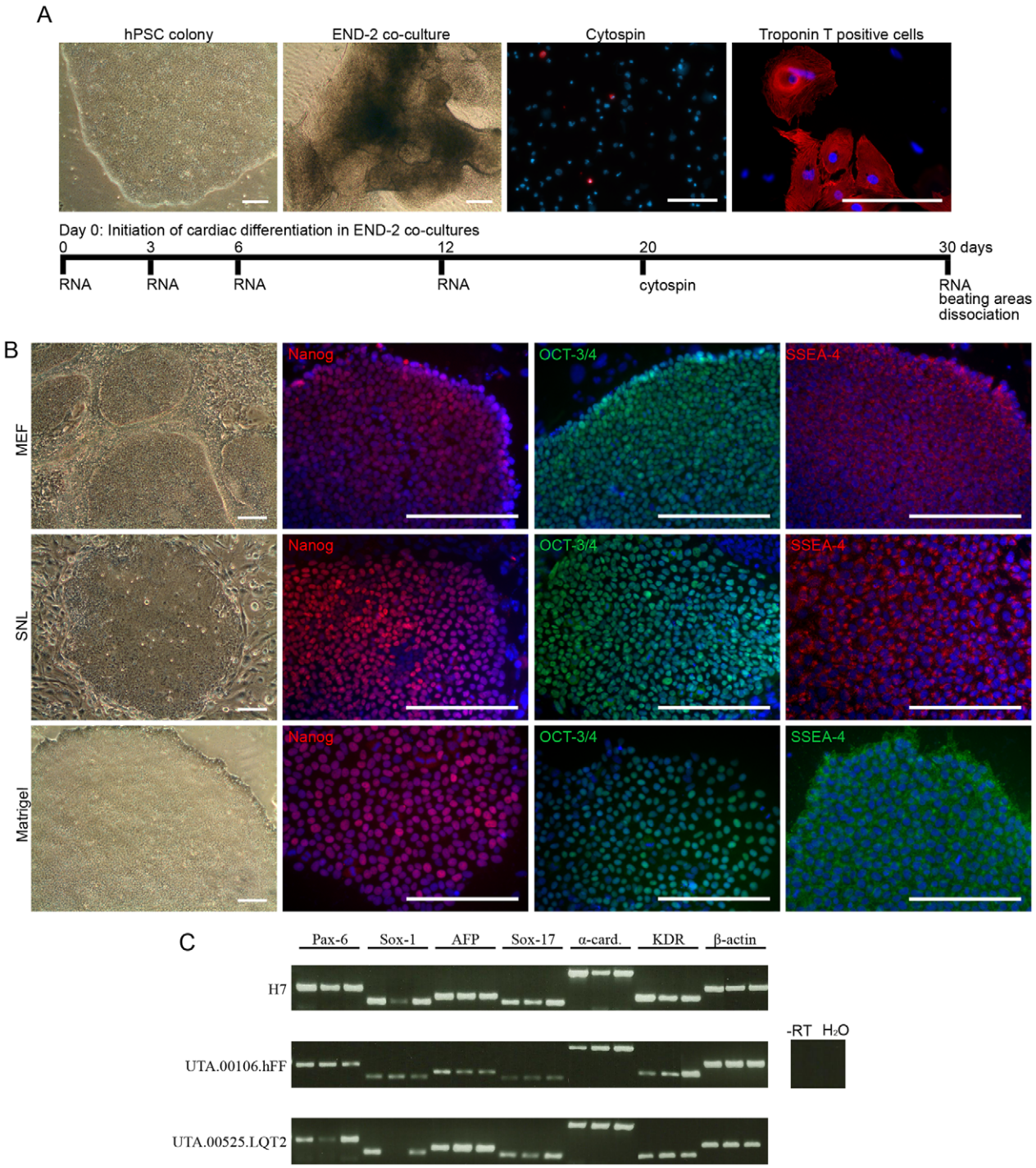

Figure 1. hPSCs were cultured with three different culture methods. A) Schematic presentation of cardiac differentiation in END-2 co-culture and the experimental design. hPSC = human pluripotent stem cell, END-2 = mouse visceral endodermal-like cells. Scale bars, 200 μm. B) All five hPSC lines cultured on MEF and SNL feeder cell layers in conventional stem cell culture medium and on Matrigel in mTeSR1 medium at least for 14 passages formed undifferentiated colonies, which expressed pluripotency markers Nanog, OCT-3/4 and SSEA-4. Representative images of UTA.00112.hFF (phase contrast microscope images) and H7 (immunofluorescence images) cell lines are presented. Scale bars, 200 μm. C) H7, UTA.00106.hFF and UTA.00525.LQT2 cell lines cultured in all three culture conditions (in figure: first band MEF, second band SNL, third band Matrigel) formed embryoid bodies (EBs) expressing markers from all germ layers: ectoderm (*PAX-6* and *SOX-1*), endoderm (*AFP* and *SOX-17*) and mesoderm (*α-cardiac actin* and *KDR*).
doi:10.1371/journal.pone.0048659.g001

OCT-3/4 expression was significantly higher than on MEF and SNL feeder cell layers on day 0 (MEF vs. Matrigel, $p = 0.003$; and SNL vs. Matrigel, $p = 0.009$) and on day 3 (MEF vs. Matrigel, $p = 0.004$; SNL vs. Matrigel, $p = 0.018$). On day 6, the expression of *OCT-3/4* was significantly higher in cells taken from Matrigel than those from MEF feeder cell layers ($p = 0.007$). Thus, the

Table 1. Cell lines and their passages used in this study.

		Passage during differentiation experiments							
Cell line	**Culture condition**	**1.**	**2.**	**3.**	**4.**	**5.**	**6.**	**TNE**	**TNW**
H7	MEF	44	51	55	47	51	57	6	105
H7	SNL	44(6)*	53(15)	–	49(6)	53(10)	63(20)	5	67
H7	Matrigel	50(6)	59(15)	–	48(5)	53(10)	60(17)	5	89
UTA.00112.hFF	MEF	–	–	–	15	18	22	3	48
UTA.00112.hFF	SNL	–	–	–	16(5)	21(10)	25(14)	3	42
UTA.00112.hFF	Matrigel	–	–	–	23(12)	26(15)	29(18)	3	54
UTA.04602.WT	MEF	–	–	–	35	40	44	3	51
UTA.04602.WT	SNL	–	–	–	37(5)	48(16)	52(20)	3	46
UTA.04602.WT	Matrigel	–	–	–	37(5)	47(15)	51(19)	3	45
UTA.00525.LQT2	MEF	45	33	37	–	–	–	3	36
UTA.00525.LQT2	SNL	44(6)	53(15)	–	–	–	–	2	18
UTA.00525.LQT2	Matrigel	44(6)	53(15)	–	–	–	–	2	30
UTA.00106.hFF	MEF	24	30	34	–	–	–	3	40
UTA.00106.hFF	SNL	23(6)	32(15)	–	–	–	–	2	25
UTA.00106.hFF	Matrigel	23(6)	32(15)	–	–	–	–	2	31

*The passages, indicating for how long hPSCs were cultured in SNL and Matrigel conditions, are given in parenthesis.
TNE = Total number of experiments.
TNW = Total number of wells from which the beating areas were counted.
doi:10.1371/journal.pone.0048659.t001

expression of *OCT-3/4* persisted for a longer time in hPSCs cultured on Matrigel as opposed to MEF or SNL feeder cell layers (Figure 3A).

In cells originating on MEF or SNL feeder cell layers, the peak level of *Brachyury T* expression was observed on day 3, while cells originating on Matrigel showed peak *Brachyury T* expression later on day 6 (Figure 3B). The highest expression level of *Brachyury T* was observed on day 3 in cells cultured on a MEF feeder cell layer prior to differentiation (MEF vs. SNL, $p = 0.004$; MEF vs. Matrigel, $p<0.001$). On day 3, the expression of *Brachyury T* in cells originating on Matrigel was significantly lower than the expression level in cells cultured on MEF ($p<0.001$) or SNL ($p = 0.016$) feeder cell layers. On day 6 and 12, the expression of *Brachyury T* was significantly higher in cells cultured on Matrigel than those cultured on MEF (day 6, $p = 0.040$; day 12, $p = 0.001$) or SNL (day 6, $p = 0.009$; day 12, $p = 0.001$) feeder cell layers prior to differentiation.

The expression of endodermal *SOX-17* was similar when compared to mesodermal *Brachyury T* expression (Figure 3C). The highest level of *SOX-17* expression was found in cells originating on MEF feeder cell layers on day 3. *SOX-17* peaked on day 3 in cells cultured on MEF and SNL feeder cell layers, whereas the peak level of *SOX-17* expression in cells cultured on Matrigel was observed on day 6. On day 3, *SOX-17* expression in cells originating on Matrigel was significantly lower than in cells cultured on MEF ($p<0.001$) or SNL ($p = 0.001$) feeder cell layers, while on day 6, *SOX-17* expression was significantly higher in cells originating on Matrigel than on an SNL feeder cell layer ($p = 0.016$).

The highest expression of *NKX2.5* was observed on day 3 in cells from SNL feeder cells, and it was significantly higher ($p = 0.047$) than expression levels in cells cultured on Matrigel. On day 12, the situation was just the opposite, in that the expression of *NKX2.5* was higher in cells originating on Matrigel than on MEF ($p = 0.018$) or SNL ($p<0.001$) feeder cell layers. On day 30, *NKX2.5* expression was significantly higher in cells originating on MEF than on SNL feeder cell layers or Matrigel ($p<0.001$ for both conditions).

PSA-NCAM positive cells can be detected in all culture conditions

All five hPSC lines cultured in all three conditions were analyzed with cytometric analysis of pluripotency marker tumor-related antigen (TRA)-1-81 and polysialylated-neural cell adhesion molecule (PSA-NCAM), which is mainly expressed in embryonic and neonatal neural tissue. PSA-NCAM positive cells could be detected from all hPSC culture conditions (Figure 4A–B). The lowest amount of PSA-NCAM positive cells about 2.5% was found in MEF cultures, while in SNL and Matrigel cultures the amount of PSA-NCAM positive cells was about 11%. H7 and UTA.00112.hFF cell lines had the highest amount of PSA-NCAM positive cells in Matrigel cultures, UTA.00106.hFF and UTA.00525.LQT2 in SNL cultures and UTA.04602.WT cell line in MEF cultures. In general, the amount of TRA-1-81 positive cells positive cells correlated with the amount of PSA-NCAM positive cells. It was highest in MEF cultures and lowest in SNL and Matrigel cultures (Figure 4A). In all hPSC lines, the amount of TRA-1-81 positive cells was highest in MEF cultures indicating the superiority of MEF feeder layer over SNL feeders and Matrigel in maintaining the pluripotency of hPSCs. PSA-NCAM positive cells were not detected in MEF cultures in immunocytochemical stainings, while on SNL feeder cell layers and on Matrigel cultures PSA-NCAM positive cells were detected. Example of TRA-1-81 and PSA-NCAM positive cells and immunocytochemical staining with PSA-NCAM antibody are presented in Figure 4C for H7 cell line. H7 cell line is widely used in cardiac differentiation

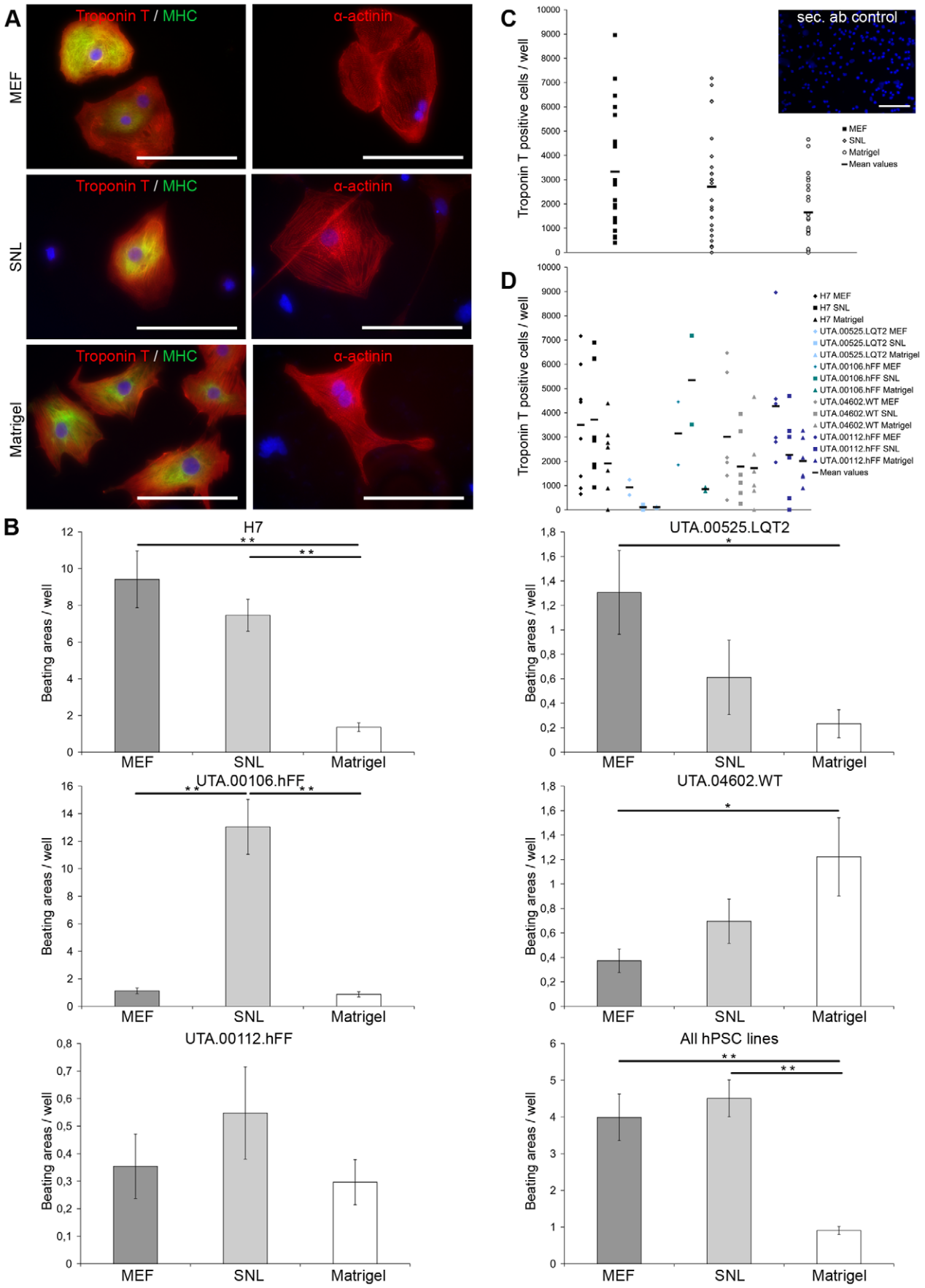
A
Troponin T / MHC
α-actinin
MEF
SNL
Matrigel
C
sec. ab control
Troponin T positive cells / well
MEF
SNL
Matrigel
Mean values
D
H7 MEF
H7 SNL
H7 Matrigel
UTA.00525.LQT2 MEF
UTA.00525.LQT2 SNL
UTA.00525.LQT2 Matrigel
UTA.00106.hFF MEF
UTA.00106.hFF SNL
UTA.00106.hFF Matrigel
UTA.04602.WT MEF
UTA.04602.WT SNL
UTA.04602.WT Matrigel
UTA.00112.hFF MEF
UTA.00112.hFF SNL
UTA.00112.hFF Matrigel
Mean values
B
H7
UTA.00525.LQT2
UTA.00106.hFF
UTA.04602.WT
UTA.00112.hFF
All hPSC lines
Beating areas / well
MEF
SNL
Matrigel

Figure 2. All hPSC lines cultured with different culture methods differentiated into cardiomyocytes with varying efficiencies. A) Cardiomyocytes derived from hPSCs cultured in all three culture conditions expressed Troponin T, myosin ventricular heavy chain α/β (MHC) and α-actinin. Representative images from H7 and UTA.00112.hFF cell lines. Scale bars, 200 μm. B) The columns show the average amount of beating areas in one well with different hPSC lines cultured in all three culture conditions. The number of wells from which beating areas were counted in different conditions for each cell line can be found in Table 1. In figure where all hPSC lines are collected into one histogram, the columns show the average amount of beating areas in one well of all cell lines (MEF n = 280, SNL n = 198, Matrigel n = 249). Error bars show the standard error of the mean (SEM). ** $p<0.01$, * $p<0.05$. Representative image of secondary antibody control is from H7 cell line cultured on Matrigel prior differentiation. Scale bar, 200 μm. C) Scatter plot show the amount of Troponin T positive cells in one well of all hPSC lines collected together in different conditions. The amount of Troponin T positive cells was significantly higher on MEF feeder cell layers than on Matrigel ($p = 0.012$). D) The scatter plot show the amount of Troponin T positive cells in one well separately for each cell line cultured in all three culture conditions.
doi:10.1371/journal.pone.0048659.g002

experiments and it had the best cardiac differentiation efficiency of all hPSC lines used in this experiment.

Neural cells are more abundant in Matrigel cultures than in feeder cultures

On Matrigel matrix combined with mTeSR1 medium, hPSCs tended to differentiate into neural-like cells, which was observed primarily along the edges of the undifferentiated hPSC colonies (Figure 5A). Neural-like cells were observed occasionally in all cell lines cultured on Matrigel in mTeSR1 medium and two hPSC lines H7 and UTA.00112.hFF were hard to adapt on Matrigel because of the neural differentiation. The H7 cell line was hard to maintain on Matrigel in mTeSR1 medium, and as a result of differentiation into neural-like cells, the H7 cell line was lost after 7 passages in culture. At first, there were only a few neural-like cells observed in the culture, but the number of neural cells expanded during the culture period, even though the differentiated areas were carefully removed before passaging the cells. Finally, only colonies with MAP-2 expressing, rosette-like structures (Figure 5A–B) and neural-like cells (Figure 5C) were observed in the cultures. H7, UTA.00112.hFF, UTA00525.LQT2 and UTA.04602.WT cell lines cultured in all three culture conditions were characterized by immunocytochemical staining with MAP-2. Only a few MAP-2 positive cells were found in SNL and MEF cultures, but none were found to the same extent as in cells cultured on Matrigel in mTeSR1 medium (Figure 5E). On SNL feeders, the only MAP-2 positive cells were found from H7 cell line and on MEF feeders from UTA.00525.LQT2 cell line (Figure 5E).

The expression of ectodermal *PAX-6, Musashi* and *Neurofilament 68* (*NF-68*) was measured by q-RT-PCR in cells cultured for 0, 3,

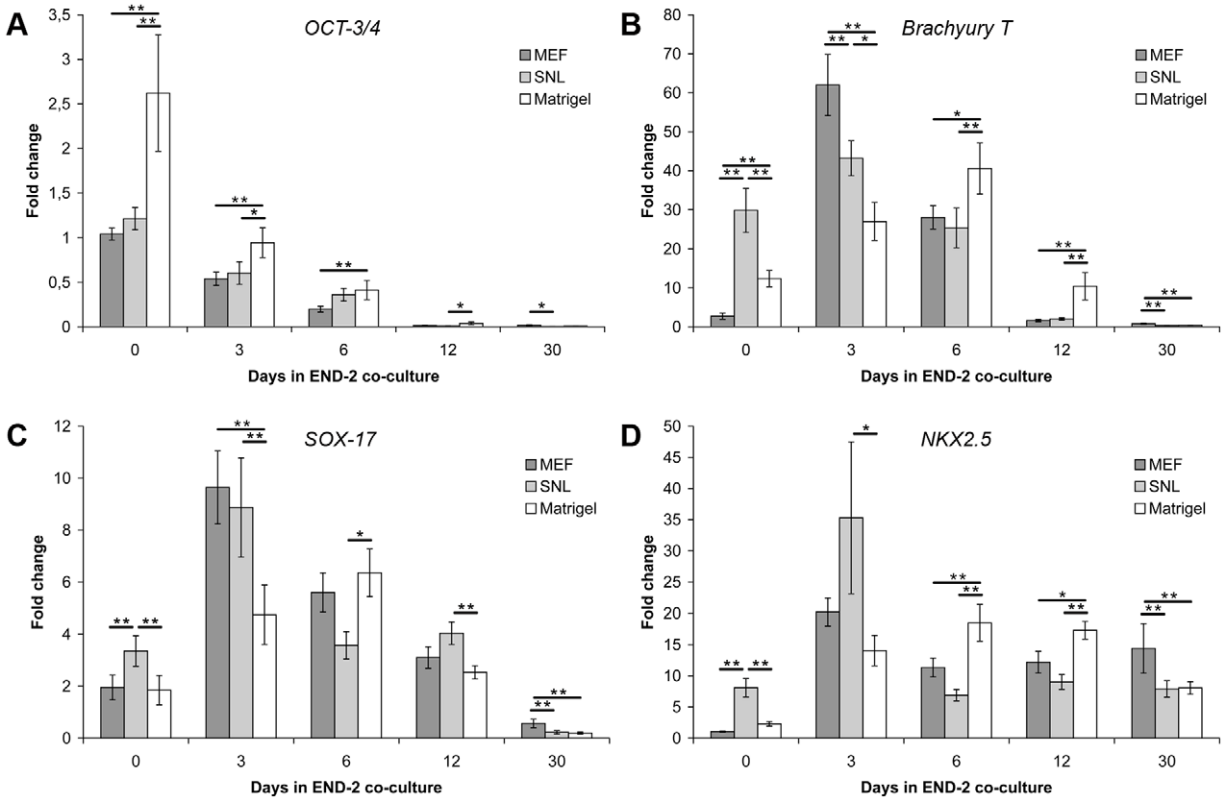

Figure 3. The expression profiles of *OCT-3/4, Brachyury T, SOX-17* and *NKX2.5* in END-2 co-cultures. A) The expression of *OCT-3/4* in END-2 co-cultures originating from Matrigel decreased slower than in MEF and SNL feeder cell layer. B) The expression of *Brachyury T* peaked on day 3 in END-2 co-cultures originating from MEF and SNL feeder cell layers, while from Matrigel the peak was delayed to day 6. C) The expression of *SOX-17* behaved in the same way than *Brachyury T* expression. *SOX-17* peaked on day 3 in END-2 co-cultures originating from MEF and SNL feeders, while in co-cultures originating from Matrigel, the *SOX-17* peak was delayed to day 6. D) The expression of *NKX2.5* was highest on MEF feeder cell layers in the end of END-2 co-culture. The data is collected from two individual differentiation experiments of H7, UTA.00112.hFF and UTA.04602.WT hPSC lines (n = 6 in all three conditions). Error bars show the standard error of the mean (SEM). ** $p<0.01$, * $p<0.05$.
doi:10.1371/journal.pone.0048659.g003

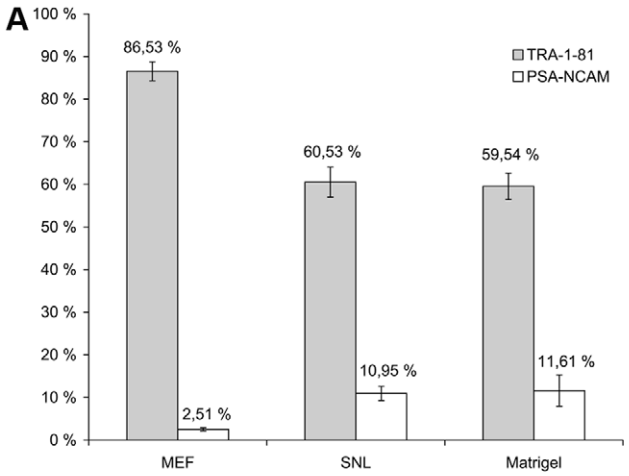

B

Cell line and condition	n	TRA-1-81	SEM	PSA-NCAM	SEM
H7 MEF	3	90,33 %	3,04 %	0,97 %	0,27 %
H7 SNL	4	60,05 %	3,80 %	18,33 %	2,97 %
H7 Matrigel	3	52,07 %	5,33 %	30,77 %	9,27 %
UTA.00106.hFF MEF	3	74,53 %	3,45 %	2,10 %	0,06 %
UTA.00106.hFF SNL	4	41,73 %	1,43 %	14,73 %	3,15 %
UTA.00106.hFF Matrigel	3	56,50 %	6,13 %	8,37 %	0,72 %
UTA.00112.hFF MEF	3	80,97 %	1,01 %	1,67 %	0,20 %
UTA.00112.hFF SNL	4	58,23 %	1,48 %	7,50 %	1,29 %
UTA.00112.hFF Matrigel	3	52,80 %	9,31 %	15,63 %	9,38 %
UTA.00525.LQT2 MEF	4	88,33 %	2,73 %	4,08 %	0,44 %
UTA.00525.LQT2 SNL	4	55,73 %	1,78 %	13,30 %	2,30 %
UTA.00525.LQT2 Matrigel	3	70,37 %	6,90 %	2,13 %	0,99 %
UTA.04602.WT MEF	3	97,87 %	0,38 %	3,23 %	1,08 %
UTA.04602.WT SNL	4	86,90 %	3,58 %	0,90 %	0,16 %
UTA.04602.WT Matrigel	3	65,97 %	0,12 %	1,17 %	0,24 %

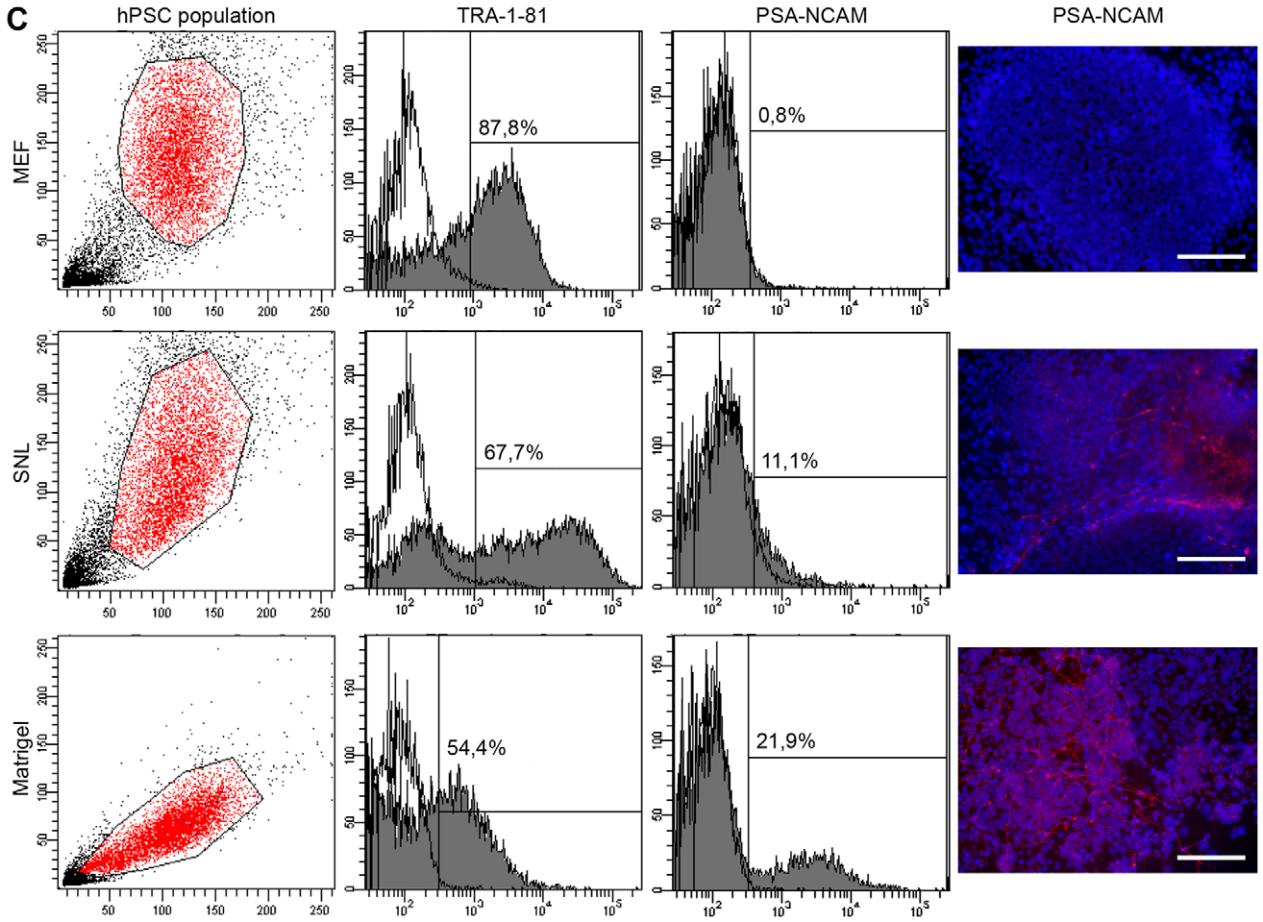

Figure 4. The amount of TRA-1-81 and PSA-NCAM positive cells in hPSC cultures. A) The amount of TRA-1-81 positive cells was higher and the expression of PSA-NCAM positive cells was lower in MEF feeder cultures than in SNL or Matrigel cultures. Columns show the average of TRA-1-81 and PSA-NCAM positive cells of all hPSC lines cultured in three different conditions (MEF n = 16, SNL n = 20 and Matrigel n = 15). Error bars show the standard error of the mean (SEM). B) The amount of TRA-1-81 and PSA-NCAM cells for each hPSC lines cultured in all three conditions. C) Examples of TRA-1-81 and PSA-NCAM expressions in H7 cell line in all three conditions. Dot plots show the determination of hPSC population and histograms show the percentage of TRA-1-81 and PSA-NCAM positive cells. Unstained cells were used for background determination (white). The highest amount of PSA-NCAM positive cells in immunocytochemical stainings were found on Matrigel. PSA-NCAM positive cells were not detected on MEF feeder cell cultures. Scale bars, 200 μm.
doi:10.1371/journal.pone.0048659.g004

6, 12 and 30 days in END-2 co-cultures (Figure 5F–H). Samples were collected during two individual differentiation experiments of the H7, UTA.00112.hFF and UTA.04602.WT cell lines. The expression of *PAX-6* increased in all conditions from day 0 to day 30 (Figure 5F). However, the expression of *PAX-6* in cells originating from Matrigel was significantly higher than on MEF of SNL feeder layers on day 3 (Matrigel vs. MEF $p<0.001$, Matrigel vs. SNL $p<0.001$), 6 (Matrigel vs. MEF $p<0.001$, Matrigel vs.

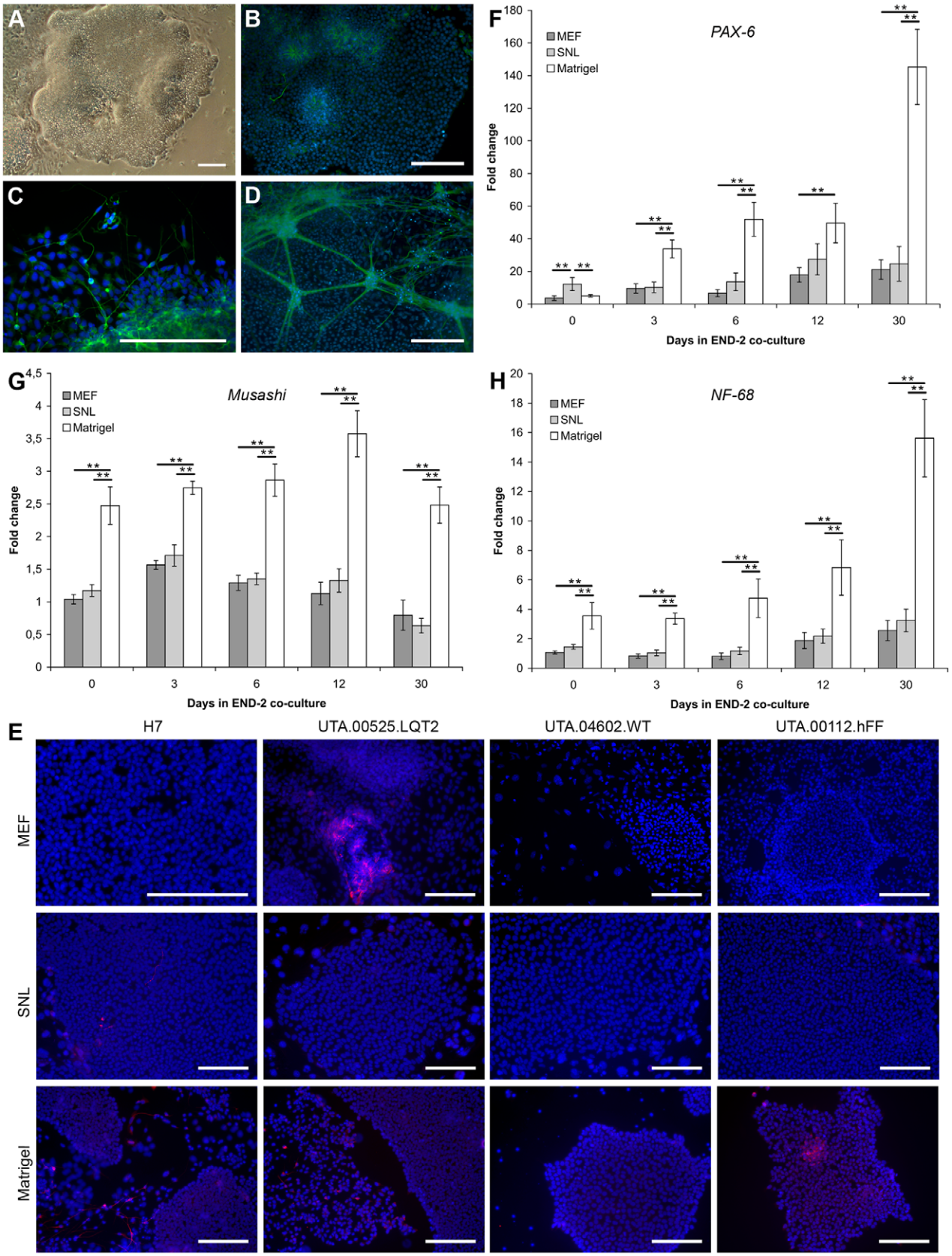

Figure 5. The expression of neural markers was highest in hPSCs originating from Matrigel. A) H7 cell line was hard to adapt on Matrigel combined with mTeSR1 medium. At first, the neural differentiation was observed primarily along the edges of the colonies on Matrigel in mTeSR1 medium. Finally, uneven neural rosette-like structures were formed in the colonies and the cell line was lost. B) Uneven neural rosette-like structures

found in colonies of H7 cell line cultured on Matrigel in mTeSR1 medium stained with MAP-2. C) MAP-2 expressing neural-like cells and structures were found on Matrigel in mTeSR1 medium in all hPSC lines. Representative image of UTA.04602.WT cell line. D) MAP-2 expressing neural structures appeared also in END-2 co-cultures when hPSCs originated from Matrigel and mTeSR1 cultures with all hPSC lines. Representative image of H7 cell line. Scale bars, 200 μm. E) The highest amount of MAP-2 positive cells were found in Matrigel cultures. Scale bars, 200 μm. The expression of *PAX-6 (F), Musashi (G)* and *Neurofilament (NF-68)* (H) in END-2 co-cultures was significantly higher in cells originating from Matrigel and mTeSR1 medium than from MEF or SNL feeder cell layers almost in all time points. The data is collected from two individual differentiation experiments of H7, UTA.00112.hFF and UTA.04602.WT hPSC lines (n = 6 in all three conditions). Error bars show the standard error of the mean (SEM). ** $p<0.01$, * $p<0.05$.

doi:10.1371/journal.pone.0048659.g005

SNL $p<0.001$) and 30 (Matrigel vs. MEF $p<0.001$, Matrigel vs. SNL $p<0.001$). On day 30 the expression of *PAX-6* was about 7 times higher in cells originating from Matrigel than from feeder cell layers. The expression of *Musashi* (Figure 5G) and *NF-68* (Figure 5H) remained stable in cells originating on MEF and SNL feeder cell layers. The expression of *Musashi* was significantly higher in all time points in cells originating from Matrigel than from MEF or SNL feeder cell layers ($p<0.001$) (Figure 5G). There were no significant differences between MEF and SNL feeder cell layers in the expression of *Musashi*. The expression of *NF-68* increased steadily from day 0 to day 30 (Figure 5H): day 0 (Matrigel vs. MEF, $p<0.001$; Matrigel vs. SNL, $p = 0.003$); day 3 and day 6 ($p<0.001$ for both conditions); day 12 (Matrigel vs. MEF, $p = 0.002$; Matrigel vs. SNL, $p = 0.005$) and day 30 ($p<0.001$ for both conditions). Interestingly, MAP-2 expressing neural-like cells and nerve bundles could also be detected in END-2 co-cultures when hPSCs were cultured on Matrigel prior to differentiation (Figure 5D). These structures were not found in END-2 co-cultures originating from mouse feeder cell layers.

Discussion

Several studies have evaluated the pluripotent and undifferentiated growth of hPSCs in serum-, xeno- and feeder cell-free conditions [26–29]. Previously we have shown that MEF feeder cells support cardiac differentiation better than human foreskin fibroblast (hFF) feeder cells [30]. In this study, we cultured hPSCs with three different culture methods: on MEF [1] and on SNL [31] feeder cell layers combined with conventional ko-SR and bFGF containing stem cell culture medium and on Matrigel with mTeSR1 medium [9], and evaluated the influence of the culture method on the cardiac differentiation potential of hPSCs. The cardiac differentiation efficiency varied between hPSC lines and separate differentiation experiments. In general our results suggest that hPSCs cultured on MEF and SNL feeder cell layers together with conventional stem cell culture medium are more prone to cardiac differentiation than hPSCs cultured on Matrigel combined with mTeSR1 medium, with one cell line UTA.04602.WT as an exception.

In this study, all hPSC lines differentiated into cardiomyocytes, but the differentiation efficiency varied considerably depending on the individual cell line, separate differentiation experiments and on the conditions under which the cell lines had been cultured prior to differentiation. Each hPSC line has a unique gene expression profile and thus vary in their cardiac differentiation potential [32]. In addition, it has been shown that hPSC lines change over time in culture due to genomic alterations [20]. For example enzymes used in hPSC passaging might have an effect to the pluripotent growth of hPSCs [22]. In our study the same enzymes which were used as in the original publications of the culture methods. The highest cardiac differentiation efficiency was observed in cells cultured on MEF or SNL feeder cell layers together with stem cell culture medium and the lowest in cells cultured on Matrigel in mTeSR1 medium. However, one cell line UTA.04602.WT was an exception and produced the highest amount of beating areas when cultured previously on Matrigel in mTeSR1. We characterized the starting population of hPSCs in all three conditions with flow cytometric analysis of TRA-1-81 and PSA-NCAM to determine the amount of pluripotent cells and if more cells were already committed to ectodermal lineages in some culture condition. The amount of PSA-NCAM positive cells was lower and the amount of TRA-1-81 positive cells was higher on MEF feeder cell cultures than in SNL feeder cell cultures and Matrigel cultures, indicating the superiority of MEF feeders in maintaining the pluripotency of hPSCs.

Mouse feeder cells express high levels of Activin A and low levels of bone morphogenetic protein 4 (BMP-4), which together have been reported to induce cardiac differentiation [33–35]. Normally, the peak *Brachyury T* expression is observed on day 3 in END-2 co-cultures [36]. Previously, we showed that peak *Brachyury T* expression was delayed to day 6 in cells cultured on hFF feeder cell layers [30]. The delayed peak of *Brachyury T* expression has been shown to lead to poor cardiac differentiation efficiency [37]. In this study, the expression peak of *Brachyury T* in cells cultured on Activin A expressing MEF and SNL feeder cells prior the differentiation was observed on day 3 and the peak *Brachyury T* expression was delayed to day 6 in cells cultured on Matrigel in mTeSR1 medium. Furthermore, endodermal *SOX-17* expression has been shown to enhance the cardiac differentiation and should peak on the same day on day 3 as *Brachyury T* [36,37]. The peak *SOX-17* expression was observed on day 3 in co-cultures originating from MEF and SNL feeder cell layers while the expression peak of *SOX-17* in END-2 co-cultures originating on Matrigel was delayed to day 6 in the same way than the expression peak of *Brachyury T*. The delayed expression of *Brachyury T* and *SOX-17* might indicate that hPSCs grown on Matrigel in mTeSR1 medium need more time to the initiation of the differentiation to mesodermal lineages. However, we counted the Troponin T positive cells 20 days and the beating areas 30 days after the initiation of END-2 co-culture and all our data suggest that hPSCs cultured on MEF and SNL feeder cell layers were more prone to cardiac differentiation than hPSCs cultured on Matrigel. The delayed expression of *Brachyury T* and *SOX-17* may be one reason for differences in cardiac differentiation efficiencies. However, to explain this phenomenon additional experiments are required.

Matrigel matrix together with mTeSR1 medium is widely used in different laboratories, and several research groups have reported this culture condition to maintain the undifferentiated growth of hPSCs [8,9,26,27,38]. In these studies, the pluripotency of hPSCs was confirmed by teratoma and EB formation and analysis of the expression of markers specific to all three germ layers present in these structures. Recently, Hudson and co-workers adapted hESCs to Matrigel in mTeSR1 medium and demonstrated that passaging the cells as single-cells prior to their cardiac differentiation reduced the heterogeneity of the cell population and enhanced cardiac differentiation [39]. However, they cultured hESCs on Matrigel in mTeSR1 medium for only one passage. To our knowledge, this is the first study reporting the long-term effects of this culture method on cardiac differentiation.

In this study, more MAP-2 positive cells could be detected in long-term culture of hPSCs on Matrigel matrix together with mTeSR1 medium than in MEF and SNL feeder cell cultures. The expression of *PAX-6, Musashi* and *NF-68* increased during END-2 co-culture in cells cultured on Matrigel in mTeSR1 medium prior to differentiation, and the emergence of neuronal cells in END-2 co-cultures was confirmed by MAP-2 staining. Beqqali and co-workers have reported that the expression of ectodermal genes in the END-2 co-culture method is low when compared to endodermal and mesodermal genes [36]. Erceg and co-workers have described the efficient differentiation of hESCs into neural lineages, using a mixed ECM protein (collagen IV, vitronectin and fibronectin) coating together with TeSR1 [8] medium, in which human serum albumin was replaced by Voluven [40]. In addition, laminin is one of the major constituents of Matrigel [41,42], and both Matrigel [43] and laminin are widely used as a matrix when generating neuronal cells and their derivatives from hPSCs [44–46]. In fact, Ma and co-workers tested five substrates, including poly-D-lysine, fibronectin, laminin, collagen and Matrigel; and they observed that laminin and laminin-rich Matrigel significantly enhanced directed differentiation into neural progenitors and neurons [44]. Axell and co-workers reported that hESCs cultured on Matrigel were more efficient source of neural progenitors than hESCs cultured on MEF feeder cell layers [45]. They assumed that this was due to the fact that cells cultured on Matrigel were already adapted to feeder cell-free cultures for 6–12 passages before their transfer to neural differentiation conditions. In addition to the neural differentiation inducing properties of Matrigel, mTeSR1 medium contains high concentrations of bFGF, transforming growth factor beta (TGF-β), gamma amino-butyric acid (GABA), pipecolinic acid and lithium chloride [9]. Further, mTeSR1 medium contains a higher concentration of insulin (0.023 g/l) than conventional stem cell culture medium (0.01 g/l) and insulin has been suggested to inhibit cardiac differentiation in END-2 co-cultures and actually redirecting the differentiation from cardiac mesoderm and endoderm into neuroectoderm [47]. The concentration of bFGF in mTeSR1 medium (100 ng/ml) is extremely high when compared to basic stem cell culture medium (4 ng/ml), and mouse feeder cells do not express bFGF [33]. In neural precursor media, the concentration of bFGF is normally 10–20 ng/ml [43,48–51] and bFGF has been found to play a role in the derivation, proliferation and maintenance of the neural progenitor state [43,45,52]. Thus, it is possible that, together with the laminin found in Matrigel, some of these factors: bFGF, TGF-β, GABA, pipecolinic acid, lithium chloride and insulin somehow induce more neural differentiation of hPSCs than differentiation to mesoendodermal lineages.

In our study, the expression of *OCT-3/4* was significantly higher in hPSCs cultured on Matrigel in mTeSR1 medium than on MEF or SNL feeder cell layers. Retention of *OCT-3/4* expression has been observed in neural progenitor populations, and the rapid loss of *OCT-3/4* expression during neural progenitor differentiation has been reported to induce hPSCs to develop into flattened extraembryonic cells rather than neural cells [45,53,54]. In fact, prolonged expression of *OCT-3/4* could be required for the neural differentiation while the rapid downregulation of *OCT-3/4* may be required to promote the formation of primitive endoderm that is essential for mesodermal differentiation [53]. Our results suggest that hPSCs cultured on Matrigel in mTeSR1 medium are more prone to neural lineages as to mesoendodermal lineages after long-term culture, and thus, the cardiac differentiation efficiency remains low.

Here, we have studied the effects of hPSC culture methods on the cardiac differentiation efficiency of hPSCs. Five hPSC lines cultured in three different culture conditions differentiated into beating cardiomyocytes, but the differentiation efficiency varied depending on the cell line, the specific differentiation experiment conducted and most importantly on the different culture conditions used. Mouse feeder cell layers (MEF and SNL) were found to be superior to the Matrigel matrix used together with mTeSR1 medium in inducing cardiac differentiation with one cell line as an exception out of all five hPSC lines. In fact, more MAP-2 expressing cells could be found in Matrigel and mTeSR1 cultures than from MEF and SNL feeder cell cultures. Our suggestion is that, in addition to the specific differentiation method, the hPSC culture method should also be optimized when differentiating hPSCs into specific lineages. In addition, the combination of culture conditions and differentiation conditions might be important for cardiac differentiation. At least our results show that mouse feeder cells should be used instead of Matrigel and mTeSR1 medium in combination of END-2 differentiation method.

Materials and Methods

Ethical issues

The study was conducted in accordance with the Ethics Committee of Pirkanmaa Hospital District to establish, culture and differentiate hESC and hiPSC lines (R08070, R05116). Skin biopsies for hiPSC establishment were received from the Heart Center, Tampere University Hospital. Patients donating skin biopsies signed an informed consent form after receiving both an oral and written description of the study.

Cell lines and cell culture

The hESC line H7 (46, XX) (WiCell Research Institute, Madison, WI, USA) [1] and four hiPSC lines including UTA.00112.hFF (46, XY) and UTA.00106.hFF from hFFs, and UTA.04602.WT (46, XX) and UTA.00525.LQT2 (46, XY) from adult human dermal fibroblasts were used in this study. hiPSC lines were reprogrammed with four retroviral vectors (*SOX-2, OCT-3/4, KLF4* and *C-MYC*) as described previously [55,56]. The UTA.00106.hFF cell line was found to be karyotypically abnormal with inversion in chromosome 12 (46, XY inv(12)). All five cell lines were cultured for at least for 14 passages at +37°C and 5% CO_2 in three different culture conditions, as described below.

All hPSC lines used in this study were normally cultured on mitomycin C treated MEF feeder cell layers (26000 cells/cm^2) (Millipore Corporate, Billerica, MA, USA) in stem cell culture medium consisting of ko-DMEM (Invitrogen, Carlsbad, CA, USA) supplemented with 20% ko-SR (Invitrogen), 1% non-essential amino acids (NEAA, Cambrex Bio Science Inc., Walkersville, MD, USA), 2 mM GlutaMax (Invitrogen), 50 U/ml penicillin/streptomycin (Lonza Group Ltd, Basel, Switzerland), 0.1 mM 2-mercaptoethanol (Invitrogen) and 4 ng/ml bFGF (R&D Systems Inc., Minneapolis, MN, USA). The medium was changed three times per week, and the cells were passaged enzymatically onto a new MEF feeder cell layer once per week. The MEF feeder cell layer was removed manually with a pipette tip before detaching the hPSC colonies with 1 mg/ml Collagenase IV (Invitrogen).

All hPSC lines were cultured on irradiated (40 Gy) SNL 76/7 (HPA Culture Collections, Salisbury, UK) feeder cell layers (29000 cells/cm^2) in stem cell culture medium. The medium was changed 6 times per week and hPSCs were passaged mostly in every five days (range 4–7 days) onto new SNL feeder cell layers. Before passaging, SNL feeder cells were removed with the previously described CTK solution [56] with a minor modification: ko-SR was replaced by stem cell culture medium without bFGF. CTK

solution consisted of 10% Trypsin (10x, Lonza), 0.1 mg/ml Collagenase IV (Invitrogen), 0.001 M $CaCl_2$ and 20% stem cell culture medium in H_2O. After CTK treatment, the remaining SNL feeder cells were carefully rinsed with ko-DMEM (Invitrogen), and colonies were scraped into stem cell culture medium with a pipette tip and plated onto new SNL feeder cell layers.

All hPSC lines were cultured on hESC-qualified Matrigel (BD Biosciences, Franklin Lakes, NJ, USA) in mTeSR1 medium (StemCell Technologies Inc., Vancouver, Canada) supplemented with 50 U/ml penicillin/streptomycin (Lonza). MEF feeder cell layer was manually removed as described above; colonies were scraped into mTeSR1 medium and plated onto Matrigel-coated 6-well culture plates. Plates were coated with Matrigel for at least 1 hour at room temperature (RT) following manufacturer's instructions. mTeSR1 medium was changed 6 times per week, and the cells were passaged using 1 mg/ml dispase (Invitrogen) mostly in every 5 days (range 4–6 days). Differentiated areas were carefully removed before passaging.

The growth of hPSC lines in different conditions was monitored daily under Nikon Eclipse TS100 phase contrast microscope (Nikon Instruments Europe B.V. Amstelveen, The Netherlands) and pictured with Altra-Cell-D-Bundle camera (Olympus Corporation, Tokyo, Japan).

Cardiac differentiation

Differentiation experiments were performed 2 to 6 times in hPSC lines cultured in all three conditions. hPSC lines and their passages in 6 separate differentiation experiments are presented in Table 1 and the cardiac differentiation experiments are outlined in Figure 1A. Altogether differentiation experiments were performed 18 times from MEF feeder cell layers and 15 times from both SNL feeder cell layers and Matrigel. All differentiation experiments with the UTA.00106.hFF cell line were performed with karyotypically abnormal (46, XY inv(12)) cells. To initiate cardiac differentiation, hPSCs were co-cultured in 12-well culture plates with Mitomycin C (Sigma-Aldrich, St. Louis, MO, USA) treated END-2 cells (50000 cells/cm^2), which were a kind gift from Professor Mummery (Humbrecht Institute, Utrecht, The Netherlands) [57]. MEF feeder cell layers were removed manually, and SNL feeder cells enzymatically with CTK solution before differentiation. Cell colonies cultured in all three conditions were detached with a cell scraper or pipette tip. Approximately 30 colony pieces per well were transferred onto END-2 cells in stem cell culture medium without ko-SR or bFGF and supplemented with 3 mg/ml ascorbic acid (Sigma-Aldrich). Medium was changed after 5, 8 and 12 days of culturing. After 15 days of culturing, 10% ko-SR was included and ascorbic acid was excluded from the culture medium; subsequently, the medium was changed three times per week.

Cardiac differentiation efficiency

Cardiac differentiation efficiency was determined by cytospin analysis on day 16–21 (herein on day 20) and by counting the number of beating areas on day 28–35 (herein day 30). Cytospin analysis was performed and beating areas were counted from all five hPSC lines cultured in all three conditions. The total number of wells from which the beating areas were counted is presented in Table 1. For cytospin analysis, the whole differentiating pool of cells from three wells (A1, B1 and C1), and a replicate sample of all cells from another three wells (A2, B2 and C2) were treated with trypsin (Lonza) at 37°C for 45 minutes. After the incubation, the aggregates were pipetted into a single-cell suspension and resuspended in EB medium, consisting of ko-DMEM supplemented with 20% fetal bovine serum (FBS, PAA Laboratories GmbH, Pasching, Austria), 1% NEAA (Cambrex Bio Science), 2 mM GlutaMax (Invitrogen) and 50 U/ml penicillin/streptomycin (Lonza). Approximately 1×10^6 cells were centrifuged at 800–1000 rpm for 5 minutes onto polysine slides (Thermo Scientific, Rochester, NY) using the cytospin system (Sakura Finetek, Alphen aan den Rijn, The Netherlands). Adherent cells on slides were fixed with 4% paraformaldehyde (Sigma-Aldrich) at RT for 20 minutes, permeabilized and blocked with 0.1% Triton X-100 (Sigma-Aldrich), 1% bovine serum albumin (BSA, Sigma-Aldrich) and 10% normal donkey serum (Sigma-Aldrich) in phosphate-buffered saline (PBS, Lonza) for 45 min at RT, and stained with mouse or goat anti-cardiac Troponin T primary antibodies (Table S1) diluted in 1% normal donkey serum, 0.1% TritonX-100, and 1% BSA in PBS (Lonza) over night at +4°C. The next day, the cells were probed with Alexa Fluor 568 secondary antibody (Invitrogen) diluted in 1% BSA (Sigma-Aldrich) in PBS (Lonza) for 1 h at RT in the dark. Finally, cells were mounted with Vectashield (Vector Laboratories Inc., Burlingame, CA, USA) containing 40,6-diamidino-2-phenylindole (DAPI) for nuclear staining, and the percentage of Troponin T positive cells versus the total cell number was determined. Counted areas were randomly selected in the DAPI channel using 20 x magnification, and a total of 1500 cells was counted. Cells were pictured with Olympus IX51 phase contrast microscope with fluorescence optics and Olympus DP30BW camera (Olympus Corporation).

Dissociation of beating areas and immunocytochemistry

Beating areas were cut out manually and dissociated into a single-cell suspension using Collagenase A (Roche Diagnostics GmbH, Mannheim, Germany) treatment, as previously described [58]. Dissociated cells were plated onto 0.1% gelatin coated 24-well plates in EB medium.

The undifferentiated growth and neural differentiation of hPSCs under different culture conditions was judged by the morphology of the cells. The morphologic characterization was confirmed by immunocytochemical stainings for hPSCs cultured at least for 14 passages in three different culture conditions. hPSC colonies were stained with primary antibodies specific for undifferentiated hPSCs including Nanog, OCT-3/4 and SSEA-4. Neural progenitor cells and neuronal cells were detected from undifferentiated cultures by staining cells for PSA-NCAM and MAP-2. Dissociated cardiomyocytes were stained for connexin-43, α-actinin, Troponin T and MHC. The primary antibodies are summarized in Table S1 and staining was performed as described above. All Alexa Fluor 568 or 488-conjugated secondary antibodies were from Invitrogen.

In vitro analysis of pluripotency

The pluripotency of the H7, UTA.00106.hFF and UTA.00525.LQT2 cell lines cultured in all three culture conditions was verified by the formation of EBs. To form EBs, feeder cells were removed mechanically (MEF) or enzymatically (SNL), and hPSCs were scraped with a cell scraper and placed into suspension culture in EB medium. Media was changed every 2 to 3 days, and EBs were cultured for 5 weeks. Total RNA was extracted from EBs and 200 ng of cDNA was transcripted. The expression of the three germ layers, ectoderm (*Paired box 6* (*PAX-6*) and *SRY-box 1* (*SOX-1*)), endoderm (*Alpha-fetoprotein* (*AFP*) and *SOX-17*) and mesoderm (*α-cardiac actin* and *Kinase insert domain receptor* (*KDR*)) was studied in the EBs using RT-PCR primers. *β-actin* was used as housekeeping control. Primer sequences are presented in Table S2.

Quantitative-RT-PCR

Quantitative RT-PCR was performed on H7, UTA.00112.hFF and UTA.04602.WT cell samples collected from the fourth and sixth differentiation experiments (Table 1). Each of two replicate samples were collected from two wells of co-cultures and lysed into RA1 buffer supplemented with β-mercaptoethanol at time points of 3, 5–6, 12–13 and 28–35 days, herein reported as 3, 6, 12 and 30 days. Undifferentiated cells were used as day 0 samples. Samples were stored at −70°C until the total-RNA was extracted with the NucleoSpin® RNA II kit, which included DNAase treatment (Macherey-Nagel, Duren, Germany) as described in the manufacturer's instructions. The concentration and quality of RNA was measured using a NanoDrop 1000 spectrophotometer (NanoDrop Technologies, Wilmington, DE). Biological replicates were pooled into one sample during cDNA transcription, and 250 ng of RNA from both biological replicates (totaling 500 ng) were transcribed into cDNA in a total volume of 20 µl with a High-Capacity cDNA Reverse-Transcription kit (Applied Biosystems, Foster City, CA, USA) in the presence of RiboLock RNase inhibitor (Thermo Scientific). The expression of *Brachyury T, NKX2.5* and *SOX-17* were studied with SYBR chemistry and *Ribosomal protein large p0* (*RPLP0*), *OCT-3/4, PAX-6, Musashi* and *NF-68* were studied with Taqman chemistry. The PCR reaction for SYBR primers consisted of 1 µl of cDNA at a 1:3 dilution, 14 µl of 2× SYBR green PCR mastermix (Applied Biosystems) and 300 nM of each primer. The following Taqman assays were used: NM_053275.3 for *RPLP0*, Hs00999632_g1 for *OCT-3/4* (*POU5F1*), Hs00240871_m1 for *PAX-6*, Hs01045894_m1 for *Musashi* and Hs00196245_m1 for *NF-68*. SYBR primer sequences are presented in Table S2. All samples were analyzed in triplicate, C_τ values were determined, and the fold changes were calculated by the $2^{-\Delta\Delta C\tau}$ method [59]. The data were normalized to the expression of the endogenous control *RPLP0*. The average of d0 samples from MEF feeder cell layers were used as a calibrator.

Flow cytometric analysis

All five hPSC lines cultured in all three conditions were analyzed by flow cytometry using antibodies against TRA-1-81-FITC (BD Biosciences) and PSA-NCAM-APC (Miltenyi Biotec, Teterow, Germany). Samples were collected from one day before or same day as passaging was done. MEF and SNL feeder cells were removed prior the sample collections. FITC mouse IgM isotype control antibody (BD Biosciences) was used as isotype control. Labeled hPSCs were analyzed using BD FACSAria™ (BD Biosciences). The samples were analyzed as duplicates and the acquisition was set for 10000 events per sample. The data were analyzed using FACSDiva Software version 6.1.3 (BD Biosciences).

Statistical analysis

The number of beating areas is presented as the mean value over all differentiation experiments; error bars represent the standard error of the mean (SEM). The number of the Troponin T positive cells in one well detected in cytospin analysis and are presented in scatter blots. Quantitative RT-PCR data are presented as the mean value ± SEM. For beating areas, cytospin and q-RT-PCR results statistical significance was determined using one-way ANOVA with Bonferroni's correction for multiple comparisons. Results were confirmed by Poisson regression analysis. However, for the sake of simplicity, only the ANOVA results are reported. A p-value <0.05 was considered statistically significant.

Supporting Information

Table S1 Primary antibodies used in this study.
(DOC)

Table S2 RT-PCR and quantitative RT-PCR primers used in this study.
(DOC)

Acknowledgments

We thank professor Christine Mummery for providing us the END-2 cells, Anna Lahti, Henna Venäläinen, Markus Haponen and Janne Koivisto for their contribution to the laboratory work, as well as Neuro Group especially Anu Hyysalo, Susanna Narkilahti and Riikka Äänismaa for the consult with immunocytochemical stainings and FACS analysis for the neuronal markers.

Author Contributions

Conceived and designed the experiments: MO KR MPM KAS. Performed the experiments: MO KR MM. Analyzed the data: MO KR MPM HH. Wrote the paper: MO KR KAS.

References

1. Thomson JA, Itskovitz-Eldor J, Shapiro SS, Waknitz MA, Swiergiel JJ, et al. (1998) Embryonic stem cell lines derived from human blastocysts. Science 282: 1145–1147.
2. Amit M, Margulets V, Segev H, Shariki K, Laevsky I, et al. (2003) Human feeder layers for human embryonic stem cells. Biol Reprod 68: 2150–2156.
3. Richards M, Fong CY, Chan WK, Wong PC, Bongso A (2002) Human feeders support prolonged undifferentiated growth of human inner cell masses and embryonic stem cells. Nat Biotechnol 20: 933–936.
4. Takahashi K, Narita M, Yokura M, Ichisaka T, Yamanaka S (2009) Human induced pluripotent stem cells on autologous feeders. PLoS One 4: e8067.
5. Xu C, Jiang J, Sottile V, McWhir J, Lebkowski J, et al. (2004) Immortalized fibroblast-like cells derived from human embryonic stem cells support undifferentiated cell growth. Stem Cells 22: 972–980.
6. Amit M, Shariki C, Margulets V, Itskovitz-Eldor J (2004) Feeder layer- and serum-free culture of human embryonic stem cells. Biol Reprod 70: 837–845.
7. Beattie GM, Lopez AD, Bucay N, Hinton A, Firpo MT, et al. (2005) Activin A maintains pluripotency of human embryonic stem cells in the absence of feeder layers. Stem Cells 23: 489–495.
8. Ludwig T, Levenstein M, Jones J, Berggren W, Mitchen E, et al. (2006) Derivation of human embryonic stem cells in defined conditions. Nat Biotechnol 24: 185–187.
9. Ludwig TE, Bergendahl V, Levenstein ME, Yu J, Probasco MD, et al. (2006) Feeder-independent culture of human embryonic stem cells. Nat Methods 3: 637–646.
10. Xu C, Inokuma MS, Denham J, Golds K, Kundu P, et al. (2001) Feeder-free growth of undifferentiated human embryonic stem cells. Nat Biotechnol 19: 971–974.
11. Larijani MR, Seifinejad A, Pournasr B, Hajihoseini V, Hassani SN, et al. (2011) Long-term maintenance of undifferentiated human embryonic and induced pluripotent stem cells in suspension. Stem Cells Dev 20: 1911–1923.
12. Martin MJ, Muotri A, Gage F, Varki A (2005) Human embryonic stem cells express an immunogenic nonhuman sialic acid. Nat Med 11: 228–232.
13. Hisamatsu-Sakamoto M, Sakamoto N, Rosenberg AS (2008) Embryonic stem cells cultured in serum-free medium acquire bovine apolipoprotein B-100 from feeder cell layers and serum replacement medium. Stem Cells 26: 72–78.
14. Skottman H, Mikkola M, Lundin K, Olsson C, Stromberg AM, et al. (2005) Gene expression signatures of seven individual human embryonic stem cell lines. Stem Cells 23: 1343–1356.
15. Abeyta MJ, Clark AT, Rodriguez RT, Bodnar MS, Pera RA, et al. (2004) Unique gene expression signatures of independently-derived human embryonic stem cell lines. Hum Mol Genet 13: 601–608.
16. Tavakoli T, Xu X, Derby E, Serebryakova Y, Reid Y, et al. (2009) Self-renewal and differentiation capabilities are variable between human embryonic stem cell lines I3, I6 and BG01V. BMC Cell Biol 10: 44.
17. Peterson SE, Westra JW, Rehen SK, Young H, Bushman DM, et al. (2011) Normal human pluripotent stem cell lines exhibit pervasive mosaic aneuploidy. PLoS One 6: e23018.

18. Narsinh KH, Sun N, Sanchez-Freire V, Lee AS, Almeida P, et al. (2011) Single cell transcriptional profiling reveals heterogeneity of human induced pluripotent stem cells. J Clin Invest 121: 1217–1221.
19. Hussein SM, Batada NN, Vuoristo S, Ching RW, Autio R, et al. (2011) Copy number variation and selection during reprogramming to pluripotency. Nature 471: 58–62.
20. Laurent LC, Ulitsky I, Slavin I, Tran H, Schork A, et al. (2011) Dynamic changes in the copy number of pluripotency and cell proliferation genes in human ESCs and iPSCs during reprogramming and time in culture. Cell Stem Cell 8: 106–118.
21. Mayshar Y, Ben-David U, Lavon N, Biancotti JC, Yakir B, et al. (2010) Identification and classification of chromosomal aberrations in human induced pluripotent stem cells. Cell Stem Cell 7: 521–531.
22. Allegrucci C, Wu YZ, Thurston A, Denning CN, Priddle H, et al. (2007) Restriction landmark genome scanning identifies culture-induced DNA methylation instability in the human embryonic stem cell epigenome. Hum Mol Genet 16: 1253–1268.
23. Forsyth NR, Kay A, Hampson K, Downing A, Talbot R, et al. (2008) Transcriptome alterations due to physiological normoxic (2% O2) culture of human embryonic stem cells. Regen Med 3: 817–833.
24. Skottman H, Stromberg AM, Matilainen E, Inzunza J, Hovatta O, et al. (2006) Unique gene expression signature by human embryonic stem cells cultured under serum-free conditions correlates with their enhanced and prolonged growth in an undifferentiated stage. Stem Cells 24: 151–167.
25. Kattman SJ, Witty AD, Gagliardi M, Dubois NC, Niapour M, et al. (2011) Stage-specific optimization of activin/nodal and BMP signaling promotes cardiac differentiation of mouse and human pluripotent stem cell lines. Cell Stem Cell 8: 228–240.
26. Hakala H, Rajala K, Ojala M, Panula S, Areva S, et al. (2009) Comparison of biomaterials and extracellular matrices as a culture platform for multiple, independently derived human embryonic stem cell lines. Tissue Eng Part A 15: 1775–1785.
27. Akopian V, Andrews PW, Beil S, Benvenisty N, Brehm J, et al. (2010) Comparison of defined culture systems for feeder cell free propagation of human embryonic stem cells. In Vitro Cell Dev Biol Anim 46: 247–258.
28. Chin AC, Padmanabhan J, Oh SK, Choo AB (2010) Defined and serum-free media support undifferentiated human embryonic stem cell growth. Stem Cells Dev 19: 753–761.
29. Rajala K, Hakala H, Panula S, Aivio S, Pihlajamaki H, et al. (2007) Testing of nine different xeno-free culture media for human embryonic stem cell cultures. Hum Reprod 22: 1231–1238.
30. Pekkanen-Mattila M, Ojala M, Kerkela E, Rajala K, Skottman H, et al. (2012) The effect of human and mouse fibroblast feeder cells on cardiac differentiation of human pluripotent stem cells. Stem Cells Int: 875059.
31. Takahashi K, Tanabe K, Ohnuki M, Narita M, Ichisaka T, et al. (2007) Induction of pluripotent stem cells from adult human fibroblasts by defined factors. Cell 131: 861–872.
32. Pekkanen-Mattila M, Kerkela E, Tanskanen JM, Pietila M, Pelto-Huikko M, et al. (2009) Substantial variation in the cardiac differentiation of human embryonic stem cell lines derived and propagated under the same conditions–a comparison of multiple cell lines. Ann Med 41: 360–370.
33. Eiselleova L, Peterkova I, Neradil J, Slaninova I, Hampl A, et al. (2008) Comparative study of mouse and human feeder cells for human embryonic stem cells. Int J Dev Biol 52: 353–363.
34. Laflamme MA, Chen KY, Naumova AV, Muskheli V, Fugate JA, et al. (2007) Cardiomyocytes derived from human embryonic stem cells in pro-survival factors enhance function of infarcted rat hearts. Nat Biotechnol 25: 1015–1024.
35. Yang L, Soonpaa MH, Adler ED, Roepke TK, Kattman SJ, et al. (2008) Human cardiovascular progenitor cells develop from a KDR+ embryonic-stem-cell-derived population. Nature 453: 524–528.
36. Beqqali A, Kloots J, Ward-van Oostwaard D, Mummery C, Passier R (2006) Genome-wide transcriptional profiling of human embryonic stem cells differentiating to cardiomyocytes. Stem Cells 24: 1956–1967.
37. Bettiol E, Sartiani L, Chicha L, Krause KH, Cerbai E, et al. (2007) Fetal bovine serum enables cardiac differentiation of human embryonic stem cells. Differentiation 75: 669–681.
38. Lagarkova MA, Eremeev AV, Svetlakov AV, Rubtsov NB, Kiselev SL (2010) Human embryonic stem cell lines isolation, cultivation, and characterization. In Vitro Cell Dev Biol Anim 46: 284–293.
39. Hudson JE, Titmarsh DM, Hidalgo A, Wolvetang EJ, Cooper-White JJ (2011) Primitive Cardiac Cells from Human Embryonic Stem Cells. Stem Cells Dev.
40. Erceg S, Lainez S, Ronaghi M, Stojkovic P, Perez-Arago MA, et al. (2008) Differentiation of human embryonic stem cells to regional specific neural precursors in chemically defined medium conditions. PLoS One 3: e2122.
41. Kleinman HK, McGarvey ML, Hassell JR, Star VL, Cannon FB, et al. (1986) Basement membrane complexes with biological activity. Biochemistry 25: 312–318.
42. Kleinman HK, Martin GR (2005) Matrigel: basement membrane matrix with biological activity. Semin Cancer Biol 15: 378–386.
43. Benzing C, Segschneider M, Leinhaas A, Itskovitz-Eldor J, Brustle O (2006) Neural conversion of human embryonic stem cell colonies in the presence of fibroblast growth factor-2. Neuroreport 17: 1675–1681.
44. Ma W, Tavakoli T, Derby E, Serebryakova Y, Rao MS, et al. (2008) Cell-extracellular matrix interactions regulate neural differentiation of human embryonic stem cells. BMC Dev Biol 8: 90.
45. Axell MZ, Zlateva S, Curtis M (2009) A method for rapid derivation and propagation of neural progenitors from human embryonic stem cells. J Neurosci Methods 184: 275–284.
46. Nat R, Nilbratt M, Narkilahti S, Winblad B, Hovatta O, et al. (2007) Neurogenic neuroepithelial and radial glial cell generated form six human embryonic stem cell lines in serum-free adherent and suspension cultures. Glia 55: 385–399.
47. Freund C, Ward-van Oostwaard D, Monshouwer-Kloots J, van den Brink S, van Rooijen M, et al. (2008) Insulin redirects differentiation from cardiogenic mesoderm and endoderm to neuroectoderm in differentiating human embryonic stem cells. Stem Cells 26: 724–733.
48. Carpenter MK, Inokuma MS, Denham J, Mujtaba T, Chiu CP, et al. (2001) Enrichment of neurons and neural precursors from human embryonic stem cells. Exp Neurol 172: 383–397.
49. Reubinoff BE, Itsykson P, Turetsky T, Pera MF, Reinhartz E, et al. (2001) Neural progenitors from human embryonic stem cells. Nat Biotechnol 19: 1134–1140.
50. Zhang SC, Wernig M, Duncan ID, Brustle O, Thomson JA (2001) In vitro differentiation of transplantable neural precursors from human embryonic stem cells. Nat Biotechnol 19: 1129–1133.
51. Itsykson P, Ilouz N, Turetsky T, Goldstein RS, Pera MF, et al. (2005) Derivation of neural precursors from human embryonic stem cells in the presence of noggin. Mol Cell Neurosci 30: 24–36.
52. Joannides AJ, Fiore-Heriche C, Battersby AA, Athauda-Arachchi P, Bouhon IA, et al. (2006) A scaleable and defined system for generating neural stem cells from human embryonic stem cells. Stem Cells 25: 731–737.
53. Gerrard L, Rodgers L, Cui W (2005) Differentiation of human embryonic stem cells to neural lineages in adherent culture by blocking bone morphogenetic protein signaling. Stem Cells 23: 1234–1241.
54. Rathjen J, Haines BP, Hudson KM, Nesci A, Dunn S, et al. (2002) Directed differentiation of pluripotent cells to neural lineages: homogeneous formation and differentiation of a neurectoderm population. Development 129: 2649–2661.
55. Lahti AL, Kujala VJ, Chapman H, Koivisto AP, Pekkanen-Mattila M, et al. (2011) Model for long QT syndrome type 2 using human iPS cells demonstrates arrhythmogenic characteristics in cell culture. Dis Model Mech.
56. Ohnuki M, Takahashi K, Yamanaka S (2009) Generation and characterization of human induced pluripotent stem cells. Curr Protoc Stem Cell Biol Chapter 4: Unit 4A 2.
57. Mummery CL, van Achterberg TA, van den Eijnden-van Raaij AJ, van Haaster L, Willemse A, et al. (1991) Visceral-endoderm-like cell lines induce differentiation of murine P19 embryonal carcinoma cells. Differentiation 46: 51–60.
58. Mummery C, Ward-van Oostwaard D, Doevendans P, Spijker R, van den Brink S, et al. (2003) Differentiation of human embryonic stem cells to cardiomyocytes: role of coculture with visceral endoderm-like cells. Circulation 107: 2733–2740.
59. Livak KJ, Schmittgen TD (2001) Analysis of relative gene expression data using real-time quantitative PCR and the 2(-Delta Delta C(T)) Method. Methods 25: 402–408.